

Article

Comprehensive Second-Order Adjoint Sensitivity Analysis Methodology (2nd-ASAM) Applied to a Subcritical Experimental Reactor Physics Benchmark: IV. Effects of Imprecisely Known Source Parameters

Ruixian Fang  and Dan Gabriel Cacuci * 

Center for Nuclear Science and Energy, Department of Mechanical Engineering, University of South Carolina, Columbia, SC 29208, USA; fangr@cec.sc.edu

* Correspondence: cacuci@cec.sc.edu; Tel.: +1-(803)-777-9751

Received: 26 January 2020; Accepted: 11 March 2020; Published: 19 March 2020



Abstract: By applying the Second-Order Adjoint Sensitivity Analysis Methodology (2nd-ASAM) to the polyethylene-reflected plutonium (PERP) benchmark, this work presents results for the first- and second-order sensitivities of this benchmark's leakage response with respect to the spontaneous fission source parameters. The numerical results obtained for these sensitivities indicate that the 1st-order relative sensitivity of the leakage response to the source parameters for the two fissionable isotopes in the benchmark are all positive, signifying that an increase in the source parameters will cause an increase in the total neutron leakage from the PERP sphere. The 1st- and 2nd-order relative sensitivities with respect to the source parameters for ^{239}Pu are very small (10^{-4} or less). In contradistinction, the 1st-order and several 2nd-order relative sensitivities of the leakage response with respect to the source parameters of ^{240}Pu are large. Large values (e.g., greater than 1.0) are also displayed by several mixed 2nd-order relative sensitivities of the leakage response with respect to parameters involving the source and: (i) the total cross sections; (ii) the average neutrons per fission; and (iii) the isotopic number densities. On the other hand, the values of the mixed 2nd-order relative sensitivities with respect to parameters involving the source and: (iv) the scattering cross sections; and (v) and the fission cross sections are smaller than 1.0. It is also shown that the effects of the 1st- and 2nd-order sensitivities of the PERP benchmark's leakage response with respect to the benchmark's source parameters on the moments (expected value, variance and skewness) of the PERP benchmark's leakage response distribution are negligibly smaller than the corresponding effects (on the response distribution) stemming from uncertainties in the total, fission and scattering cross sections.

Keywords: polyethylene-reflected plutonium sphere; 1st- and 2nd-order sensitivities; fission source parameters; fission spectrum; expected value; variance and skewness of leakage response

1. Introduction

In previous works [1–3], the Second-Order Adjoint Sensitivity Analysis Methodology (2nd-ASAM) conceived by Cacuci [4–6] has been applied to the subcritical polyethylene-reflected plutonium (acronym: PERP) metal OECD/NEA-benchmark [7], to compute efficiently the exact values of the 1st-order and 2nd-order sensitivities of the PERP's leakage response with respect to the following model parameters: (i) 180 group-averaged total microscopic cross sections [1]; (ii) 21,600 group-averaged scattering microscopic cross sections [2]; and (iii) 120 fission process parameters [3]. This work, designated as Part IV, presents the results of having applied the 2nd-ASAM to compute the 1st- and 2nd-order sensitivities of the PERP's leakage response with respect to the PERP benchmark's 12 source

parameters. The remaining results obtained by applying the 2nd-ASAM to compute the 1st- and 2nd-order sensitivities of the PERP's leakage response with respect to the PERP's 6 isotopic number densities will be presented in Part V [8]. The overall conclusions drawn from this massive sensitivity analysis endeavor will be presented in Part VI [9].

Although the physical characteristics of the PERP metal sphere benchmark have been detailed in Part I [1], it is convenient, for easy reference, to recall the dimensional and material composition of the benchmark in Table 1.

Table 1. Dimensions and material composition of the PERP benchmark.

Materials	Isotopes	Weight Fraction	Density (g/cm ³)	Zones
Material 1 (plutonium metal)	Isotope 1 (²³⁹ Pu)	9.3804×10^{-1}	19.6	Material 1 is assigned to zone 1, which has a radius of 3.794 cm.
	Isotope 2 (²⁴⁰ Pu)	5.9411×10^{-2}		
	Isotope 3 (⁶⁹ Ga)	1.5152×10^{-3}		
	Isotope 4 (⁷¹ Ga)	1.0346×10^{-3}		
Material 2 (polyethylene)	Isotope 5 (C)	8.5630×10^{-1}	0.95	Material 2 is assigned to zone 2, which has an inner radius of 3.794 cm and an outer radius of 7.604 cm.
	Isotope 6 (¹ H)	1.4370×10^{-1}		

The PERP benchmark has no delayed neutron or (α, n) source; the sole source of neutrons is provided by the spontaneous fissions stemming from ²³⁹Pu (Isotope 1) and ²⁴⁰Pu (Isotope 2). This source has been computed using the code SOURCES4C [10]. For an actinide nuclide k , where $k = 1, 2$ for the PERP benchmark, the spontaneous source depends on the following 12 model parameters [10]: the decay constant λ_k , the atom density N_k , the average number of neutrons per spontaneous fission ν_k^{SF} , the spontaneous fission branching ratio F_k^{SF} , and the two parameters a_k and b_k used in a Watt's fission spectra to approximate the spontaneous fission neutron spectra. The nominal values of these parameters (except for N_k) are available from a library file contained in SOURCES4C [10], and the nominal values for N_k are specified from the PERP benchmark. These imprecisely known source parameters also contribute to the accuracy of the neutron transport calculation. To evaluate the uncertainties induced in the leakage response by the imprecisely known source parameters, the 1st-order and 2nd-order sensitivities of the leakage response with respect to the source parameters will be computed by specializing the general expressions derived by Cacuci [6] to the PERP benchmark.

This work is organized, as follows: Section 2 presents the computational results for the 12 first-order sensitivities and 12×12 second-order sensitivities of the leakage response with respect to the benchmark's source parameters. Section 3 reports the numerical results for the 12×180 mixed 2nd-order sensitivities to the source parameters and total microscopic cross sections. Section 4 reports the numerical results for the $12 \times 21,600$ matrix of mixed 2nd-order sensitivities to the source parameters and scattering microscopic cross sections. Section 5 presents the numerical results for the 12×60 mixed 2nd-order sensitivities to the source parameters and fission microscopic cross sections. Section 6 reports the computational results for the 12×60 mixed 2nd-order sensitivities to source parameters and the average number of neutrons per fission of all the fissionable isotopes in the PERP benchmark. Section 7 reports the numerical results for the 12×6 mixed 2nd-order sensitivities to source parameters and the isotopic number densities of all isotopes in the PERP benchmark. Section 8 presents the impact of the 1st- and 2nd-order sensitivities on the uncertainties induced in the PERP's leakage response by the imprecisely known source parameters. Section 9 offers conclusions based upon the computational results presented in this work.

2. Computation of 1st- and 2nd-Order Sensitivities of the PERP Leakage Response to Source Parameters

As described in Part I [1], the neutron flux is computed by solving numerically the neutron transport equation using the PARTISN [11] multigroup discrete ordinates transport code. These PARTISN [11]

computations were performed using the MENDF71X 618-group cross sections [12] collapsed to $G = 30$ energy groups, with group boundaries, E^g , as presented in [1]. The MENDF71X library uses ENDF/B-VII.1 Nuclear Data [13].

For the PERP benchmark under consideration, PARTISN [11] solves the following multi-group approximation of the neutron transport equation with a spontaneous fission source provided by the code SOURCES4C [10]:

$$B^g(\boldsymbol{\alpha})\varphi^g(r, \boldsymbol{\Omega}) = Q^g(r), \quad g = 1, \dots, G, \quad (1)$$

$$\varphi^g(r_d, \boldsymbol{\Omega}) = 0, \quad \boldsymbol{\Omega} \cdot \mathbf{n} < 0, \quad g = 1, \dots, G, \quad (2)$$

where $\varphi^g(r, \boldsymbol{\Omega})$ is the customary “group-flux” for group g , and r_d denotes the external radius of the PERP benchmark, and where:

$$B^g(\boldsymbol{\alpha})\varphi^g(r, \boldsymbol{\Omega}) \triangleq \boldsymbol{\Omega} \cdot \nabla \varphi^g(r, \boldsymbol{\Omega}) + \Sigma_t^g(r) \varphi^g(r, \boldsymbol{\Omega}) - \sum_{g'=1}^G \int_{4\pi} \Sigma_s^{g' \rightarrow g}(r, \boldsymbol{\Omega}' \rightarrow \boldsymbol{\Omega}) \varphi^{g'}(r, \boldsymbol{\Omega}') d\boldsymbol{\Omega}' - \chi^g(r) \sum_{g'=1}^G \int_{4\pi} (v\Sigma_f)^{g'}(r) \varphi^{g'}(r, \boldsymbol{\Omega}') d\boldsymbol{\Omega}', \quad (3)$$

$$Q^g(r) \triangleq \sum_{i=1}^{N_f} \lambda_i N_{i,1} F_i^{SF} v_i^{SF} \frac{1}{I_0} \int_{E^{g+1}}^{E^g} dE e^{-E/a_i} \sinh \sqrt{b_i E}, \quad (4)$$

with:

$$I_0 = \frac{\sqrt{\pi a_i^3 b_i}}{2} e^{\frac{a_i b_i}{4}}. \quad (5)$$

In Equations (4) and (5), the subscript “ i ” is the number of nuclides with spontaneous fission source. In Equation (1), the vector $\boldsymbol{\alpha}$ denotes the “vector of imprecisely known model parameters”, which has been defined in Part I [1] as $\boldsymbol{\alpha} \triangleq [\sigma_t; \sigma_s; \sigma_f; \mathbf{v}; \mathbf{p}; \mathbf{q}; \mathbf{N}]^\dagger$, with vector-components σ_t , σ_s , σ_f , \mathbf{v} , \mathbf{p} , \mathbf{q} and \mathbf{N} , which comprise the various model parameters for the microscopic total cross sections, scattering cross sections, fission cross sections, average number of neutrons per fission, fission spectra, sources, and isotopic number densities, respectively. For convenient reference, the components of the vector of model parameters $\boldsymbol{\alpha}$ are reproduced in Appendix A.

The total neutron leakage from the PERP sphere, denoted as $L(\boldsymbol{\alpha})$, will depend (indirectly, through the neutron flux) on all of the imprecisely known model parameters and is defined as follows:

$$L(\boldsymbol{\alpha}) \triangleq \int_{S_b} dS \sum_{g=1}^G \int_{\boldsymbol{\Omega} \cdot \mathbf{n} > 0} d\boldsymbol{\Omega} \boldsymbol{\Omega} \cdot \mathbf{n} \varphi^g(r, \boldsymbol{\Omega}), \quad (6)$$

where S_b is the external surface area of the PERP ball. Figure 1 shows the histogram plot of the leakage for each energy group for the PERP benchmark. The total leakage computed using Equation (6) for the PERP benchmark is 1.7648×10^6 neutrons/sec. Table 2 summarizes the integrals for the source, fission source, absorption, in-scattering, self-scattering, out-scattering, and particle balance.

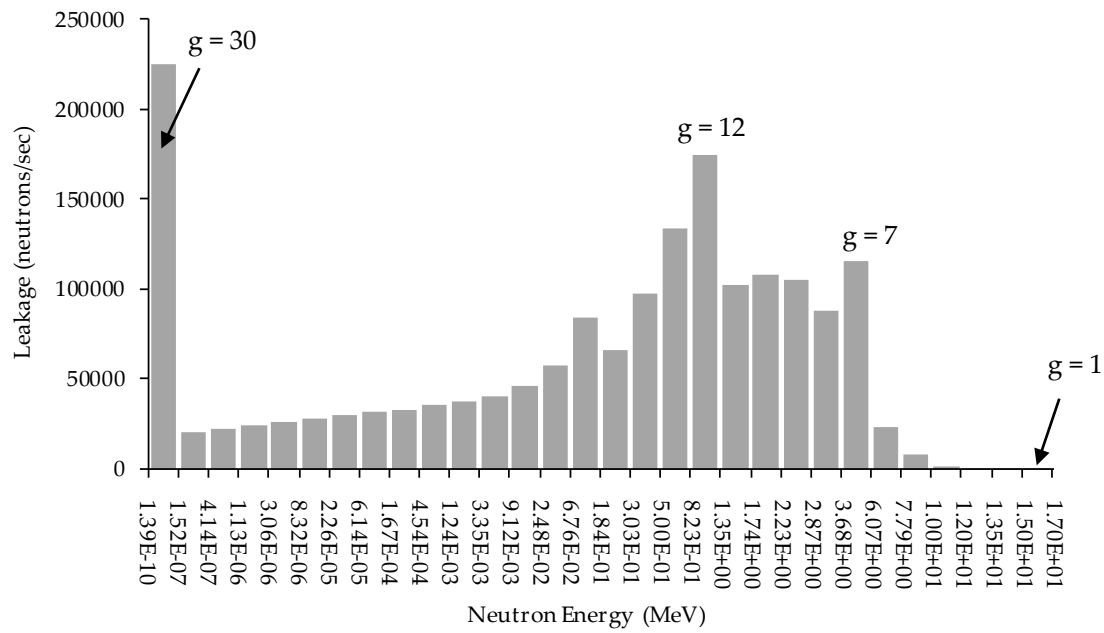


Figure 1. Histogram plot of the leakage for each energy group for the PERP benchmark.

Table 2. Summary of integrals of neutrons for the PERP benchmark.

Quantity	Values (neutrons/s)
Integral source	2.7839×10^5
Integral fission	2.4584×10^6
Integral absorption	9.7201×10^5
Integral in-scattering	8.3842×10^6
Integral self-scattering	1.3558×10^7
Integral out-scattering	8.3842×10^6
Integral net leakage	1.7648×10^6
Integral particle balance	8.3526×10^{-6}

The sub-sections to follow will report computational results for the 1st- and 2nd-order sensitivities of the leakage response with respect to the source parameters for $\partial L(\alpha)/\partial \mathbf{q}$ and $\partial^2 L(\alpha)/\partial \mathbf{q} \partial \mathbf{q}$, and the 2nd-order mixed sensitivities $\partial^2 L(\alpha)/\partial \mathbf{q} \partial \sigma_t$, $\partial^2 L(\alpha)/\partial \mathbf{q} \partial \sigma_s$, $\partial^2 L(\alpha)/\partial \mathbf{q} \partial \sigma_f$, $\partial^2 L(\alpha)/\partial \mathbf{q} \partial \nu$ and $\partial^2 L(\alpha)/\partial \mathbf{q} \partial \mathbf{N}$.

2.1. First-Order Sensitivities $\partial L(\alpha)/\partial \mathbf{q}$

In view of Equation (4), the source $Q^S(r)$ for the PERP benchmark depends on the vector of model parameters \mathbf{q} , having components defined as follows:

$$\mathbf{q} \triangleq [q_1, \dots, q_{J_q}]^\dagger \triangleq [\lambda_1, \lambda_2; F_1^{SF}, F_2^{SF}; a_1, a_2; b_1, b_2; v_1^{SF}, v_2^{SF}; N_{1,1}, N_{2,1}]^\dagger, \quad J_q = 12. \quad (7)$$

The nominal values of the source parameters for the PERP benchmark are listed in Table 3 below.

Table 3. Nominal values of the source parameters for the PERP benchmark [10].

Parameters	λ_1 [1/sec]	F_1^{SF} [-]	a_1 [-]	b_1 [-]	ν_1^{SF} [-]	$N_{1,1}$ [atoms/cm ³]
Values	9.11029×10^{-13}	3.0×10^{-12}	0.885247	3.80269	2.16	4.631644×10^{22}
Parameters	λ_2 [1/sec]	F_2^{SF} [-]	a_2 [-]	b_2 [-]	ν_2^{SF} [-]	$N_{2,1}$ [atoms/cm ³]
Values	3.35340×10^{-12}	5.75×10^{-8}	0.794930	4.68927	2.16	2.921242×10^{21}

The first-order sensitivity of the PERP leakage response to the source parameters are computed from the following particular form of Equation (154) from Reference [6]:

$$\frac{\partial L(\alpha)}{\partial q_j} = \sum_{g=1}^G \int_V dV \int_{4\pi} d\Omega \psi^{(1),g}(r, \Omega) \frac{\partial Q^g(\mathbf{q}; r, \Omega)}{\partial q_j}, \quad j = 1, \dots, J_q. \tag{8}$$

The multigroup adjoint fluxes $\psi^{(1),g}(r, \Omega)$, $g = 1, \dots, G$ appearing in Equation (8) are the solutions of the following 1st-Level Adjoint Sensitivity System (1st-LASS) presented in Equations (156) and (157) of [6]:

$$A^{(1),g}(\alpha) \psi^{(1),g}(r, \Omega) = \Omega \cdot \mathbf{n} \delta(r - r_d), \quad g = 1, \dots, G, \tag{9}$$

$$\psi^{(1),g}(r_d, \Omega) = 0, \Omega \cdot \mathbf{n} > 0, \quad g = 1, \dots, G, \tag{10}$$

where the adjoint operator $A^{(1),g}(\alpha)$ takes on the following particular form of Equation (149) from Reference [6]:

$$\begin{aligned} &A^{(1),g}(\alpha) \psi^{(1),g}(r, \Omega) \\ &\triangleq -\Omega \cdot \nabla \psi^{(1),g}(r, \Omega) + \Sigma_t^g(\mathbf{t}) \psi^{(1),g}(r, \Omega) - \sum_{g'=1}^G \int_{4\pi} d\Omega' \Sigma_s^{g \rightarrow g'}(\mathbf{s}; \Omega \rightarrow \Omega') \psi^{(1),g'}(r, \Omega') \\ &- \nu \Sigma_f^g(\mathbf{f}) \sum_{g'=1}^G \int_{4\pi} d\Omega' \chi^{g'} \psi^{(1),g'}(r, \Omega'), \quad g = 1, \dots, G. \end{aligned} \tag{11}$$

Performing the integration over the energy interval in Equation (4) yields the following expression for the PERP benchmark’s spontaneous fission source:

$$Q^g = Q_{SF}^g = \sum_{i=1}^{N_f} Q_{SF,i}^g \tag{12}$$

with:

$$Q_{SF,i}^g = \lambda_i N_{i,1} F_i^{SF} \nu_i^{SF} \left[\frac{\text{erf}(c_2) - \text{erf}(c_1) + \text{erf}(c_4) - \text{erf}(c_3)}{2} + \frac{e^{-(c_1)^2} - e^{-(c_2)^2} - e^{-(c_3)^2} + e^{-(c_4)^2}}{\sqrt{\pi a_i b_i}} \right], \tag{13}$$

where:

$$c_1 = \left(\sqrt{E^{g+1}} - \sqrt{a_i^2 b_i / 4} \right) / \sqrt{a_i}, \tag{14}$$

$$c_2 = \left(\sqrt{E^g} - \sqrt{a_i^2 b_i / 4} \right) / \sqrt{a_i}, \tag{15}$$

$$c_3 = \left(\sqrt{E^{g+1}} + \sqrt{a_i^2 b_i / 4} \right) / \sqrt{a_i}, \tag{16}$$

$$c_4 = \left(\sqrt{E^g} + \sqrt{a_i^2 b_i / 4} \right) / \sqrt{a_i}. \tag{17}$$

The first-order derivatives of the spontaneous fission source with respect to the parameters $q_{j=1} \equiv \lambda_{i=1}$ and $q_{j=2} \equiv \lambda_{i=2}$ are as follows:

$$\frac{\partial Q^g(\mathbf{q}; r, \Omega)}{\partial q_j} = \frac{\partial Q_{SF}^g}{\partial \lambda_i} = N_{i,1} F_i^{SF} v_i^{SF} \frac{1}{I_0} \int_{E^g+1}^{E^g} dE e^{-E/a_i} \sinh \sqrt{b_i E} = \frac{Q_{SF,i}^g}{\lambda_i}, \quad i, j = 1, 2. \quad (18)$$

The first-order derivatives of the spontaneous fission source with respect to the parameters $q_{j=3} \equiv F_{i=1}^{SF}$ and $q_{j=4} \equiv F_{i=2}^{SF}$ are as follows:

$$\frac{\partial Q^g(\mathbf{q}; r, \Omega)}{\partial q_j} = \frac{\partial Q_{SF}^g}{\partial F_i^{SF}} = \frac{Q_{SF,i}^g}{F_i^{SF}}, \quad j = 3, 4; i = 1, 2. \quad (19)$$

The first-order derivatives of the spontaneous fission source with respect to the parameters $q_{j=5} \equiv a_{i=1}$ and $q_{j=6} \equiv a_{i=2}$ are as follows:

$$\frac{\partial Q^g(\mathbf{q}; r, \Omega)}{\partial q_j} = \frac{\partial Q_{SF}^g}{\partial a_i} = \frac{\partial \left(\sum_{m=1}^M \sum_{k=1}^I Q_{SF,k}^g \right)}{\partial a_i} = \lambda_i N_{i,1} F_i^{SF} v_i^{SF} Da(g; a_i, b_i), \quad j = 5, 6; i = 1, 2, \quad (20)$$

where:

$$Da(g; a_i, b_i) = \frac{1}{2a_i \sqrt{\pi}} \left[c_3 e^{-c_1^2} - c_4 e^{-c_2^2} + c_1 e^{-c_3^2} - c_2 e^{-c_4^2} \right] + \frac{1}{2a_i \sqrt{\pi a_i b_i}} \left[(1 - 2c_1 c_3) (e^{-c_3^2} - e^{-c_1^2}) + (1 - 2c_2 c_4) (e^{-c_2^2} - e^{-c_4^2}) \right]. \quad (21)$$

The first-order derivatives of the spontaneous fission source with respect to the parameters $q_{j=7} \equiv b_{i=1}$ and $q_{j=8} \equiv b_{i=2}$ are as follows:

$$\frac{\partial Q^g(\mathbf{q}; r, \Omega)}{\partial q_j} = \frac{\partial Q_{SF}^g}{\partial b_i} = \frac{\partial \left(\sum_{m=1}^M \sum_{k=1}^I Q_{SF,k}^g \right)}{\partial b_i} = \lambda_i N_{i,1} F_i^{SF} v_i^{SF} Db(g; a_i, b_i), \quad j = 7, 8; i = 1, 2, \quad (22)$$

where:

$$Db(g; a_i, b_i) = \frac{\sqrt{a_i}}{4 \sqrt{\pi b_i}} \left[e^{-c_1^2} - e^{-c_2^2} + e^{-c_4^2} - e^{-c_3^2} \right] + \frac{1}{2b_i \sqrt{\pi a_i b_i}} \left[(e^{-c_2^2} - e^{-c_1^2} + e^{-c_3^2} - e^{-c_4^2}) + \sqrt{a_i b_i} (c_1 e^{-c_1^2} - c_2 e^{-c_2^2} + c_3 e^{-c_3^2} - c_4 e^{-c_4^2}) \right]. \quad (23)$$

The first-order derivatives of the spontaneous fission source with respect to the parameters $q_{j=9} \equiv v_{i=1}^{SF}$ and $q_{j=10} \equiv v_{i=2}^{SF}$ are as follows:

$$\begin{aligned} \frac{\partial Q^g(\mathbf{q}; r, \Omega)}{\partial q_j} &= \frac{\partial Q_{SF}^g}{\partial v_i^{SF}} = \frac{\partial \left(\sum_{m=1}^M \sum_{k=1}^I \lambda_k N_{k,m} F_k^{SF} v_k^{SF} \frac{1}{I_0} \int_{E^g+1}^{E^g} dE e^{-E/a_k} \sinh \sqrt{b_k E} \right)}{\partial v_i^{SF}} \\ &= \lambda_i N_{i,1} F_i^{SF} \frac{1}{I_0} \int_{E^g+1}^{E^g} dE e^{-E/a_i} \sinh \sqrt{b_i E} = \frac{Q_{SF,i}^g}{v_i^{SF}}, \quad j = 9, 10; i = 1, 2. \end{aligned} \quad (24)$$

The first-order derivatives of the spontaneous fission source with respect to the parameters $q_{j=11} \equiv N_{1,1}$ and $q_{j=12} \equiv N_{2,1}$ are as follows:

$$\begin{aligned} \frac{\partial Q^g(\mathbf{q}; r, \Omega)}{\partial q_j} &= \frac{\partial Q_{SF}^g}{\partial N_{i,1}} = \frac{\partial \left(\sum_{m=1}^M \sum_{k=1}^I \lambda_k N_{k,m} F_k^{SF} v_k^{SF} \frac{1}{I_0} \int_{E^g+1}^{E^g} dE e^{-E/a_k} \sinh \sqrt{b_k E} \right)}{\partial N_{i,1}} = \frac{Q_{SF,i}^g}{N_{i,1}}, \\ j &= 11, 12; i = 1, 2. \end{aligned} \quad (25)$$

Inserting the expressions obtained in Equations (18)–(25) into Equation (8) yields the following expressions for the 1st-order sensitivities of the leakage response with respect to the source parameters:

$$\text{For } j = 1, 2 : \frac{\partial L(\boldsymbol{\alpha})}{\partial q_j} \triangleq \frac{\partial L(\boldsymbol{\alpha})}{\partial \lambda_i} = \frac{1}{\lambda_i} \sum_{g=1}^G \int_V dV \xi_0^{(1),g}(r) Q_{SF,i'}^g \quad i = 1, 2; \tag{26}$$

$$\text{For } j = 3, 4 : \frac{\partial L(\boldsymbol{\alpha})}{\partial q_j} \triangleq \frac{\partial L(\boldsymbol{\alpha})}{\partial F_i^{SF}} = \frac{1}{F_i^{SF}} \sum_{g=1}^G \int_V dV \xi_0^{(1),g}(r) Q_{SF,i'}^g \quad i = 1, 2; \tag{27}$$

$$\text{For } j = 5, 6 : \frac{\partial L(\boldsymbol{\alpha})}{\partial q_j} \triangleq \frac{\partial L(\boldsymbol{\alpha})}{\partial a_i} = \lambda_i N_{i,1} F_i^{SF} v_i^{SF} \sum_{g=1}^G \int_V dV \xi_0^{(1),g}(r) Da(g; a_i, b_i), \quad i = 1, 2; \tag{28}$$

$$\text{For } j = 7, 8 : \frac{\partial L(\boldsymbol{\alpha})}{\partial q_j} \triangleq \frac{\partial L(\boldsymbol{\alpha})}{\partial b_i} = \lambda_i N_{i,1} F_i^{SF} v_i^{SF} \sum_{g=1}^G \int_V dV \xi_0^{(1),g}(r) Db(g; a_i, b_i), \quad i = 1, 2; \tag{29}$$

$$\text{For } j = 9, 10 : \frac{\partial L(\boldsymbol{\alpha})}{\partial q_j} \triangleq \frac{\partial L(\boldsymbol{\alpha})}{\partial v_i^{SF}} = \frac{1}{v_i^{SF}} \sum_{g=1}^G \int_V dV \xi_0^{(1),g}(r) Q_{SF,i'}^g \quad i = 1, 2; \tag{30}$$

$$\text{For } j = 11, 12 : \frac{\partial L(\boldsymbol{\alpha})}{\partial q_j} \triangleq \frac{\partial L(\boldsymbol{\alpha}; Q_{SF}^g)}{\partial N_{i,1}} = \frac{1}{N_{i,1}} \sum_{g=1}^G \int_V dV \xi_0^{(1),g}(r) Q_{SF,i'}^g \quad i = 1, 2, \tag{31}$$

where:

$$\xi_0^{(1),g}(r) \triangleq \int_{4\pi} d\boldsymbol{\Omega} \psi^{(1),g}(r, \boldsymbol{\Omega}). \tag{32}$$

The 1st-order absolute sensitivities of the PERP’s leakage response with respect to the source parameters for the PERP benchmark are computed using Equations (26)–(31). It is important to note that the parameters $q_{j=1} \equiv \lambda_{i=1}$, $q_{j=2} \equiv \lambda_{i=2}$, $q_{j=3} \equiv F_{i=1}^{SF}$, $q_{j=4} \equiv F_{i=2}^{SF}$, $q_{j=5} \equiv a_{i=1}$, $q_{j=6} \equiv a_{i=2}$, $q_{j=7} \equiv b_{i=1}$, $q_{j=8} \equiv b_{i=2}$, $q_{j=9} \equiv v_{i=1}^{SF}$ and $q_{j=10} \equiv v_{i=2}^{SF}$ appear solely in the expression of the spontaneous fission source, Q_{SF}^g , for the PERP benchmark. Therefore, the expressions provided in Equations (26)–(30) represent the total 1st-order sensitivities of the leakage response with respect to these parameters. In contradistinction, however, the isotopic densities $N_{1,1}$ and $N_{2,1}$ appear not only in the expression of the PERP’s source Q_{SF}^g , but also appear as parameters in the definitions of the various macroscopic cross sections that enter as coefficients of the various terms in the definition of the forward and adjoint Boltzmann operator (i.e., on the left side of the various forward and adjoint transport equations). Therefore, the expression shown on the right-most side of Equation (31) represents the partial 1st-order sensitivity of the PERP’s leakage response with respect to the isotopic densities $N_{1,1}$ and $N_{2,1}$ appearing solely in the source Q_{SF}^g . This fact has been emphasized by using the notation $\partial L(\boldsymbol{\alpha}; Q_{SF}^g)$ in Equation (31).

The sensitivities obtained in Equations (26)–(31) are absolute, as opposed to relative sensitivities, which makes it difficult to rank the importance of these sensitivities in affecting to the PERP’s leakage response. Therefore, to facilitate the direct comparison of the importance ranking of the sensitivities obtained in Equations (26)–(31), the numerical results for these sensitivities will be presented in unit-less values of the respective *relative* sensitivities, which are denoted as $S^{(1)}(q_j)$ and are defined as follows:

$$S^{(1)}(q_j) = \left(\partial L / \partial q_j \right) (q_j / L), \quad j = 1, \dots, J_q. \tag{33}$$

Applying Equation (33) to Equations (26), (27), (30) and (31), yields the same expression for the 1st-order relative sensitivities for $S^{(1)}(\lambda_i)$, $S^{(1)}(F_i^{SF})$, $S^{(1)}(v_i^{SF})$ and $S^{(1)}(N_{i,1})$ for $i = 1, 2$, namely:

$$S^{(1)}(\lambda_i) = S^{(1)}(F_i^{SF}) = S^{(1)}(v_i^{SF}) = S^{(1)}(N_{i,1}) = \frac{1}{L} \sum_{g=1}^G \int_V dV \xi_0^{(1),g}(r) Q_{SF,i}^g \quad i = 1, 2, \quad (34)$$

which means that these sensitivities will all have the same relative values, although their absolute values differ from each other.

The numerical values of the 1st-order relative sensitivities of the PERP leakage response with respect to the source parameters are presented in Tables 4 and 5, below. All the values obtained for the 1st-order sensitivities, as shown in Tables 4 and 5, have been independently verified with the results calculated from the central-difference estimates obtained by repeated forward PARTISN computations, in which the source parameters were individually perturbed by a small amount. These verifications showed good agreements between the sensitivities computed using the 1st-LASS and the corresponding ones computed using central-difference methods.

Table 4. First-order relative sensitivities $S^{(1)}(q_j)$ for isotope ^{239}Pu .

	$S^{(1)}(\lambda_1)$	$S^{(1)}(F_1^{SF})$	$S^{(1)}(a_1)$	$S^{(1)}(b_1)$	$S^{(1)}(v_1^{SF})$	$S^{(1)}(N_{1,1})$
values	2.252×10^{-4}	2.252×10^{-4}	1.119×10^{-5}	2.801×10^{-6}	2.252×10^{-4}	2.252×10^{-4}

Table 5. First-order relative sensitivities $S^{(1)}(q_j)$ for isotope ^{240}Pu .

	$S^{(1)}(\lambda_2)$	$S^{(1)}(F_2^{SF})$	$S^{(1)}(a_2)$	$S^{(1)}(b_2)$	$S^{(1)}(v_2^{SF})$	$S^{(1)}(N_{2,1})$
values	9.998×10^{-1}	9.998×10^{-1}	4.372×10^{-2}	1.165×10^{-2}	9.998×10^{-1}	9.998×10^{-1}

The results shown in Table 4 indicate that the 1st-order relative sensitivities with respect to the source parameters of isotope ^{239}Pu are very small, in the order of 10^{-4} or less. However, as shown in Table 5, the 1st-order relative sensitivities with respect to the source parameters λ_2 , F_2^{SF} , v_2^{SF} , and $N_{2,1}$ of isotope ^{240}Pu are quite large, with values close to 1.0. Also, it can be seen that the leakage response is less sensitive to spectrum effects (i.e., to parameters a and b of the normalized Watt’s spectrum) than to the parameters affecting the magnitudes of the respective sources. Moreover, the 1st-order relative sensitivities with respect to the Watt’s coefficients a_2 and b_2 of isotope ^{240}Pu are also much larger than the ones with respect to the Watt’s coefficients a_1 and b_1 of isotope ^{239}Pu .

As indicated in Table 4, the 1st-order sensitivities of the leakage response with respect to the source parameters of isotope ^{239}Pu (i.e., λ_1 , F_1^{SF} , v_1^{SF} , a_1 , b_1 and $N_{1,1}$) are all negligibly small by comparison to the corresponding results shown in Table 5 for ^{240}Pu .

2.2. Second-Order Sensitivities $\partial^2 L(\alpha) / \partial q \partial q$

The equations needed for deriving the expression of the 2nd-order sensitivities $\partial^2 L(\alpha) / \partial q \partial q$ are obtained by particularizing Equation (208) from Reference [6] to the PERP benchmark, which yields:

$$\frac{\partial^2 L(\alpha)}{\partial q_j \partial q_{m_2}} = \sum_{g=1}^G \int_V dV \int_{4\pi} d\Omega \psi^{(1),g}(r, \Omega) \frac{\partial Q^g(\mathbf{q}; r, \Omega)}{\partial q_j \partial q_{m_2}}, \quad j = 1, \dots, J_q; \quad m_2 = 1, \dots, J_q. \quad (35)$$

Computing the unmixed 2nd-order derivatives of the spontaneous fission source with respect to λ_i , F_i^{SF} , v_i^{SF} and $N_{i,1}$ shows that they vanish, i.e.,

$$\frac{\partial Q^g(\mathbf{q}; r, \Omega)}{\partial \lambda_i \partial \lambda_i} = \frac{\partial Q^g(\mathbf{q}; r, \Omega)}{\partial F_i^{SF} \partial F_i^{SF}} = \frac{\partial Q^g(\mathbf{q}; r, \Omega)}{\partial v_i^{SF} \partial v_i^{SF}} = \frac{\partial Q^g(\mathbf{q}; r, \Omega)}{\partial N_{i,1} \partial N_{i,1}} = 0, \quad \text{for } i = 1, 2. \quad (36)$$

The mixed 2nd-order derivatives with respect to the source parameters that do not belong to the same isotope also vanish, i.e.,

$$\frac{\partial Q^g(\mathbf{q}; r, \Omega)}{\partial q_j \partial q_{m_2}} = 0, \text{ if } i_j \neq i_{m_2}, \quad (37)$$

where i_j and i_{m_2} denote the isotope associated with the source parameters q_j and q_{m_2} , respectively.

The expressions of the five non-zero 2nd-order derivatives of the spontaneous fission source with respect to $q_{j=1,2} \equiv \lambda_i$ and other source parameters are provided in Equations (38) through (42), below:

$$\frac{\partial Q^g(\mathbf{q}; r, \Omega)}{\partial \lambda_i \partial F_i^{SF}} = \frac{\partial(\partial Q_{SF}^g / \partial \lambda_i)}{\partial F_i^{SF}} = \frac{\partial\left(N_{i,1} F_i^{SF} v_i^{SF} \frac{1}{I_0} \int_{E_{S+1}}^{E_S} dE e^{-E/a_i} \sinh \sqrt{b_i E}\right)}{\partial F_i^{SF}} = \frac{Q_{SF,i}^g}{\lambda_i F_i^{SF}}, \quad i = 1, 2; \quad (38)$$

$$\frac{\partial Q^g(\mathbf{q}; r, \Omega)}{\partial \lambda_i \partial a_i} = \frac{\partial(\partial Q_{SF}^g / \partial a_i)}{\partial \lambda_i} = \frac{\partial\left[\lambda_i N_{i,1} F_i^{SF} v_i^{SF} Da(g; a_i, b_i)\right]}{\partial \lambda_i} = N_{i,1} F_i^{SF} v_i^{SF} Da(g; a_i, b_i), \quad i = 1, 2; \quad (39)$$

$$\frac{\partial Q^g(\mathbf{q}; r, \Omega)}{\partial \lambda_i \partial b_i} = \frac{\partial(\partial Q_{SF}^g / \partial b_i)}{\partial \lambda_i} = \frac{\partial\left[\lambda_i N_{i,1} F_i^{SF} v_i^{SF} Db(g; a_i, b_i)\right]}{\partial \lambda_i} = N_{i,1} F_i^{SF} v_i^{SF} Db(g; a_i, b_i), \quad i = 1, 2; \quad (40)$$

$$\frac{\partial Q^g(\mathbf{q}; r, \Omega)}{\partial \lambda_i \partial v_i^{SF}} = \frac{\partial(\partial Q_{SF}^g / \partial v_i^{SF})}{\partial v_i^{SF}} = \frac{\partial\left(N_{i,1} F_i^{SF} v_i^{SF} \frac{1}{I_0} \int_{E_{S+1}}^{E_S} dE e^{-E/a_i} \sinh \sqrt{b_i E}\right)}{\partial v_i^{SF}} = \frac{Q_{SF,i}^g}{\lambda_i v_i^{SF}}, \quad i = 1, 2; \quad (41)$$

$$\frac{\partial Q^g(\mathbf{q}; r, \Omega)}{\partial \lambda_i \partial N_{i,1}} = \frac{\partial(\partial Q_{SF}^g / \partial \lambda_i)}{\partial N_{i,1}} = \frac{\partial\left(N_{i,1} F_i^{SF} v_i^{SF} \frac{1}{I_0} \int_{E_{S+1}}^{E_S} dE e^{-E/a_i} \sinh \sqrt{b_i E}\right)}{\partial N_{i,1}} = \frac{Q_{SF,i}^g}{\lambda_i N_{i,1}}, \quad i = 1, 2. \quad (42)$$

The expressions of the four non-zero 2nd-order derivatives of the spontaneous fission source with respect to $q_{j=3,4} \equiv F_i^{SF}$ and other source parameters are given in Equations (43) through (46), below:

$$\frac{\partial Q^g(\mathbf{q}; r, \Omega)}{\partial F_i^{SF} \partial a_i} = \frac{\partial(\partial Q_{SF}^g / \partial a_i)}{\partial F_i^{SF}} = \frac{\partial\left[\lambda_i N_{i,1} F_i^{SF} v_i^{SF} Da(g; a_i, b_i)\right]}{\partial F_i^{SF}} = \lambda_i N_{i,1} v_i^{SF} Da(g; a_i, b_i), \quad i = 1, 2; \quad (43)$$

$$\frac{\partial Q^g(\mathbf{q}; r, \Omega)}{\partial F_i^{SF} \partial b_i} = \frac{\partial(\partial Q_{SF}^g / \partial b_i)}{\partial F_i^{SF}} = \frac{\partial\left[\lambda_i N_{i,1} F_i^{SF} v_i^{SF} Db(g; a_i, b_i)\right]}{\partial F_i^{SF}} = \lambda_i N_{i,1} v_i^{SF} Db(g; a_i, b_i), \quad i = 1, 2; \quad (44)$$

$$\frac{\partial Q^g(\mathbf{q}; r, \Omega)}{\partial F_i^{SF} \partial v_i^{SF}} = \frac{\partial(\partial Q_{SF}^g / \partial v_i^{SF})}{\partial v_i^{SF}} = \frac{\partial\left(\lambda_i N_{i,1} v_i^{SF} \frac{1}{I_0} \int_{E_{S+1}}^{E_S} dE e^{-E/a_i} \sinh \sqrt{b_i E}\right)}{\partial v_i^{SF}} = \frac{Q_{SF,i}^g}{F_i^{SF} v_i^{SF}}, \quad i = 1, 2; \quad (45)$$

$$\frac{\partial Q^g(\mathbf{q}; r, \Omega)}{\partial F_i^{SF} \partial N_{i,1}} = \frac{\partial(\partial Q_{SF}^g / \partial F_i^{SF})}{\partial N_{i,1}} = \frac{\partial\left(\lambda_i N_{i,1} v_i^{SF} \frac{1}{I_0} \int_{E_{S+1}}^{E_S} dE e^{-E/a_i} \sinh \sqrt{b_i E}\right)}{\partial N_{i,1}} = \frac{Q_{SF,i}^g}{F_i^{SF} N_{i,1}}, \quad i = 1, 2. \quad (46)$$

The expressions of the four non-zero 2nd-order derivatives of the spontaneous fission source with respect to $q_{j=5,6} \equiv a_i$ and other source parameters are provided in Equations (47), (49), (51) and (52), below:

$$\frac{\partial Q^g(\mathbf{q}; r, \Omega)}{\partial a_i \partial a_i} = \frac{\partial(\partial Q_{SF}^g / \partial a_i)}{\partial a_i} = \frac{\partial\left[\lambda_i N_{i,1} F_i^{SF} v_i^{SF} Da(g; a_i, b_i)\right]}{\partial a_i} = \lambda_i N_{i,1} F_i^{SF} v_i^{SF} Da2(g; a_i, b_i), \quad i = 1, 2, \quad (47)$$

where:

$$Da2(g; a_i, b_i) = \lambda_i N_{i,1} F_i^{SF} v_i^{SF} \left\{ \begin{aligned} & \frac{1}{4a_i^2 \sqrt{\pi}} \left[e^{-c_1^2} (2c_1c_3^2 - 2c_3 - c_1) + e^{-c_2^2} (2c_4 + c_2 - 2c_2c_4^2) \right] \\ & + e^{-c_3^2} (2c_3c_1^2 - 2c_1 - c_3) + e^{-c_4^2} (2c_2 + c_4 - 2c_4c_2^2) \\ & + \frac{1}{4a_i^2 \sqrt{\pi a_i b_i}} \left[(2c_3^2 + 2c_1^2 + 8c_1c_3 - 4c_1^2c_3^2 - 3)(e^{-c_3^2} - e^{-c_1^2}) \right] \\ & + (2c_4^2 + 2c_2^2 + 8c_2c_4 - 4c_2^2c_4^2 - 3)(e^{-c_2^2} - e^{-c_4^2}) \end{aligned} \right\}; \quad (48)$$

$$\frac{\partial Q^g(\mathbf{q}; r, \Omega)}{\partial a_i \partial b_i} = \frac{\partial(\partial Q_{SF}^g / \partial a_i)}{\partial b_i} = \frac{\partial[\lambda_i N_{i,1} F_i^{SF} v_i^{SF} Da(g; a_i, b_i)]}{\partial b_i} = \lambda_i N_{i,1} F_i^{SF} v_i^{SF} Dab(g; a_i, b_i), \quad i = 1, 2, \quad (49)$$

where:

$$Dab(g; a_i, b_i) = \lambda_i N_{i,1} F_i^{SF} v_i^{SF} \left\{ \begin{aligned} & \frac{1}{8\sqrt{\pi a_i b_i}} \left[(e^{-c_1^2} - e^{-c_3^2})(1 + 2c_1c_3) + (e^{-c_4^2} - e^{-c_2^2})(1 + 2c_2c_4) \right] \\ & - \frac{1}{4a_i b_i \sqrt{\pi a_i b_i}} \left[(1 - 2c_1c_3)(e^{-c_3^2} - e^{-c_1^2}) + (1 - 2c_2c_4)(e^{-c_2^2} - e^{-c_4^2}) \right] \\ & + \frac{1}{4a_i b_i \sqrt{\pi}} \left[(2c_1c_3^2 - c_1)e^{-c_3^2} + (2c_1^2c_3 - c_3)e^{-c_1^2} \right] \\ & + (c_4 - 2c_2^2c_4)e^{-c_2^2} + (c_2 - 2c_2c_4^2)e^{-c_4^2} \end{aligned} \right\}; \quad (50)$$

$$\frac{\partial Q^g(\mathbf{q}; r, \Omega)}{\partial a_i \partial v_i^{SF}} = \frac{\partial(\partial Q_{SF}^g / \partial a_i)}{\partial v_i^{SF}} = \frac{\partial[\lambda_i N_{i,1} F_i^{SF} v_i^{SF} Da(g; a_i, b_i)]}{\partial v_i^{SF}} = \lambda_i N_{i,1} F_i^{SF} Da(g; a_i, b_i), \quad i = 1, 2; \quad (51)$$

$$\frac{\partial Q^g(\mathbf{q}; r, \Omega)}{\partial a_i \partial N_{i,1}} = \frac{\partial(\partial Q_{SF}^g / \partial a_i)}{\partial N_{i,1}} = \frac{\partial[\lambda_i N_{i,1} F_i^{SF} v_i^{SF} Da(g; a_i, b_i)]}{\partial N_{i,1}} = \lambda_i F_i^{SF} v_i^{SF} Da(g; a_i, b_i), \quad i = 1, 2. \quad (52)$$

The three 2nd-order derivatives of the spontaneous fission source with respect to $q_{j=7,8} \equiv b_i$ and other source parameters are provided in Equations (53), (55) and (56), below:

$$\frac{\partial Q^g(\mathbf{q}; r, \Omega)}{\partial b_i \partial b_i} = \frac{\partial(\partial Q_{SF}^g / \partial b_i)}{\partial b_i} = \frac{\partial[\lambda_i N_{i,1} F_i^{SF} v_i^{SF} Db(g; a_i, b_i)]}{\partial b_i} = \lambda_i N_{i,1} F_i^{SF} v_i^{SF} Db2(g; a_i, b_i), \quad i = 1, 2, \quad (53)$$

where:

$$Db2(g; a_i, b_i) = \lambda_i N_{i,1} F_i^{SF} v_i^{SF} \left\{ \begin{aligned} & \left(\frac{3 - a_i b_i}{4b_i^2 \sqrt{\pi a_i b_i}} \right) (e^{-c_1^2} - e^{-c_2^2} + e^{-c_4^2} - e^{-c_3^2}) \\ & + \left(\frac{a_i b_i - 6}{8b_i^2 \sqrt{\pi}} \right) (c_1 e^{-c_1^2} - c_2 e^{-c_2^2} - c_4 e^{-c_4^2} + c_3 e^{-c_3^2}) \\ & + \frac{\sqrt{a_i}}{4b_i \sqrt{\pi b_i}} (c_1^2 e^{-c_1^2} - c_2^2 e^{-c_2^2} - c_3^2 e^{-c_3^2} + c_4^2 e^{-c_4^2}) \end{aligned} \right\}; \quad (54)$$

$$\frac{\partial Q^g(\mathbf{q}; r, \Omega)}{\partial b_i \partial v_i^{SF}} = \frac{\partial(\partial Q_{SF}^g / \partial b_i)}{\partial v_i^{SF}} = \frac{\partial[\lambda_i N_{i,1} F_i^{SF} v_i^{SF} Db(g; a_i, b_i)]}{\partial v_i^{SF}} = \lambda_i N_{i,1} F_i^{SF} Db(g; a_i, b_i), \quad i = 1, 2; \quad (55)$$

$$\frac{\partial Q^g(\mathbf{q}; r, \Omega)}{\partial b_i \partial N_{i,1}} = \frac{\partial(\partial Q_{SF}^g / \partial b_i)}{\partial N_{i,1}} = \frac{\partial[\lambda_i N_{i,1} F_i^{SF} v_i^{SF} Db(g; a_i, b_i)]}{\partial N_{i,1}} = \lambda_i F_i^{SF} v_i^{SF} Db(g; a_i, b_i), \quad i = 1, 2. \quad (56)$$

The 2nd-order derivatives of the spontaneous fission source with respect to $q_{j=9,10} \equiv v_i^{SF}$ and $q_{j=11,12} \equiv N_{i,1}$ are as follows:

$$\frac{\partial Q^g(\mathbf{q}; r, \Omega)}{\partial v_i^{SF} \partial N_{i,1}} = \frac{\partial(\partial Q_{SF}^g / \partial v_i^{SF})}{\partial N_{i,1}} = \frac{\partial[\lambda_i N_{i,1} F_i^{SF} \frac{1}{I_0} \int_{E_8+1}^{E_8} dE e^{-E/a_i} \sinh \sqrt{b_i E}]}{\partial N_{i,1}} = \frac{Q_{SF,i}^g}{v_i^{SF} N_{i,1}}, \quad i = 1, 2. \quad (57)$$

Inserting the 2nd-order derivatives obtained in Equations (38)–(57) into Equation (35), yields the following expressions for the 2nd-order sensitivities of the leakage response with respect to the source parameters:

For $j = 1, m_2 = 3$ or $j = 2, m_2 = 4$:

$$\frac{\partial^2 L(\alpha)}{\partial q_j \partial q_{m_2}} = \frac{\partial^2 L(\alpha)}{\partial \lambda_i \partial F_i^{SF}} = \frac{1}{\lambda_i F_i^{SF}} \sum_{g=1}^G \int_V dV \xi_0^{(1),g}(r) Q_{SF,i'}^g, \quad i = 1, 2; \quad (58)$$

For $j = 1, m_2 = 5$ or $j = 2, m_2 = 6$:

$$\frac{\partial^2 L(\alpha)}{\partial q_j \partial q_{m_2}} = \frac{\partial^2 L(\alpha)}{\partial \lambda_i \partial a_i} = N_{i,1} F_i^{SF} v_i^{SF} \sum_{g=1}^G \int_V dV \xi_0^{(1),g}(r) Da(g; a_i, b_i), \quad i = 1, 2; \quad (59)$$

For $j = 1, m_2 = 7$ or $j = 2, m_2 = 8$:

$$\frac{\partial^2 L(\alpha)}{\partial q_j \partial q_{m_2}} = \frac{\partial^2 L(\alpha)}{\partial \lambda_i \partial b_i} = N_{i,1} F_i^{SF} v_i^{SF} \sum_{g=1}^G \int_V dV \xi_0^{(1),g}(r) Db(g; a_i, b_i), \quad i = 1, 2; \quad (60)$$

For $j = 1, m_2 = 9$ or $j = 2, m_2 = 10$:

$$\frac{\partial^2 L(\alpha)}{\partial q_j \partial q_{m_2}} = \frac{\partial^2 L(\alpha)}{\partial \lambda_i \partial v_i^{SF}} = \frac{1}{\lambda_i v_i^{SF}} \sum_{g=1}^G \int_V dV \xi_0^{(1),g}(r) Q_{SF,i'}^g, \quad i = 1, 2; \quad (61)$$

For $j = 1, m_2 = 11$ or $j = 2, m_2 = 12$:

$$\frac{\partial^2 L(\alpha)}{\partial q_j \partial q_{m_2}} = \frac{\partial^2 L(\alpha; Q_{SF}^g)}{\partial \lambda_i \partial N_{i,1}} = \frac{1}{\lambda_i N_{i,1}} \sum_{g=1}^G \int_V dV \xi_0^{(1),g}(r) Q_{SF,i'}^g, \quad i = 1, 2; \quad (62)$$

For $j = 3, m_2 = 5$ or $j = 4, m_2 = 6$:

$$\frac{\partial^2 L(\alpha)}{\partial q_j \partial q_{m_2}} = \frac{\partial^2 L(\alpha)}{\partial F_i^{SF} \partial a_i} = \lambda_i N_{i,1} v_i^{SF} \sum_{g=1}^G \int_V dV \xi_0^{(1),g}(r) Da(g; a_i, b_i), \quad i = 1, 2; \quad (63)$$

For $j = 3, m_2 = 7$ or $j = 4, m_2 = 8$:

$$\frac{\partial^2 L(\alpha)}{\partial q_j \partial q_{m_2}} = \frac{\partial^2 L(\alpha)}{\partial F_i^{SF} \partial b_i} = \lambda_i N_{i,1} v_i^{SF} \sum_{g=1}^G \int_V dV \xi_0^{(1),g}(r) Db(g; a_i, b_i), \quad i = 1, 2; \quad (64)$$

For $j = 3, m_2 = 9$ or $j = 4, m_2 = 10$:

$$\frac{\partial^2 L(\alpha)}{\partial q_j \partial q_{m_2}} = \frac{\partial^2 L(\alpha)}{\partial F_i^{SF} \partial v_i^{SF}} = \frac{1}{F_i^{SF} v_i^{SF}} \sum_{g=1}^G \int_V dV \xi_0^{(1),g}(r) Q_{SF,i'}^g, \quad i = 1, 2; \quad (65)$$

For $j = 3, m_2 = 11$ or $j = 4, m_2 = 12$:

$$\frac{\partial^2 L(\alpha)}{\partial q_j \partial q_{m_2}} = \frac{\partial^2 L(\alpha; Q_{SF}^g)}{\partial F_i^{SF} \partial N_{i,1}} = \frac{1}{F_i^{SF} N_{i,1}} \sum_{g=1}^G \int_V dV \xi_0^{(1),g}(r) Q_{SF,i'}^g, \quad i = 1, 2; \quad (66)$$

For $j = 5, m_2 = 5$ or $j = 6, m_2 = 6$:

$$\frac{\partial^2 L(\alpha)}{\partial q_j \partial q_{m_2}} = \frac{\partial^2 L(\alpha)}{\partial a_i \partial a_i} = \lambda_i N_{i,1} F_i^{SF} v_i^{SF} \sum_{g=1}^G \int_V dV \xi_0^{(1),g}(r) Da2(g; a_i, b_i), \quad i = 1, 2; \quad (67)$$

For $j = 5, m_2 = 7$ or $j = 6, m_2 = 8$:

$$\frac{\partial^2 L(\alpha)}{\partial q_j \partial q_{m_2}} = \frac{\partial^2 L(\alpha)}{\partial a_i \partial b_i} = \lambda_i N_{i,1} F_i^{SF} v_i^{SF} \sum_{g=1}^G \int_V dV \xi_0^{(1),g}(r) Dab(g; a_i, b_i), \quad i = 1, 2; \tag{68}$$

For $j = 5, m_2 = 9$ or $j = 6, m_2 = 10$:

$$\frac{\partial^2 L(\alpha)}{\partial q_j \partial q_{m_2}} = \frac{\partial^2 L(\alpha)}{\partial a_i \partial v_i^{SF}} = \lambda_i N_{i,1} F_i^{SF} \sum_{g=1}^G \int_V dV \xi_0^{(1),g}(r) Da(g; a_i, b_i), \quad i = 1, 2; \tag{69}$$

For $j = 5, m_2 = 11$ or $j = 6, m_2 = 12$:

$$\frac{\partial^2 L(\alpha)}{\partial q_j \partial q_{m_2}} = \frac{\partial^2 L(\alpha; Q_{SF}^g)}{\partial a_i \partial N_{i,1}} = \lambda_i F_i^{SF} v_i^{SF} \sum_{g=1}^G \int_V dV \xi_0^{(1),g}(r) Da(g; a_i, b_i), \quad i = 1, 2; \tag{70}$$

For $j = 7, m_2 = 7$ or $j = 8, m_2 = 8$:

$$\frac{\partial^2 L(\alpha)}{\partial q_j \partial q_{m_2}} = \frac{\partial^2 L(\alpha)}{\partial b_i \partial b_i} = \lambda_i N_{i,1} F_i^{SF} v_i^{SF} \sum_{g=1}^G \int_V dV \xi_0^{(1),g}(r) Db2(g; a_i, b_i), \quad i = 1, 2; \tag{71}$$

For $j = 7, m_2 = 9$ or $j = 8, m_2 = 10$:

$$\frac{\partial^2 L(\alpha)}{\partial q_j \partial q_{m_2}} = \frac{\partial^2 L(\alpha)}{\partial b_i \partial v_i^{SF}} = \lambda_i N_{i,1} F_i^{SF} \sum_{g=1}^G \int_V dV \xi_0^{(1),g}(r) Db(g; a_i, b_i), \quad i = 1, 2; \tag{72}$$

For $j = 7, m_2 = 11$ or $j = 8, m_2 = 12$:

$$\frac{\partial^2 L(\alpha)}{\partial q_j \partial q_{m_2}} = \frac{\partial^2 L(\alpha; Q_{SF}^g)}{\partial b_i \partial N_{i,1}} = \lambda_i F_i^{SF} v_i^{SF} \sum_{g=1}^G \int_V dV \xi_0^{(1),g}(r) Db(g; a_i, b_i), \quad i = 1, 2; \tag{73}$$

For $j = 9, m_2 = 11$ or $j = 10, m_2 = 12$:

$$\frac{\partial^2 L(\alpha)}{\partial q_j \partial q_{m_2}} = \frac{\partial^2 L(\alpha; Q_{SF}^g)}{\partial v_i^{SF} \partial N_{i,1}} = \frac{1}{v_i^{SF} N_{i,1}} \sum_{g=1}^G \int_V dV \xi_0^{(1),g}(r) Q_{SF,i}^g, \quad i = 1, 2. \tag{74}$$

The 2nd-order absolute sensitivities of the leakage response with respect to the source parameters for the PERP benchmark are computed using Equations (58)–(74). The corresponding relative sensitivities are defined as follows:

$$\mathbf{S}^{(2)}(q_j, q_{m_2}) = (\partial^2 L / \partial q_j \partial q_{m_2})(q_j q_{m_2} / L), \quad j, m_2 = 1, \dots, J_q. \tag{75}$$

It is noteworthy that the 2nd-order relative sensitivities for $S^{(2)}(\lambda_i, F_i^{SF})$, $S^{(2)}(\lambda_i, v_i^{SF})$, $S^{(2)}(\lambda_i, N_{i,1})$, $S^{(2)}(F_i^{SF}, v_i^{SF})$, $S^{(2)}(F_i^{SF}, N_{i,1})$, and $S^{(2)}(v_i^{SF}, N_{i,1})$ for $i = 1, 2$ all have the same expression, namely:

$$\begin{aligned} S^{(2)}(\lambda_i, F_i^{SF}) &= S^{(2)}(\lambda_i, v_i^{SF}) = S^{(2)}(\lambda_i, N_{i,1}) = S^{(2)}(F_i^{SF}, v_i^{SF}) = S^{(2)}(F_i^{SF}, N_{i,1}) = S^{(2)}(v_i^{SF}, N_{i,1}) \\ &= \frac{1}{L} \sum_{g=1}^G \int_V dV \xi_0^{(1),g}(r) Q_{SF,i}^g, \quad i = 1, 2. \end{aligned} \tag{76}$$

Furthermore, the right side of Equation (76) is the same as rightmost side of Equation (34). Hence, the respective mixed 2nd-order relative sensitivities have the same values as the 1st-order sensitivities of the leakage response with respect to the source parameters $\lambda_i, F_i^{SF}, v_i^{SF}$, and $N_{i,1}$, for $i = 1, 2$, namely,

$$S^{(2)}(\lambda_i, F_i^{SF}) = S^{(2)}(\lambda_i, v_i^{SF}) = S^{(2)}(\lambda_i, N_{i,1}) = S^{(2)}(F_i^{SF}, v_i^{SF}) = S^{(2)}(F_i^{SF}, N_{i,1}) = S^{(2)}(v_i^{SF}, N_{i,1}) = S^{(1)}(\lambda_i) = S^{(1)}(F_i^{SF}) = S^{(1)}(v_i^{SF}) = S^{(1)}(N_{i,1}) = \frac{1}{L} \sum_{g=1}^G \int_V dV \xi_0^{(1),g}(r) Q_{SF,i}^g, \quad i = 1, 2. \tag{77}$$

Similarly, the following relations hold for the 2nd-order sensitivities with respect to the Watt’s spectrum coefficients a_i and b_i :

$$S^{(2)}(\lambda_i, a_i) = S^{(2)}(F_i^{SF}, a_i) = S^{(2)}(a_i, v_i^{SF}) = S^{(2)}(a_i, N_{i,1}) = S^{(1)}(a_i) = \frac{\lambda_i N_{i,1} F_i^{SF} v_i^{SF} a_i}{L} \sum_{g=1}^G \int_V dV \xi_0^{(1),g}(r) Da(g; a_i, b_i), \quad i = 1, 2; \tag{78}$$

$$S^{(2)}(\lambda_i, b_i) = S^{(2)}(F_i^{SF}, b_i) = S^{(2)}(b_i, v_i^{SF}) = S^{(2)}(b_i, N_{i,1}) = S^{(1)}(b_i) = \frac{\lambda_i N_{i,1} F_i^{SF} v_i^{SF} b_i}{L} \sum_{g=1}^G \int_V dV \xi_0^{(1),g}(r) Db(g; a_i, b_i), \quad i = 1, 2. \tag{79}$$

The computations which were performed to obtain the numerical values of the corresponding 2nd-order sensitivities of the PERP leakage response with respect to the source parameters for ^{239}Pu have yielded results that are several orders of magnitude smaller than the corresponding 1st-order sensitivities shown in Table 4. Therefore, the 2nd-order sensitivities of the leakage response with respect to the source parameters for ^{239}Pu will not be presented in this work, since they are inconsequential for applications to uncertainty quantification and/or predictive modeling. Hence, the remainder of this work will present only the 2nd-order sensitivities of the leakage response with respect to the source parameters (i.e., $\lambda_2, F_2^{SF}, v_2^{SF}, a_2, b_2$ and $N_{2,1}$) for isotope ^{240}Pu .

The numerical results obtained for the 2nd-order relative sensitivities to the source parameters of isotope ^{240}Pu are presented in Table 6. Since the matrix $\mathbf{S}^{(2)}(q_j, q_{m_2}), j, m_2 = 1, \dots, J_q$, is symmetrical with respect to its main diagonal, only the results for the elements of the upper triangular segment of this matrix are shown in Table 6.

Table 6. 2nd-order relative sensitivities $\mathbf{S}^{(2)}(q_j, q_{m_2}), j, m_2 = 1, \dots, J_q$ of the leakage response with respect to the source parameters of isotope ^{240}Pu .

	λ_2	F_2^{SF}	a_2	b_2	v_2^{SF}	$N_{2,1}$
λ_2	$S^{(2)}(\lambda_2, \lambda_2) = 0$	$S^{(2)}(\lambda_2, F_2^{SF}) = 9.998 \times 10^{-1}$	$S^{(2)}(\lambda_2, a_2) = 4.373 \times 10^{-2}$	$S^{(2)}(\lambda_2, b_2) = 1.165 \times 10^{-2}$	$S^{(2)}(\lambda_2, v_2^{SF}) = 9.998 \times 10^{-1}$	$S^{(2)}(\lambda_2, N_{2,1}) = 9.998 \times 10^{-1}$
F_2^{SF}		$S^{(2)}(F_2^{SF}, F_2^{SF}) = 0$	$S^{(2)}(F_2^{SF}, a_2) = 4.373 \times 10^{-2}$	$S^{(2)}(F_2^{SF}, b_2) = 1.165 \times 10^{-2}$	$S^{(2)}(F_2^{SF}, v_2^{SF}) = 9.998 \times 10^{-1}$	$S^{(2)}(F_2^{SF}, N_{2,1}) = 9.998 \times 10^{-1}$
a_2			$S^{(2)}(a_2, a_2) = 6.594 \times 10^{-2}$	$S^{(2)}(a_2, b_2) = 3.179 \times 10^{-2}$	$S^{(2)}(a_2, v_2^{SF}) = 4.373 \times 10^{-2}$	$S^{(2)}(a_2, N_{2,1}) = 4.373 \times 10^{-2}$
b_2				$S^{(2)}(b_2, b_2) = 1.571 \times 10^{-3}$	$S^{(2)}(b_2, v_2^{SF}) = 1.165 \times 10^{-2}$	$S^{(2)}(b_2, N_{2,1}) = 1.165 \times 10^{-2}$
v_2^{SF}					$S^{(2)}(v_2^{SF}, v_2^{SF}) = 0$	$S^{(2)}(v_2^{SF}, N_{2,1}) = 9.998 \times 10^{-1}$
$N_{2,1}$						$S^{(2)}(N_{2,1}, N_{2,1}) = 0$

The results shown in Table 6 indicate that the 2nd-order relative sensitivities of the leakage response with respect to the source parameters are all positive. The unmixed 2nd-order sensitivities, i.e., the elements on the main diagonal in Table 6, are mostly zero, except for $S^{(2)}(a_2, a_2)$ and $S^{(2)}(b_2, b_2)$. The largest 2nd-order sensitivities are $S^{(2)}(\lambda_2, F_2^{SF}) = S^{(2)}(\lambda_2, v_2^{SF}) = S^{(2)}(\lambda_2, N_{2,1}) = S^{(2)}(F_2^{SF}, v_2^{SF}) = S^{(2)}(F_2^{SF}, N_{2,1}) = S^{(2)}(v_2^{SF}, N_{2,1}) = 0.9998$ which are the same as the 1st-order sensitivities $S^{(1)}(\lambda_2) = S^{(1)}(F_2^{SF}) = S^{(1)}(v_2^{SF}) = S^{(1)}(N_{2,1}) = 0.9998$. Furthermore, the 2nd-order sensitivities $S^{(2)}(\lambda_2, a_2) = S^{(2)}(F_2^{SF}, a_2) = S^{(2)}(a_2, v_2^{SF}) = S^{(2)}(a_2, N_{2,1}) = 0.04373$ have the same values as the 1st-order relative sensitivity of $S^{(1)}(a_2)$, which was presented in Table 5. Similarly, the 2nd-order sensitivities $S^{(2)}(\lambda_2, b_2) = S^{(2)}(F_2^{SF}, b_2) = S^{(2)}(b_2, v_2^{SF}) = S^{(2)}(b_2, N_{2,1}) = 0.01165$ have the same values as the 1st-order relative sensitivity of $S^{(1)}(b_2)$. The unmixed 2nd-order relative sensitivity $S^{(2)}(a_2, a_2)$ with respect to the Watt's coefficient a_2 , is about 50% larger than the corresponding 1st-order sensitivity. However, the value of the 2nd-order relative sensitivity $S^{(2)}(b_2, b_2)$ with respect to the Watt's coefficient b_2 is about 1/7 of the value of the corresponding 1st-order sensitivity $S^{(1)}(b_2)$.

3. Mixed Second-Order Sensitivities of the PERP Total Leakage Response with Respect to the Benchmark's Source Parameters and Total Cross Sections

This Section presents the computation and analysis of the numerical results for the 2nd-order mixed sensitivities $\partial^2 L(\boldsymbol{\alpha}) / \partial \mathbf{q} \partial \sigma_t$, of the PERP's leakage response with respect to the source parameters and group-averaged total microscopic cross sections of all isotopes of the PERP benchmark. As has been shown by Cacuci [6], these mixed sensitivities can be computed using either one of two distinct expressions, involving distinct 2nd-level adjoint systems and corresponding adjoint functions, by considering either the computation of $\partial^2 L(\boldsymbol{\alpha}) / \partial \mathbf{q} \partial \sigma_t$ or the computation of $\partial^2 L(\boldsymbol{\alpha}) / \partial \sigma_t \partial \mathbf{q}$. These two distinct paths will be presented in Sections 3.1 and 3.2, respectively. The corresponding end results produced by these two distinct paths must be identical to one another, thus providing a mutual "solution verification", ensuring that the respective computations were performed correctly.

3.1. Computing the Second-Order Sensitivities $\partial^2 L(\boldsymbol{\alpha}) / \partial \mathbf{q} \partial \sigma_t$

The equation needed for deriving the expression of the 2nd-order sensitivities $\partial^2 L(\boldsymbol{\alpha}) / \partial \mathbf{q} \partial \sigma_t$ is obtained by particularizing Equation (204) from Reference [6] to the PERP benchmark, which takes on the following form:

$$\frac{\partial^2 L(\boldsymbol{\alpha})}{\partial q_j \partial t_{m_2}} = - \sum_{g=1}^G \int_V dV \int_{4\pi} d\boldsymbol{\Omega} h_{1,j}^{(2),g}(r, \boldsymbol{\Omega}) \psi^{(1),g}(r, \boldsymbol{\Omega}) \frac{\partial \Sigma_t^g(\mathbf{t})}{\partial t_{m_2}}, \quad j = 1, \dots, J_q; \quad m_2 = 1, \dots, J_{\sigma t}, \quad (80)$$

where the 2nd-level adjoint functions $h_{1,j}^{(2),g}, j = 1, \dots, J_n; \quad g = 1, \dots, G$, are the solutions of the following 2nd-Level Adjoint Sensitivity System (2nd-LASS) presented in Equations (200) and (202) of [6]:

$$B^g(\boldsymbol{\alpha}^0) h_{1,j}^{(2),g}(r, \boldsymbol{\Omega}) = \frac{\partial Q^g(\mathbf{q}; r, \boldsymbol{\Omega})}{\partial q_j}, \quad j = 1, \dots, J_q; \quad g = 1, \dots, G, \quad (81)$$

$$h_{1,j}^{(2),g}(r_d, \boldsymbol{\Omega}) = 0, \quad \boldsymbol{\Omega} \cdot \mathbf{n} < 0; \quad j = 1, \dots, J_n; \quad g = 1, \dots, G. \quad (82)$$

The derivatives appearing on the right-side of Equation (81) have been defined previously in Equations (18)–(25) for each of the respective source parameters.

In Equation (80), the parameters t_{m_2} correspond to the total cross sections, i.e., $t_{m_2} \equiv \sigma_{t,i_{m_2}}^{g_{m_2}}$, where the subscripts i_{m_2} , g_{m_2} and m_{m_2} denote the isotope, energy group and material associated with the parameter t_{m_2} , respectively. The following relation holds:

$$\frac{\partial \Sigma_t^g(\mathbf{t})}{\partial t_{m_2}} = \frac{\partial \Sigma_t^g(\mathbf{t})}{\partial \sigma_{t,i_{m_2}}^{g_{m_2}}} = \frac{\partial \left(\sum_{m=1}^M \sum_{i=1}^I N_{i,m} \sigma_{t,i}^g \right)}{\partial \sigma_{t,i_{m_2}}^{g_{m_2}}} = \delta_{g_{m_2}g} N_{i_{m_2},m_{m_2}}, \quad (83)$$

where $\delta_{g_{m_2}g}$ denotes the Kronecker-delta functional ($\delta_{g_{m_2}g} = 1$ if $g_{m_2} = g$; $\delta_{g_{m_2}g} = 0$ if $g_{m_2} \neq g$). Inserting the result obtained in Equation (83) into Equation (80) yields:

$$\frac{\partial^2 L(\boldsymbol{\alpha})}{\partial q_j \partial t_{m_2}} = -N_{i_{m_2},m_{m_2}} \int_V dV \int_{4\pi} d\boldsymbol{\Omega} h_{1,j}^{(2),g_{m_2}}(r, \boldsymbol{\Omega}) \psi^{(1),g_{m_2}}(r, \boldsymbol{\Omega}), \quad j = 1, \dots, J_q; \quad m_2 = 1, \dots, J_{ot}. \quad (84)$$

3.2. Alternative Path: Computing the Second-Order Sensitivities $\partial^2 L(\boldsymbol{\alpha}) / \partial \boldsymbol{\sigma}_t \partial \mathbf{q}$

The equation needed for deriving the expression for $\partial^2 L(\boldsymbol{\alpha}) / \partial \boldsymbol{\sigma}_t \partial \mathbf{q}$ is obtained by particularizing Equation (162) from Reference [6] to the PERP benchmark, which yields:

$$\frac{\partial^2 L(\boldsymbol{\alpha})}{\partial t_j \partial q_{m_2}} = \sum_{g=1}^G \int_V dV \int_{4\pi} d\boldsymbol{\Omega} \psi_{2,j}^{(2),g}(r, \boldsymbol{\Omega}) \frac{\partial Q^g(\mathbf{q}; r, \boldsymbol{\Omega})}{\partial q_{m_2}}, \quad j = 1, \dots, J_{ot}; \quad m_2 = 1, \dots, J_q, \quad (85)$$

where the adjoint functions $\psi_{2,j}^{(2),g}$; $j = 1, \dots, J_{ot}$; $g = 1, \dots, G$; are the solutions of the 2nd-Level Adjoint Sensitivity System (2nd-LASS) presented in Equations (34) and (40) of Part I [1], which are reproduced below for convenient reference:

$$A^{(1),g}(\boldsymbol{\alpha}^0) \psi_{2,j}^{(2),g}(r, \boldsymbol{\Omega}) = -\delta_{g,j} N_{i_j, m_j} \psi^{(1),g}(r, \boldsymbol{\Omega}), \quad j = 1, \dots, J_{ot}; \quad g = 1, \dots, G, \quad (86)$$

$$\psi_{2,j}^{(2),g}(r_d, \boldsymbol{\Omega}) = 0, \quad \boldsymbol{\Omega} \cdot \mathbf{n} > 0; \quad j = 1, \dots, J_{ot}; \quad g = 1, \dots, G. \quad (87)$$

The parameters t_j and q_{m_2} in Equation (85) correspond to the total cross sections and source parameters, respectively. Inserting the results obtained in Equations (18)–(25) into Equation (85), and performing the respective angular integrations, yields the following simplified expressions for Equation (85):

$$\text{For } j = 1, \dots, J_{ot}; m_2 = 1, 2: \quad \frac{\partial^2 L(\boldsymbol{\alpha})}{\partial t_j \partial q_{m_2}} = \frac{\partial^2 L(\boldsymbol{\alpha})}{\partial \sigma_{t,i_j}^g \partial \lambda_{i_{m_2}}} = \frac{1}{\lambda_{i_{m_2}}} \sum_{g=1}^G \int_V dV \xi_{2,j;0}^{(2),g}(r) Q_{SF,i_{m_2}}^g; \quad (88)$$

$$\text{For } j = 1, \dots, J_{ot}; m_2 = 3, 4: \quad \frac{\partial^2 L(\boldsymbol{\alpha})}{\partial t_j \partial q_{m_2}} = \frac{\partial^2 L(\boldsymbol{\alpha})}{\partial \sigma_{t,i_j}^g \partial F_{i_{m_2}}^{SF}} = \frac{1}{F_{i_{m_2}}^{SF}} \sum_{g=1}^G \int_V dV \xi_{2,j;0}^{(2),g}(r) Q_{SF,i_{m_2}}^g; \quad (89)$$

$$\text{For } j = 1, \dots, J_{ot}; m_2 = 5, 6: \quad \frac{\partial^2 L(\boldsymbol{\alpha})}{\partial t_j \partial q_{m_2}} = \frac{\partial^2 L(\boldsymbol{\alpha})}{\partial \sigma_{t,i_j}^g \partial a_{i_{m_2}}} = \lambda_{i_{m_2}} N_{i_{m_2},1} F_{i_{m_2}}^{SF} v_{i_{m_2}}^{SF} \sum_{g=1}^G \int_V dV \xi_{2,j;0}^{(2),g}(r) Da(g; a_{i_{m_2}}, b_{i_{m_2}}); \quad (90)$$

$$\text{For } j = 1, \dots, J_{ot}; m_2 = 7, 8: \quad \frac{\partial^2 L(\boldsymbol{\alpha})}{\partial t_j \partial q_{m_2}} = \frac{\partial^2 L(\boldsymbol{\alpha})}{\partial \sigma_{t,i_j}^g \partial b_{i_{m_2}}} = \lambda_{i_{m_2}} N_{i_{m_2},1} F_{i_{m_2}}^{SF} v_{i_{m_2}}^{SF} \sum_{g=1}^G \int_V dV \xi_{2,j;0}^{(2),g}(r) Db(g; a_{i_{m_2}}, b_{i_{m_2}}); \quad (91)$$

$$\text{For } j = 1, \dots, J_{ot}; m_2 = 9, 10: \quad \frac{\partial^2 L(\boldsymbol{\alpha})}{\partial t_j \partial q_{m_2}} = \frac{\partial^2 L(\boldsymbol{\alpha})}{\partial \sigma_{t,i_j}^g \partial v_{i_{m_2}}^{SF}} = \frac{1}{v_{i_{m_2}}^{SF}} \sum_{g=1}^G \int_V dV \xi_{2,j;0}^{(2),g}(r) Q_{SF,i_{m_2}}^g; \quad (92)$$

$$\text{For } j = 1, \dots, J_{\sigma t}; m_2 = 11, 12 : \frac{\partial^2 L(\boldsymbol{\alpha})}{\partial t_j \partial q_{m_2}} = \frac{\partial^2 L(\boldsymbol{\alpha}; Q_{SF}^g)}{\partial \sigma_{t_j}^g \partial N_{i_{m_2}, 1}} = \frac{1}{N_{i_{m_2}, 1}} \sum_{g=1}^G \int_V dV \xi_{2,j;0}^{(2),g}(r) Q_{SF, i_{m_2}}^g, \quad (93)$$

where:

$$\xi_{2,j;0}^{(2),g}(r) \triangleq \int_{4\pi} d\boldsymbol{\Omega} \psi_{2,j}^{(2),g}(r, \boldsymbol{\Omega}), \quad (94)$$

and where the subscripts $i_j = 1, \dots, 6$ and $i_{m_2} = 1, 2$ denote the isotopes associated with the parameters t_j and q_{m_2} , respectively.

3.3. Numerical Results for $\partial^2 L(\boldsymbol{\alpha}) / \partial q \partial \sigma_t$

The second-order absolute sensitivities of the leakage response with respect to the source parameters and the total cross sections for all isotopes of the PERP benchmark, $\partial^2 L(\boldsymbol{\alpha}) / \partial q \partial \sigma_t$, have been computed using Equation (84), and have been independently verified by computing $\partial^2 L(\boldsymbol{\alpha}) / \partial \sigma_t \partial q$ using Equations (88)–(93). Computing $\partial^2 L(\boldsymbol{\alpha}) / \partial q \partial \sigma_t$ requires 12 forward PARTISN transport computations for obtaining the 2nd-level adjoint functions $h_{1,j}^{(2),g}, j = 1, \dots, J_q; g = 1, \dots, G$, needed in Equation (84). In contradistinction, computing $\partial^2 L(\boldsymbol{\alpha}) / \partial \sigma_t \partial \mathbf{N}$ would require $J_{\sigma t} = G \times I = 30 \times 6 = 180$ adjoint PARTISN computations for obtaining the adjoint functions $\psi_{2,j}^{(2),g}, j = 1, \dots, J_{\sigma t}; g = 1, \dots, G$, which are needed in Equations (88)–(93). It is thus evident that computing $\partial^2 L(\boldsymbol{\alpha}) / \partial q \partial \sigma_t$ using Equation (84) is 15 times more efficient than computing $\partial^2 L(\boldsymbol{\alpha}) / \partial \sigma_t \partial q$ using Equations (88)–(93).

The matrix $\partial^2 L / \partial q_j \partial t_{m_2}, j = 1, \dots, J_q; m_2 = 1, \dots, J_{\sigma t}$ has dimensions $J_q \times J_{\sigma t} (= 12 \times 180)$. The corresponding matrix for the 2nd-order relative sensitivities is defined as follows:

$$\mathbf{S}^{(2)}(q_j, t_{m_2}) \triangleq \frac{\partial^2 L}{\partial q_j \partial t_{m_2}} \left(\frac{q_j t_{m_2}}{L} \right), \quad j = 1, \dots, J_q; \quad m_2 = 1, \dots, J_{\sigma t}. \quad (95)$$

Applying Equation (95) to Equations (88), (89), (92) and (93) yields the following relations:

$$S^{(2)}(\sigma_{t,k}^g, \lambda_i) = S^{(2)}(\sigma_{t,k}^g, F_i^{SF}) = S^{(2)}(\sigma_{t,k}^g, v_i^{SF}) = S^{(2)}(\sigma_{t,k}^g, N_{i,1}) = \frac{1}{L} \sum_{g=1}^G \sigma_{t,k}^g \int_V dV \xi_{2,j;0}^{(2),g}(r) Q_{SF, i'}^g \quad (96)$$

for $i = 1, 2; k = 1, \dots, 6; g = 1, \dots, 30$.

Therefore, the mixed 2nd-order relative sensitivities $S^{(2)}(\lambda_i, \sigma_{t,k}^g), S^{(2)}(F_i^{SF}, \sigma_{t,k}^g), S^{(2)}(v_i^{SF}, \sigma_{t,k}^g)$ and $S^{(2)}(N_{i,1}, \sigma_{t,k}^g)$ of the PERP's leakage response with respect to the total cross section parameter $\sigma_{t,k}^g$ and the source parameters $\lambda_i, F_i^{SF}, v_i^{SF}, N_{i,1}$, have the same value, which can also be confirmed by using Equation (84) together with Equation (95).

To facilitate the presentation and interpretation of the numerical results, the matrix $\mathbf{S}^{(2)}(q_j, t_{m_2})$ has been partitioned into $J_q \times I = 12 \times 6$ submatrices, each of dimensions $1 \times G = 1 \times 30$. The summary of the main features of these submatrices involving the source parameters of isotope ^{240}Pu is presented in Table 7 in the following form: when a submatrix comprises elements with relative sensitivities having absolute values greater than 1.0, the total number of such elements is shown in the shaded cells of the table. Otherwise, if the relative sensitivities of all the elements of a submatrix have values that lie in the interval $(-1.0, 1.0)$, only the element having the largest absolute value in the submatrix is listed in Table 7, together with the phase-space coordinates of that element. The submatrices in Table 7, which comprise components with absolute values greater than 1.0, will be discussed in detail in subsequent sub-sections of this Section.

Table 7. Summary presentation of the matrix $S^{(2)}(q_j, \sigma_{t,k}^g)$, $j = 2, 4, 6, 8, 10, 12$; $k = 1, \dots, 6$; $g = 1, \dots, 30$, for 2nd-order relative sensitivities of the leakage response with respect to the source parameters of isotope ^{240}Pu and total cross sections for all isotopes.

	$k=1$ (^{239}Pu)	$k=2$ (^{240}Pu)	$k=3$ (^{69}Ga)	$k=4$ (^{71}Ga)	$k=5$ (C)	$k=6$ (^1H)
λ_2	$S^{(2)}(\lambda_2, \sigma_{t,1}^g)$ 2 elements with absolute values >1.0	$S^{(2)}(\lambda_2, \sigma_{t,2}^g)$ Min. value = -8.36×10^{-2} at $g = 12$	$S^{(2)}(\lambda_2, \sigma_{t,3}^g)$ Min. value = -3.76×10^{-3} at $g = 12$	$S^{(2)}(\lambda_2, \sigma_{t,4}^g)$ Min. value = -2.55×10^{-3} at $g = 12$	$S^{(2)}(\lambda_2, \sigma_{t,5}^g)$ Min. value = -7.85×10^{-1} at $g = 30$	$S^{(2)}(\lambda_2, \sigma_{t,6}^g)$ 6 elements with absolute values >1.0
F_2^{SF}	$S^{(2)}(F_2^{SF}, \sigma_{t,1}^g)$ 2 elements with absolute values >1.0	$S^{(2)}(F_2^{SF}, \sigma_{t,2}^g)$ Min. value = -8.36×10^{-2} at $g = 12$	$S^{(2)}(F_2^{SF}, \sigma_{t,3}^g)$ Min. value = -3.76×10^{-3} at $g = 12$	$S^{(2)}(F_2^{SF}, \sigma_{t,4}^g)$ Min. value = -2.55×10^{-3} at $g = 12$	$S^{(2)}(F_2^{SF}, \sigma_{t,5}^g)$ Min. value = -7.85×10^{-1} at $g = 30$	$S^{(2)}(F_2^{SF}, \sigma_{t,6}^g)$ 6 elements with absolute values >1.0
a_2	$S^{(2)}(a_2, \sigma_{t,1}^g)$ Min. value = -2.54×10^{-1} at $g = 7$	$S^{(2)}(a_2, \sigma_{t,2}^g)$ Min. value = -1.60×10^{-2} at $g = 7$	$S^{(2)}(a_2, \sigma_{t,3}^g)$ Min. value = -6.79×10^{-4} at $g = 7$	$S^{(2)}(a_2, \sigma_{t,4}^g)$ Min. value = -4.50×10^{-4} at $g = 7$	$S^{(2)}(a_2, \sigma_{t,5}^g)$ Max. value = 3.47×10^{-2} at $g = 30$	$S^{(2)}(a_2, \sigma_{t,6}^g)$ Max. value = 4.14×10^{-1} at $g = 30$
b_2	$S^{(2)}(b_2, \sigma_{t,1}^g)$ Min. value = -6.72×10^{-2} at $g = 7$	$S^{(2)}(b_2, \sigma_{t,2}^g)$ Min. value = -4.22×10^{-3} at $g = 7$	$S^{(2)}(b_2, \sigma_{t,3}^g)$ Min. value = -1.79×10^{-4} at $g = 7$	$S^{(2)}(b_2, \sigma_{t,4}^g)$ Min. value = -1.19×10^{-4} at $g = 7$	$S^{(2)}(b_2, \sigma_{t,5}^g)$ Max. value = 1.24×10^{-2} at $g = 30$	$S^{(2)}(b_2, \sigma_{t,6}^g)$ Max. value = 1.48×10^{-1} at $g = 30$
v_2^{SF}	$S^{(2)}(v_2^{SF}, \sigma_{t,1}^g)$ 2 elements with absolute values >1.0	$S^{(2)}(v_2^{SF}, \sigma_{t,2}^g)$ Min. value = -8.36×10^{-2} at $g = 12$	$S^{(2)}(v_2^{SF}, \sigma_{t,3}^g)$ Min. value = -3.76×10^{-3} at $g = 12$	$S^{(2)}(v_2^{SF}, \sigma_{t,4}^g)$ Min. value = -2.55×10^{-3} at $g = 12$	$S^{(2)}(v_2^{SF}, \sigma_{t,5}^g)$ Min. value = -7.85×10^{-1} at $g = 30$	$S^{(2)}(v_2^{SF}, \sigma_{t,6}^g)$ 6 elements with absolute values >1.0
$N_{2,1}$	$S^{(2)}(N_{2,1}, \sigma_{t,1}^g)$ 2 elements with absolute values >1.0	$S^{(2)}(N_{2,1}, \sigma_{t,2}^g)$ Min. value = -8.36×10^{-2} at $g = 12$	$S^{(2)}(N_{2,1}, \sigma_{t,3}^g)$ Min. value = -3.76×10^{-3} at $g = 12$	$S^{(2)}(N_{2,1}, \sigma_{t,4}^g)$ Min. value = -2.55×10^{-3} at $g = 12$	$S^{(2)}(N_{2,1}, \sigma_{t,5}^g)$ Min. value = -7.85×10^{-1} at $g = 30$	$S^{(2)}(N_{2,1}, \sigma_{t,6}^g)$ 6 elements with absolute values >1.0

As shown in Table 7, the absolute values of most elements in the matrix $S^{(2)}(q_j, \sigma_{t,k}^g)$ are smaller than 1.0; but there are 32 elements with absolute values greater than 1.0, as indicated in the shaded submatrices. All of the elements in the submatrices $S^{(2)}(\lambda_2, \sigma_{t,k}^g)$, $S^{(2)}(F_2^{SF}, \sigma_{t,k}^g)$, $S^{(2)}(v_2^{SF}, \sigma_{t,k}^g)$ and $S^{(2)}(N_{2,1}, \sigma_{t,k}^g)$ have negative values. In these submatrices, the absolute values of the 2nd-order sensitivities involving the microscopic total cross sections of isotopes ^{240}Pu , ^{69}Ga , ^{71}Ga and C are all smaller than 1.0. In particular, the element having the maximum absolute value in each of these submatrices involves the microscopic total cross sections for the 12th energy group (namely, $\sigma_{t,k}^{g=12}$, $k = 1, 2, 3, 4$) or the 30th energy group (e.g., $\sigma_{t,k}^{g=30}$, $k = 5, 6$). The values of the elements of the submatrices $S^{(2)}(a_2, \sigma_{t,k}^g)$ and $S^{(2)}(b_2, \sigma_{t,k}^g)$ can be positive or negative, depending on the energy groups and/or the total cross sections of the respective isotopes; and the absolute values of these elements are all smaller than 1.0; moreover, the element having the maximum absolute value in each of these submatrices involves the microscopic total cross sections for the 7th energy group of isotopes ^{239}Pu , ^{240}Pu , ^{69}Ga , and ^{71}Ga , or the 30th energy group of isotopes C and ^1H . The largest absolute values in Table 7 are $S^{(2)}(\lambda_2, \sigma_{t,6}^{g=30}) = S^{(2)}(F_2^{SF}, \sigma_{t,6}^{g=30}) = S^{(2)}(v_2^{SF}, \sigma_{t,6}^{g=30}) = S^{(2)}(N_{2,1}, \sigma_{t,6}^{g=30}) = -9.364$. The largest sensitivities all involve the energy 30th group of H. It maybe because of the highest neutron leakage from that group, as shown in Figure 1. In addition, the 12th and 7th energy groups also exhibit higher neutron leakage, which may explain that the maximum absolute value in each of submatrices mostly relate to those energy groups.

3.3.1. Second-Order Relative Sensitivities $\mathbf{S}^{(2)}(\lambda_2, \sigma_{t,1}^g)$, $\mathbf{S}^{(2)}(F_2^{SF}, \sigma_{t,1}^g)$, $\mathbf{S}^{(2)}(v_2^{SF}, \sigma_{t,1}^g)$ and $\mathbf{S}^{(2)}(N_{2,1}, \sigma_{t,1}^g)$, $g = 1, \dots, 30$

Table 8 lists all the component values for the 2nd-order mixed relative sensitivities in the submatrices $\mathbf{S}^{(2)}(\lambda_2, \sigma_{t,1}^g)$, $\mathbf{S}^{(2)}(F_2^{SF}, \sigma_{t,1}^g)$, $\mathbf{S}^{(2)}(v_2^{SF}, \sigma_{t,1}^g)$ and $\mathbf{S}^{(2)}(N_{2,1}, \sigma_{t,1}^g)$. It has already been noted that the corresponding elements in these four submatrices have the same values. The 2 elements that have values greater than 1.0 in each of the submatrices are shown bold in Table 8; these large 2nd-order mixed relative sensitivities involve the total cross sections of isotope ^{239}Pu for the energy groups $g = 12$ and $g = 13$, respectively. The largest negative values in these submatrices are attained by the 2nd-order relative sensitivities $S^{(2)}(\lambda_2, \sigma_{t,1}^{g=12}) = S^{(2)}(F_2^{SF}, \sigma_{t,1}^{g=12}) = S^{(2)}(v_2^{SF}, \sigma_{t,1}^{g=12}) = S^{(2)}(N_{2,1}, \sigma_{t,1}^{g=12}) = -1.320$ of the leakage response with respect to source parameter $\lambda_2, F_2^{SF}, v_2^{SF}, N_{2,1}$, respectively, of ^{240}Pu and the 12th energy group of the total cross section for ^{239}Pu .

Table 8. Second-Order Relative Sensitivities $\mathbf{S}^{(2)}(\lambda_2, \sigma_{t,1}^g)$, $\mathbf{S}^{(2)}(F_2^{SF}, \sigma_{t,1}^g)$, $\mathbf{S}^{(2)}(v_2^{SF}, \sigma_{t,1}^g)$ and $\mathbf{S}^{(2)}(N_{2,1}, \sigma_{t,1}^g)$, $g = 1, \dots, 30$.

g	Relative Sensitivities	g	Relative Sensitivities
1	-0.0003	16	-0.779
2	-0.0006	17	-0.364
3	-0.002	18	-0.227
4	-0.009	19	-0.181
5	-0.046	20	-0.155
6	-0.135	21	-0.137
7	-0.789	22	-0.099
8	-0.725	23	-0.081
9	-0.843	24	-0.051
10	-0.845	25	-0.060
11	-0.775	26	-0.063
12	-1.320	27	-0.017
13	-1.154	28	-0.003
14	-0.952	29	-0.035
15	-0.690	30	-0.462

3.3.2. Second-Order Relative Sensitivities $\mathbf{S}^{(2)}(\lambda_2, \sigma_{t,6}^g)$, $\mathbf{S}^{(2)}(F_2^{SF}, \sigma_{t,6}^g)$, $\mathbf{S}^{(2)}(v_2^{SF}, \sigma_{t,6}^g)$ and $\mathbf{S}^{(2)}(N_{2,1}, \sigma_{t,6}^g)$, $g = 1, \dots, 30$

Table 9 shows the results obtained for the 2nd-order mixed relative sensitivity of the leakage response with respect to the source parameters ($\lambda_2, F_2^{SF}, v_2^{SF}, N_{2,1}$) of isotope 2 (^{240}Pu) and the total cross sections of isotope 6 (^1H). These submatrices are denoted as $\mathbf{S}^{(2)}(\lambda_2, \sigma_{t,6}^g)$, $\mathbf{S}^{(2)}(F_2^{SF}, \sigma_{t,6}^g)$, $\mathbf{S}^{(2)}(v_2^{SF}, \sigma_{t,6}^g)$ and $\mathbf{S}^{(2)}(N_{2,1}, \sigma_{t,6}^g)$, respectively. As has been shown in Equation (96), the corresponding elements in these four submatrices have the same values. In each submatrix, 6 elements (shown in bold) have relative 2nd-order sensitivities with absolute values greater than 1.0; these large mixed 2nd-order relative sensitivities involve the total cross sections of isotope ^1H for energy groups $g = 16, \dots, 20$ and $g = 30$, respectively. The most negative value in the respective submatrix is attained by the elements $S^{(2)}(\lambda_2, \sigma_{t,6}^{g=12}) = S^{(2)}(F_2^{SF}, \sigma_{t,6}^{g=12}) = S^{(2)}(v_2^{SF}, \sigma_{t,6}^{g=12}) = S^{(2)}(N_{2,1}, \sigma_{t,6}^{g=12}) = -9.364$, involving the 30th energy group of the total cross section of isotope ^1H .

Table 9. Second-Order Relative Sensitivities $\mathbf{S}^{(2)}(\lambda_2, \sigma_{t,6}^g)$, $\mathbf{S}^{(2)}(F_2^{SF}, \sigma_{t,6}^g)$, $\mathbf{S}^{(2)}(v_2^{SF}, \sigma_{t,6}^g)$ and $\mathbf{S}^{(2)}(N_{2,1}, \sigma_{t,6}^g)$, $g = 1, \dots, 30$.

g	Relative Sensitivities	g	Relative Sensitivities
1	-4.440×10^{-6}	16	-1.164
2	-1.169×10^{-5}	17	-1.173
3	-4.108×10^{-5}	18	-1.141
4	-2.555×10^{-4}	19	-1.094
5	-1.735×10^{-3}	20	-1.032
6	-7.360×10^{-3}	21	-0.969
7	-0.067	22	-0.892
8	-0.085	23	-0.826
9	-0.128	24	-0.749
10	-0.158	25	-0.709
11	-0.183	26	-0.653
12	-0.437	27	-0.584
13	-0.523	28	-0.547
14	-0.576	29	-0.544
15	-0.582	30	-9.364

4. Mixed Second-Order Sensitivities of the PERP Total Leakage Response with Respect to the Parameters Underlying the Benchmark’s Source Parameters and Scattering Cross Sections

This Section presents the computation and analysis of the numerical results for the 2nd-order mixed sensitivities $\partial^2 L(\alpha) / \partial \mathbf{q} \partial \sigma_s$ of the leakage response with respect to the source parameters and group-averaged scattering microscopic cross sections of all isotopes contained in the PERP benchmark. The 2nd-order mixed sensitivities $\partial^2 L(\alpha) / \partial \mathbf{q} \partial \sigma_s$ can also be computed using the alternative expressions for $\partial^2 L(\alpha) / \partial \sigma_s \partial \mathbf{q}$. These two distinct paths will be presented in Sections 4.1 and 4.2, respectively. As will be discussed in detail in Section 4.3, the pathway for computing $\partial^2 L(\alpha) / \partial \mathbf{q} \partial \sigma_s$ turns out to be about 590 times more efficient than the pathway for computing $\partial^2 L(\alpha) / \partial \sigma_s \partial \mathbf{q}$.

4.1. Computing the Second-Order Sensitivities $\partial^2 L(\alpha) / \partial \mathbf{q} \partial \sigma_s$

The equations needed for deriving the expressions of the 2nd-order sensitivities $\partial^2 L / \partial q_j \partial s_{m_2}$, $j = 1, \dots, J_q$; $m_2 = 1, \dots, J_{\sigma_s}$, will differ from each other depending on whether the parameter s_{m_2} corresponds to the 0th-order ($l = 0$) scattering cross sections or to the higher-order ($l \geq 1$) scattering cross sections, because the 0th-order scattering cross sections contribute to the total cross sections while the higher-order scattering cross sections do not. Therefore, the 0th-order order scattering cross sections must be considered separately from the higher order scattering cross sections. As described in [1–3] and Appendix A, the total number of 0th-order scattering cross sections comprised in σ_s is denoted as $J_{\sigma_s, l=0}$, where $J_{\sigma_s, l=0} = G \times G \times I$, while the total number of higher order scattering cross sections comprised in σ_s is denoted as $J_{\sigma_s, l \geq 1}$, where $J_{\sigma_s, l \geq 1} = G \times G \times I \times ISCT$, with $J_{\sigma_s, l=0} + J_{\sigma_s, l \geq 1} = J_{\sigma_s}$, where $ISCT$ is the total number of Legendre moments in the finite expansion of the scattering cross sections. There are two distinct cases, as follows:

(1) $\left(\frac{\partial^2 L}{\partial q_j \partial s_{m_2}} \right)_{(s=\sigma_{s, l=0})}$, $j = 1, \dots, J_q$; $m_2 = 1, \dots, J_{\sigma_s, l=0}$, where the quantities q_j refer to the source parameters while the quantities s_{m_2} refer to the parameters underlying the 0th-order ($l = 0$) scattering microscopic cross sections; and

(2) $\left(\frac{\partial^2 L}{\partial q_j \partial s_{m_2}} \right)_{(s=\sigma_{s, l \geq 1})}$, $j = 1, \dots, J_q$; $m_2 = 1, \dots, \sigma_{s, l \geq 1}$, where the quantities q_j refer to the source parameters while the quantities s_{m_2} refer to the parameters underlying the l^{th} -order ($l \geq 1$) scattering microscopic cross sections.

4.1.1. Second-Order Sensitivities $\left(\frac{\partial^2 L}{\partial q_j \partial s_{m_2}}\right)_{(s=\sigma_{s,l}=0)}$, $j = 1, \dots, J_q$; $m_2 = 1, \dots, J_{\sigma s, l=0}$

The equations needed for deriving the expression of the 2nd-order mixed sensitivities $\left(\frac{\partial^2 L}{\partial q_j \partial s_{m_2}}\right)_{(s=\sigma_{s,l}=0)}$ are obtained by particularizing Equations (204) and (205) from Reference [6] to the PERP benchmark. The expression obtained by particularizing Equation (204) from Reference [6] in conjunction with the relations $\frac{\partial^2 L}{\partial q_j \partial t_{m_2}} \frac{\partial t_{m_2}}{\partial s_{m_2}} = \frac{\partial^2 L}{\partial q_j \partial s_{m_2}}$ and $\frac{\partial \Sigma_t^g(\mathbf{t})}{\partial t_{m_2}} \frac{\partial t_{m_2}}{\partial s_{m_2}} = \frac{\partial \Sigma_t^g(\mathbf{t})}{\partial s_{m_2}}$ yields:

$$\left(\frac{\partial^2 L}{\partial q_j \partial s_{m_2}}\right)_{(s=\sigma_{s,l}=0)}^{(1)} = - \sum_{g=1}^G \int_V dV \int_{4\pi} d\Omega h_{1,j}^{(2),g}(r, \Omega) \psi^{(1),g}(r, \Omega) \frac{\partial \Sigma_t^g(\mathbf{t})}{\partial s_{m_2}}, \tag{97}$$

for $j = 1, \dots, J_q$; $m_2 = 1, \dots, J_{\sigma s, l=0}$,

where the 2nd-level adjoint functions $h_{1,j}^{(2),g}$, $j = 1, \dots, J_n$; $g = 1, \dots, G$, are the solutions of the 2nd-Level Adjoint Sensitivity System presented in Equations (81) and (82). In Equation (97), the parameter s_{m_2} corresponds to the 0th-order microscopic total cross sections, i.e., $s_{m_2} \equiv \sigma_{s, l_{m_2}=0, i_{m_2}}^{g' m_2 \rightarrow g m_2}$, where the subscripts i_{m_2} , l_{m_2} , $g' m_2$ and $g m_2$ refer to the isotope, order of Legendre expansion, and energy groups associated with s_{m_2} , respectively. It therefore follows that:

$$\begin{aligned} \frac{\partial \Sigma_t^g(\mathbf{t})}{\partial s_{m_2}} &= \frac{\partial \left[\sum_{m=1}^M \sum_{i=1}^I N_{i,m} \sigma_{s,i}^g(\mathbf{t}) \right]}{\partial \sigma_{s, l_{m_2}=0, i_{m_2}}^{g' m_2 \rightarrow g m_2}} = \frac{\partial \left\{ \sum_{m=1}^M \sum_{i=1}^I N_{i,m} \left[\sigma_{f,i}^g(\mathbf{t}) + \sigma_{c,i}^g(\mathbf{c}) + \sum_{g'=1}^G \sigma_{s, l=0, i}^{g \rightarrow g'}(\mathbf{s}) \right] \right\}}{\partial \sigma_{s, l_{m_2}=0, i_{m_2}}^{g' m_2 \rightarrow g m_2}} \\ &= \frac{\partial \left[\sum_{m=1}^M \sum_{i=1}^I \sum_{g'=1}^G N_{i,m} \sigma_{s, l=0, i}^{g \rightarrow g'}(\mathbf{s}) \right]}{\partial \sigma_{s, l_{m_2}=0, i_{m_2}}^{g' m_2 \rightarrow g m_2}} = \delta_{g' m_2, g} N_{i_{m_2}, m_{m_2}}. \end{aligned} \tag{98}$$

Inserting the result obtained in Equation (98) into Equation (97) yields the following relation:

$$\left(\frac{\partial^2 L}{\partial q_j \partial s_{m_2}}\right)_{(s=\sigma_{s,l}=0)}^{(1)} = -N_{i_{m_2}, m_{m_2}} \int_V dV \int_{4\pi} d\Omega h_{1,j}^{(2),g' m_2}(r, \Omega) \psi^{(1),g' m_2}(r, \Omega), \quad j = 1, \dots, J_q; \quad m_2 = 1, \dots, J_{\sigma s, l=0}. \tag{99}$$

Using Equation (205) from Reference [6] to the PERP benchmark yields the following contributions:

$$\left(\frac{\partial^2 L}{\partial q_j \partial s_{m_2}}\right)_{(s=\sigma_{s,l}=0)}^{(2)} = \sum_{g=1}^G \int_V dV \int_{4\pi} d\Omega h_{1,j}^{(2),g}(r, \Omega) \sum_{g'=1}^G \int_{4\pi} d\Omega' \psi^{(1),g'}(r, \Omega') \frac{\partial \Sigma_s^{g \rightarrow g'}(\mathbf{s}; \Omega \rightarrow \Omega')}{\partial s_{m_2}}, \tag{100}$$

for $j = 1, \dots, J_q$; $m_2 = 1, \dots, J_{\sigma s, l=0}$.

The right side of Equation (100) can be simplified by first noting that:

$$\begin{aligned} \frac{\partial \Sigma_s^{g \rightarrow g'}(\mathbf{s}; \Omega \rightarrow \Omega')}{\partial s_{m_2}} &= \frac{\partial \Sigma_s^{g \rightarrow g'}(\mathbf{s}; \Omega \rightarrow \Omega')}{\partial \sigma_{s, l_{m_2}, i_{m_2}}^{g' m_2 \rightarrow g m_2}} = \frac{\partial \left[\sum_{m=1}^M \sum_{i=1}^I N_{i,m} \sigma_{s,i}^{g \rightarrow g'}(\mathbf{s}; \Omega \rightarrow \Omega') \right]}{\partial \sigma_{s, l_{m_2}, i_{m_2}}^{g' m_2 \rightarrow g m_2}} \\ &= \frac{\partial \left[\sum_{m=1}^M \sum_{i=1}^I \sum_{l=0}^{ISCT} N_{i,m} (2l+1) \sigma_{s,i}^{g \rightarrow g'} P_l(\Omega' \cdot \Omega) \right]}{\partial \sigma_{s, l_{m_2}, i_{m_2}}^{g' m_2 \rightarrow g m_2}} = \delta_{g' m_2, g} \delta_{g m_2, g'} N_{i_{m_2}, m_{m_2}} (2l_{m_2} + 1) P_{l_{m_2}}(\Omega' \cdot \Omega). \end{aligned} \tag{101}$$

Inserting the result obtained in Equation (101) into Equation (100), using the addition theorem for spherical harmonics in one-dimensional geometry, performing the respective angular integrations, and setting $l_{m_2} = 0$ in the resulting expression yields the following simplified end-form for Equation (100):

$$\left(\frac{\partial^2 L}{\partial q_j \partial s_{m_2}}\right)_{(s=\sigma_{s,l}=0)}^{(2)} = N_{i_{m_2}, m_{m_2}} \int_V dV \xi_0^{(1),g m_2}(r) H_{1,j;0}^{(2),g' m_2}(r), \quad j = 1, \dots, J_q; \quad m_2 = 1, \dots, J_{\sigma s, l=0}, \tag{102}$$

where:

$$H_{1,j;0}^{(2),g}(r) \triangleq \int_{4\pi} d\Omega h_{1,j}^{(2),g}(r\Omega). \quad (103)$$

Collecting the partial contributions obtained in Equations (99) and (102), yields the following result:

$$\begin{aligned} \left(\frac{\partial^2 L}{\partial q_j \partial s_{m_2}}\right)_{(s=\sigma_s, l=0)} &= \left(\frac{\partial^2 L}{\partial q_j \partial s_{m_2}}\right)_{(s=\sigma_s, l=0)}^{(1)} + \left(\frac{\partial^2 L}{\partial q_j \partial s_{m_2}}\right)_{(s=\sigma_s, l=0)}^{(2)} \\ &= -N_{i_{m_2}, m_{m_2}} \int_V dV \int_{4\pi} d\Omega h_{1,j}^{(2),g' m_2}(r, \Omega) \psi^{(1),g' m_2}(r, \Omega) + N_{i_{m_2}, m_{m_2}} \int_V dV \xi_0^{(1),g m_2}(r) H_{1,j;0}^{(2),g' m_2}(r), \\ &\text{for } j = 1, \dots, J_q; m_2 = 1, \dots, J_{\sigma_s, l=0}. \end{aligned} \quad (104)$$

4.1.2. Second-Order Sensitivities $\left(\frac{\partial^2 L}{\partial q_j \partial s_{m_2}}\right)_{(s=\sigma_s, l \geq 1)}$, $j = 1, \dots, J_q; m_2 = 1, \dots, \sigma_s, l \geq 1$

For the 2nd-order sensitivities $\left(\frac{\partial^2 L}{\partial q_j \partial s_{m_2}}\right)_{(s=\sigma_s, l \geq 1)}$, $j = 1, \dots, J_q; m_2 = 1, \dots, \sigma_s, l \geq 1$, the quantities q_j correspond to the isotopic source parameters while the parameters $s_{m_2} \equiv \sigma_{s, l, m_2, i_{m_2}}^{g' m_2 \rightarrow g m_2}$ correspond to the l^{th} -order ($l \geq 1$) scattering cross sections. In this case, the expression for $\left(\frac{\partial^2 L}{\partial q_j \partial s_{m_2}}\right)_{(s=\sigma_s, l \geq 1)}$ is obtained by particularizing Equation (205) from reference [6] to the PERP benchmark, which yields,

$$\begin{aligned} \left(\frac{\partial^2 L}{\partial q_j \partial s_{m_2}}\right)_{(s=\sigma_s, l \geq 1)} &= \sum_{g=1}^G \int_V dV \int_{4\pi} d\Omega h_{1,j}^{(2),g}(r, \Omega) \sum_{g'=1}^G \int_{4\pi} d\Omega' \psi^{(1),g'}(r, \Omega') \frac{\partial \Sigma_s^{g \rightarrow g'}(s; \Omega \rightarrow \Omega')}{\partial s_{m_2}}, \\ &\text{for } j = 1, \dots, J_q; m_2 = 1, \dots, J_{\sigma_s, l \geq 1}. \end{aligned} \quad (105)$$

Inserting the results obtained in Equation (101) into Equation (105), using the addition theorem for spherical harmonics in one-dimensional geometry and performing the respective angular integrations yields the following expression:

$$\left(\frac{\partial^2 L}{\partial q_j \partial s_{m_2}}\right)_{(n=N, s=\sigma_s, l \geq 1)} = N_{i_{m_2}, m_{m_2}} (2l_{m_2} + 1) \int_V dV \xi_{l_{m_2}}^{(1),g m_2}(r) H_{1,j;l_{m_2}}^{(2),g' m_2}(r), \quad j = 1, \dots, J_q; m_2 = 1, \dots, J_{\sigma_s, l \geq 1}, \quad (106)$$

where:

$$\xi_l^{(1),g m_2}(r) \triangleq \int_{4\pi} d\Omega P_l(\Omega) \psi^{(1),g'}(r, \Omega), \quad (107)$$

$$H_{1,j;l}^{(2),g m_2}(r) \triangleq \int_{4\pi} d\Omega P_l(\Omega) h_{1,j}^{(2),g}(r\Omega). \quad (108)$$

4.2. Alternative Path: Computing the Second-Order Sensitivities $\partial^2 L(\alpha) / \partial \sigma_s \partial q$

The results computed using the expressions for $\partial^2 L(\alpha) / \partial q \partial \sigma_s$ obtained in Equations (104) and (106) can be verified by obtaining the expressions for $\partial^2 L(\alpha) / \partial \sigma_s \partial q$, which also requires separate consideration of the zeroth-order scattering cross sections. The two cases involved are as follows:

(1) $\left(\frac{\partial^2 L}{\partial s_j \partial q_{m_2}}\right)_{(s=\sigma_s, l=0)}$, $j = 1, \dots, J_{\sigma_s, l=0}; m_2 = 1, \dots, J_q$, where the quantities s_j refer to the parameters underlying the 0th-order scattering cross sections while the quantities q_{m_2} refer to the source parameters; and

(2) $\left(\frac{\partial^2 L}{\partial s_j \partial q_{m_2}}\right)_{(s=\sigma_s, l \geq 1)}$, $j = 1, \dots, \sigma_s, l \geq 1; m_2 = 1, \dots, J_q$, where the quantities s_j refer to the parameters underlying the l^{th} -order ($l \geq 1$) scattering cross sections while the quantities q_{m_2} refer to the source parameters.

4.2.1. Second-Order Sensitivities $\left(\frac{\partial^2 L}{\partial s_j \partial q_{m_2}}\right)_{(s=\sigma_{s,l}=0)}$, $j = 1, \dots, J_{\sigma_s, l=0}$; $m_2 = 1, \dots, J_q$

The equations needed for deriving the expression of the 2nd-order mixed sensitivities $\left(\frac{\partial^2 L}{\partial s_j \partial q_{m_2}}\right)_{(s=\sigma_{s,l}=0)}$ are obtained by particularizing Equations (162) and (171) from Reference [6] to the PERP benchmark, which yield:

$$\begin{aligned} \left(\frac{\partial^2 L}{\partial s_j \partial q_{m_2}}\right)_{(s=\sigma_{s,l}=0)} &= \sum_{g=1}^G \int_V dV \int_{4\pi} d\Omega \psi_{2,j}^{(2),g}(r, \Omega) \frac{\partial Q^g(\mathbf{q}r, \Omega)}{\partial q_{m_2}} \\ &+ \sum_{g=1}^G \int_V dV \int_{4\pi} d\Omega \theta_{2,j}^{(2),g}(r, \Omega) \frac{\partial Q^g(\mathbf{q}r, \Omega)}{\partial q_{m_2}}, \text{ for } j = 1, \dots, J_{\sigma_s, l=0}; m_2 = 1, \dots, J_q. \end{aligned} \tag{109}$$

In Equation (109), the adjoint functions $\psi_{2,j}^{(2),g}$, $j = 1, \dots, J_{\sigma_s, l=0}$; $g = 1, \dots, G$ are the solutions of the 2nd-Level Adjoint Sensitivity System presented in Equations (32) and (37) of Part II [2], which are reproduced below for convenient reference:

$$A^{(1),g}(\boldsymbol{\alpha}^0) \psi_{2,j}^{(2),g}(r, \Omega) = -\delta_{g',j,g} N_{i_j, m_j} \psi^{(1),g}(r, \Omega), \quad j = 1, \dots, J_{\sigma_s, l=0}; \quad g = 1, \dots, G, \tag{110}$$

$$\psi_{2,j}^{(2),g}(r_d, \Omega) = 0, \quad \Omega \cdot \mathbf{n} > 0; \quad j = 1, \dots, J_{\sigma_s, l=0}; \quad g = 1, \dots, G. \tag{111}$$

The 2nd-level adjoint functions, $\theta_{2,j}^{(2),g}$, $j = 1, \dots, J_{\sigma_s, l=0}$; $g = 1, \dots, G$, which also appear in Equation (109), are the solutions of the 2nd-Level Adjoint Sensitivity System presented in Equations (48) and (52) of Part II [2], which are reproduced below for convenient reference:

$$A^{(1),g}(\boldsymbol{\alpha}^0) \theta_{2,j}^{(2),g}(r, \Omega) = \delta_{g',j,g} N_{i_j, m_j} (2l_j + 1) P_{l_j}(\Omega) \xi_{i_j}^{(1),g_j}(r), \quad j = 1, \dots, J_{\sigma_s}; \quad g = 1, \dots, G; \quad l = 0, \dots, ISCT, \tag{112}$$

$$\theta_{2,j}^{(2),g}(r_d, \Omega) = 0, \quad \Omega \cdot \mathbf{n} > 0; \quad j = 1, \dots, J_{\sigma_s}; \quad g = 1, \dots, G. \tag{113}$$

The expressions of the derivatives $\frac{\partial Q^g(\mathbf{q}r, \Omega)}{\partial q_{m_2}}$, which appear in Equation (109), have been derived in Equations (18)–(25). Inserting the results obtained in Equations (18)–(25) into Equation (109), and performing the respective angular integrations yields the following simplified expressions for Equation (109):

For $j = 1, \dots, J_{\sigma_s, l=0}$; $m_2 = 1, 2$:

$$\left(\frac{\partial^2 L}{\partial s_j \partial q_{m_2}}\right)_{(s=\sigma_{s,l}=0)} = \frac{\partial^2 L}{\partial \sigma_{s, l_j=0, i_j}^{g_j' \rightarrow g_j} \partial \lambda_{i_{m_2}}} = \frac{1}{\lambda_{i_{m_2}}} \sum_{g=1}^G \int_V dV \left[\xi_{2,j;0}^{(2),g}(r) + \Theta_{2,j;0}^{(2),g}(r) \right] Q_{SF, i_{m_2}}^g; \tag{114}$$

For $j = 1, \dots, J_{\sigma_s, l=0}$; $m_2 = 3, 4$:

$$\left(\frac{\partial^2 L}{\partial s_j \partial q_{m_2}}\right)_{(s=\sigma_{s,l}=0)} = \frac{\partial^2 L}{\partial \sigma_{s, l_j=0, i_j}^{g_j' \rightarrow g_j} \partial F_{i_{m_2}}^{SF}} = \frac{1}{F_{i_{m_2}}^{SF}} \sum_{g=1}^G \int_V dV \left[\xi_{2,j;0}^{(2),g}(r) + \Theta_{2,j;0}^{(2),g}(r) \right] Q_{SF, i_{m_2}}^g; \tag{115}$$

For $j = 1, \dots, J_{\sigma_s, l=0}$; $m_2 = 5, 6$:

$$\left(\frac{\partial^2 L}{\partial s_j \partial q_{m_2}}\right)_{(s=\sigma_{s,l}=0)} = \frac{\partial^2 L}{\partial \sigma_{s, l_j=0, i_j}^{g_j' \rightarrow g_j} \partial a_{i_{m_2}}} = \lambda_{i_{m_2}} N_{i_{m_2}, 1} F_{i_{m_2}}^{SF} v_{i_{m_2}}^{SF} \sum_{g=1}^G \int_V dV \left[\xi_{2,j;0}^{(2),g}(r) + \Theta_{2,j;0}^{(2),g}(r) \right] Da(g; a_{i_{m_2}}, b_{i_{m_2}}); \tag{116}$$

For $j = 1, \dots, J_{\sigma_s, l=0}; m_2 = 7, 8$:

$$\left(\frac{\partial^2 L}{\partial s_j \partial q_{m_2}}\right)_{(s=\sigma_s, l=0)} = \frac{\partial^2 L}{\partial \sigma_{s, l_j=0, i_j}^{g_j' \rightarrow g_j} \partial b_{i_{m_2}}} = \lambda_{i_{m_2}} N_{i_{m_2}, 1} F_{i_{m_2}}^{SF} v_{i_{m_2}}^{SF} \sum_{g=1}^G \int_V dV [\xi_{2, j; 0}^{(2), g}(r) + \Theta_{2, j; 0}^{(2), g}(r)] Db(g; a_{i_{m_2}}, b_{i_{m_2}}); \quad (117)$$

For $j = 1, \dots, J_{\sigma_s, l=0}; m_2 = 9, 10$:

$$\left(\frac{\partial^2 L}{\partial s_j \partial q_{m_2}}\right)_{(s=\sigma_s, l=0)} = \frac{\partial^2 L}{\partial \sigma_{s, l_j=0, i_j}^{g_j' \rightarrow g_j} \partial v_{i_{m_2}}^{SF}} = \frac{1}{v_{i_{m_2}}^{SF}} \sum_{g=1}^G \int_V dV [\xi_{2, j; 0}^{(2), g}(r) + \Theta_{2, j; 0}^{(2), g}(r)] Q_{SF, i_{m_2}}^g; \quad (118)$$

For $j = 1, \dots, J_{\sigma_s, l=0}; m_2 = 11, 12$:

$$\left(\frac{\partial^2 L}{\partial s_j \partial q_{m_2}}\right)_{(s=\sigma_s, l=0)} = \frac{\partial^2 L(\alpha; Q_{SF}^g)}{\partial \sigma_{s, l_j=0, i_j}^{g_j' \rightarrow g_j} \partial N_{i_{m_2}, 1}} = \frac{1}{N_{i_{m_2}, 1}} \sum_{g=1}^G \int_V dV [\xi_{2, j; 0}^{(2), g}(r) + \Theta_{2, j; 0}^{(2), g}(r)] Q_{SF, i_{m_2}}^g, \quad (119)$$

where:

$$\Theta_{2, j; 0}^{(2), g}(r) \triangleq \int_{4\pi} d\Omega \theta_{2, j}^{(2), g}(r, \Omega). \quad (120)$$

4.2.2. Second-Order Sensitivities $\left(\frac{\partial^2 L}{\partial s_j \partial q_{m_2}}\right)_{(s=\sigma_s, l \geq 1)}$, $j = 1, \dots, \sigma_{s, l \geq 1}; m_2 = 1, \dots, J_q$

For this case, the parameters s_j correspond to the l^{th} -order ($l \geq 1$) scattering cross sections, denoted as $s_j \equiv \sigma_{s, l_j, i_j}^{g_j' \rightarrow g_j}$. Since the l^{th} -order ($l \geq 1$) scattering cross sections are not part of the total cross sections, the expression of $\left(\frac{\partial^2 L}{\partial s_j \partial q_{m_2}}\right)_{(s=\sigma_s, l \geq 1)}$ is obtained by particularizing Equation (171) from Reference [6] to the PERP benchmark, which yields,

$$\left(\frac{\partial^2 L}{\partial s_j \partial q_{m_2}}\right)_{(s=\sigma_s, l \geq 1)} = \sum_{g=1}^G \int_V dV \int_{4\pi} d\Omega \theta_{2, j}^{(2), g}(r, \Omega) \frac{\partial Q^g(\mathbf{q}; r, \Omega)}{\partial q_{m_2}}, \quad j = 1, \dots, J_{s, l \geq 1}; m_2 = 1, \dots, J_q. \quad (121)$$

The 2nd-level adjoint functions, $\theta_{2, j}^{(2), g}$, $j = 1, \dots, J_{s, l \geq 1}; g = 1, \dots, G$, which appear in Equation (121), are the solutions of the 2nd-Level Adjoint Sensitivity System presented in Equations (48) and (52) of Part II [2], as have been presented previously in Equations (112)–(113). Inserting the results obtained in Equations (18)–(25) into Equation (121), and performing the respective angular integrations, yields the following expressions:

For $j = 1, \dots, J_{\sigma_s, l \geq 1}; m_2 = 1, 2$:

$$\left(\frac{\partial^2 L}{\partial s_j \partial q_{m_2}}\right)_{(s=\sigma_s, l \geq 1)} = \frac{\partial^2 L}{\partial \sigma_{s, l_j, i_j}^{g_j' \rightarrow g_j} \partial \lambda_{i_{m_2}}} = \frac{1}{\lambda_{i_{m_2}}} \sum_{g=1}^G \int_V dV \Theta_{2, j; 0}^{(2), g}(r) Q_{SF, i_{m_2}}^g; \quad (122)$$

For $j = 1, \dots, J_{\sigma_s, l \geq 1}; m_2 = 3, 4$:

$$\left(\frac{\partial^2 L}{\partial s_j \partial q_{m_2}}\right)_{(s=\sigma_s, l \geq 1)} = \frac{\partial^2 L}{\partial \sigma_{s, l_j, i_j}^{g_j' \rightarrow g_j} \partial F_{i_{m_2}}^{SF}} = \frac{1}{F_{i_{m_2}}^{SF}} \sum_{g=1}^G \int_V dV \Theta_{2, j; 0}^{(2), g}(r) Q_{SF, i_{m_2}}^g; \quad (123)$$

For $j = 1, \dots, J_{\sigma_s, l \geq 1}; m_2 = 5, 6$:

$$\left(\frac{\partial^2 L}{\partial s_j \partial q_{m_2}}\right)_{(s=\sigma_s, l \geq 1)} = \frac{\partial^2 L}{\partial \sigma_{s, l, j}^{g_j' \rightarrow g_j} \partial a_{i_{m_2}}} = \lambda_{i_{m_2}} N_{i_{m_2}, 1} F_{i_{m_2}}^{SF} v_{i_{m_2}}^{SF} \sum_{g=1}^G \int_V dV \Theta_{2, j; 0}^{(2), g}(r) Da(g; a_{i_{m_2}}, b_{i_{m_2}}); \quad (124)$$

For $j = 1, \dots, J_{\sigma_s, l \geq 1}; m_2 = 7, 8$:

$$\left(\frac{\partial^2 L}{\partial s_j \partial q_{m_2}}\right)_{(s=\sigma_s, l \geq 1)} = \frac{\partial^2 L}{\partial \sigma_{s, l, j}^{g_j' \rightarrow g_j} \partial b_{i_{m_2}}} = \lambda_{i_{m_2}} N_{i_{m_2}, 1} F_{i_{m_2}}^{SF} v_{i_{m_2}}^{SF} \sum_{g=1}^G \int_V dV \Theta_{2, j; 0}^{(2), g}(r) Db(g; a_{i_{m_2}}, b_{i_{m_2}}); \quad (125)$$

For $j = 1, \dots, J_{\sigma_s, l \geq 1}; m_2 = 9, 10$:

$$\left(\frac{\partial^2 L}{\partial s_j \partial q_{m_2}}\right)_{(s=\sigma_s, l \geq 1)} = \frac{\partial^2 L}{\partial \sigma_{s, l, j}^{g_j' \rightarrow g_j} \partial v_{i_{m_2}}^{SF}} = \frac{1}{v_{i_{m_2}}^{SF}} \sum_{g=1}^G \int_V dV \Theta_{2, j; 0}^{(2), g}(r) Q_{SF, i_{m_2}}^g; \quad (126)$$

For $j = 1, \dots, J_{\sigma_s, l \geq 1}; m_2 = 11, 12$:

$$\left(\frac{\partial^2 L}{\partial s_j \partial q_{m_2}}\right)_{(s=\sigma_s, l \geq 1)} = \frac{\partial^2 L(\alpha; Q_{SF}^g)}{\partial \sigma_{s, l, j}^{g_j' \rightarrow g_j} \partial N_{i_{m_2}, 1}} = \frac{1}{N_{i_{m_2}, 1}} \sum_{g=1}^G \int_V dV \Theta_{2, j; 0}^{(2), g}(r) Q_{SF, i_{m_2}}^g. \quad (127)$$

4.3. Numerical Results for $\partial^2 L(\alpha) / \partial q \partial \sigma_s$

The second-order absolute sensitivities, $\partial^2 L(\alpha) / \partial q \partial \sigma_s$, of the leakage response with respect to the source parameters and the scattering cross sections for all isotopes of the PERP benchmark have been computed using Equations (104) and (106), and have been independently verified by computing $\partial^2 L(\alpha) / \partial \sigma_s \partial q$ using Equations (114)–(119) and (122)–(127). For the PERP benchmark, computing the second-order absolute sensitivities, $\partial^2 L(\alpha) / \partial q \partial \sigma_s$, using Equations (104) and (106), requires 12 forward PARTISN computations to obtain all the required adjoint functions. On the other hand, computing the alternative expression $\partial^2 L(\alpha) / \partial \sigma_s \partial q$ using Equations (114)–(119) and (122)–(127), requires 7101 adjoint PARTISN computations to obtain the needed second level adjoint functions. As has been discussed in Part III [3], the reason for needing “only” 7101, rather than 21600, PARTISN computations is that all of the up-scattering and some of the down-scattering cross sections are zero for the PERP benchmark. Therefore, computing $\partial^2 L(\alpha) / \partial q \partial \sigma_s$ using Equations (104) and (106) is about 590 ($\approx 7101/12$) times more efficient than computing $\partial^2 L(\alpha) / \partial \sigma_s \partial q$ by using Equations (114)–(119) and (122)–(127).

The dimensions of the matrix $\partial^2 L / \partial q_j \partial s_{m_2}$, $j = 1, \dots, J_q$; $m_2 = 1, \dots, J_{\sigma_s}$ is $J_q \times J_{\sigma_s}$ ($= 12 \times 21,600$), where $J_{\sigma_s} = G \times G \times (ISCT + 1) \times I = 30 \times 30 \times 4 \times 6 = 21,600$. The matrix of 2nd-order relative sensitivities corresponding to $\partial^2 L / \partial q_j \partial s_{m_2}$, $j = 1, \dots, J_q$; $m_2 = 1, \dots, J_{\sigma_s}$, denoted as $\mathbf{S}^{(2)}(q_j, \sigma_{s, l, k}^{g' \rightarrow g})$, is defined as follows:

$$\mathbf{S}^{(2)}(q_j, \sigma_{s, l, k}^{g' \rightarrow g}) \triangleq \frac{\partial^2 L}{\partial q_j \partial \sigma_{s, l, k}^{g' \rightarrow g}} \left(\frac{q_j \sigma_{s, l, k}^{g' \rightarrow g}}{L} \right), \quad j = 1, \dots, 12; l = 0, \dots, 3; k = 1, \dots, 6; g', g = 1, \dots, 30. \quad (128)$$

Applying Equation (128) to Equations (114), (115), (118), (119), (122), (123), (126) and (127), yields the following expressions:

(i) for the mixed 2nd-order relative sensitivities of the leakage response with respect to the zeroth-order scattering cross sections:

$$\begin{aligned}
 S^{(2)}\left(\sigma_{s,l=0,k'}^{g' \rightarrow g}, \lambda_i\right) &= S^{(2)}\left(\sigma_{s,l=0,k'}^{g' \rightarrow g}, F_i^{SF}\right) = S^{(2)}\left(\sigma_{s,l=0,k'}^{g' \rightarrow g}, \nu_i^{SF}\right) = S^{(2)}\left(\sigma_{s,l=0,k'}^{g' \rightarrow g}, N_{i,1}\right) \\
 &= \frac{1}{L} \sum_{g=1}^G \sigma_{s,l=0,k}^{g' \rightarrow g} \int_V dV \left[\xi_{2,j;0}^{(2),g}(r) + \Theta_{2,j;0}^{(2),g}(r) \right] Q_{SF,i'}^g \text{ for } i = 1, 2; k = 1, \dots, 6; g', g = 1, \dots, 30;
 \end{aligned}
 \tag{129}$$

(ii) for the mixed 2nd-order relative sensitivities of the leakage response with respect to the higher order (i.e., $l = 1, 2, 3$) scattering cross sections:

$$\begin{aligned}
 S^{(2)}\left(\sigma_{s,l,k}^{g' \rightarrow g}, \lambda_i\right) &= S^{(2)}\left(\sigma_{s,l,k}^{g' \rightarrow g}, F_i^{SF}\right) = S^{(2)}\left(\sigma_{s,l,k}^{g' \rightarrow g}, \nu_i^{SF}\right) = S^{(2)}\left(\sigma_{s,l,k}^{g' \rightarrow g}, N_{i,1}\right) \\
 &= \frac{1}{L} \sum_{g=1}^G \sigma_{s,l,k}^{g' \rightarrow g} \int_V dV \Theta_{2,j;0}^{(2),g}(r) Q_{SF,i'}^g \text{ for } i = 1, 2; k = 1, \dots, 6; l = 1, 2, 3; g', g = 1, \dots, 30.
 \end{aligned}
 \tag{130}$$

As expected, the results obtained in Equations (129) and (130) are the same as have been previously obtained in Equations (104) and (106), together with Equation (128).

To facilitate the presentation and interpretation of the numerical results, the $J_q \times J_{\sigma_s}$ ($= 12 \times 21, 600$) matrix $\mathbf{S}^{(2)}\left(q_j, \sigma_{s,l,k}^{g' \rightarrow g}\right)$ has first been partitioned into 4 submatrices, namely, $\mathbf{S}^{(2)}\left(q_j, \sigma_{s,l=0,k}^{g' \rightarrow g}\right)$, $\mathbf{S}^{(2)}\left(q_j, \sigma_{s,l=1,k}^{g' \rightarrow g}\right)$, $\mathbf{S}^{(2)}\left(N_{i,m}, \sigma_{s,l=2,k}^{g' \rightarrow g}\right)$ and $\mathbf{S}^{(2)}\left(q_j, \sigma_{s,l=3,k}^{g' \rightarrow g}\right)$, for the scattering orders $l = 0, l = 1, l = 2$ and $l = 3$, respectively; then each of them is further partitioned into $J_q \times I = 12 \times 6$ smaller submatrices, each of dimensions $1 \times (G \cdot G) = 1 \times 900$. The results are summarized below, in Sections 4.3.1–4.3.4.

4.3.1. Results for the Relative Sensitivities $\mathbf{S}^{(2)}\left(q_j, \sigma_{s,l=0,k}^{g' \rightarrow g}\right)$

The matrix $\mathbf{S}^{(2)}\left(q_j, \sigma_{s,l=0,k}^{g' \rightarrow g}\right)$, $j = 2, 4, 6, 8, 10, 12; k = 1, \dots, 6; g', g = 1, \dots, 30$, comprises the mixed 2nd-order relative sensitivities of the leakage response with respect to the source parameters of isotope ^{240}Pu and the 0th-order scattering microscopic cross sections for all isotopes in the PERP benchmark. Table 10 presents the summary of the numerical results obtained for these mixed 2nd-order relative sensitivities.

As shown in Table 10, the absolute values of all elements in the matrix $\mathbf{S}^{(2)}\left(q_j, \sigma_{s,l=0,k}^{g' \rightarrow g}\right)$ are smaller than 1.0. The overall largest value in the matrix $\mathbf{S}^{(2)}\left(q_j, \sigma_{s,l=0,k}^{g' \rightarrow g}\right)$ is attained by the sensitivities $S^{(2)}\left(\lambda_2, \sigma_{s,l=0,5}^{12 \rightarrow 12}\right) = S^{(2)}\left(F_2^{SF}, \sigma_{s,l=0,5}^{12 \rightarrow 12}\right) = S^{(2)}\left(\nu_2^{SF}, \sigma_{s,l=0,5}^{12 \rightarrow 12}\right) = S^{(2)}\left(N_{2,1}, \sigma_{s,l=0,5}^{12 \rightarrow 12}\right) = 0.681$, all of which involve the 0th-order self-scattering cross section for the 12th energy group of isotope 5 (C). The values of the mixed 2nd-order relative sensitivities $S^{(2)}\left(\lambda_2, \sigma_{s,l=0,k}^{g' \rightarrow g}\right)$, $S^{(2)}\left(F_2^{SF}, \sigma_{s,l=0,k}^{g' \rightarrow g}\right)$, $S^{(2)}\left(\nu_2^{SF}, \sigma_{s,l=0,k}^{g' \rightarrow g}\right)$ and $S^{(2)}\left(N_{2,1}, \sigma_{s,l=0,k}^{g' \rightarrow g}\right)$ for $k = 1, \dots, 4$, with respect to the source parameters $\lambda_2, F_2^{SF}, \nu_2^{SF}, N_{2,1}$ of isotope ^{240}Pu and the 0th-order scattering cross sections of isotopes ^{239}Pu , ^{240}Pu , ^{69}Ga and ^{71}Ga , can be positive or negative, but there are more positive values than negative ones. For instance, among the 900 elements in the submatrix $\mathbf{S}^{(2)}\left(\lambda_2, \sigma_{s,l=0,k=1}^{g' \rightarrow g}\right)$, 251 elements have positive values and 87 elements have negative values, while the remaining elements are zero. On the other hand, the nonzero values of the mixed 2nd-order relative sensitivities with respect to the source parameters $\lambda_2, F_2^{SF}, \nu_2^{SF}, N_{2,1}$ of isotope ^{240}Pu and the 0th-order scattering cross sections of isotopes C and ^1H [i.e., $S^{(2)}\left(\lambda_2, \sigma_{s,l=0,k}^{g' \rightarrow g}\right)$, $S^{(2)}\left(F_2^{SF}, \sigma_{s,l=0,k}^{g' \rightarrow g}\right)$, $S^{(2)}\left(\nu_2^{SF}, \sigma_{s,l=0,k}^{g' \rightarrow g}\right)$, $S^{(2)}\left(N_{2,1}, \sigma_{s,l=0,k}^{g' \rightarrow g}\right)$, for $k = 5, 6$] are all positive. As also shown in Table 10, the values of all of the largest elements of each of the respective sub-matrices are positive; most of these elements involve the 0th-order self-scattering cross sections for the 12th energy group of isotopes ^{239}Pu , ^{240}Pu , ^{69}Ga , ^{71}Ga and C, while the others involve the 0th-order out-scattering cross section $\sigma_{s,l=0,k=6}^{16 \rightarrow 17}$ for isotope ^1H .

Table 10. Summary presentation of the matrix $\mathbf{S}^{(2)}(q_j, \sigma_{s,l=0,k}^{g' \rightarrow g})$, for 2nd-order relative sensitivities of the leakage response with respect to the source parameters of isotope ^{240}Pu and the 0th-order ($l = 0$) scattering cross sections for all isotopes in the PERP benchmark.

	$k=1$ (^{239}Pu)	$k=2$ (^{240}Pu)	$k=3$ (^{69}Ga)	$k=4$ (^{71}Ga)	$k=5$ (C)	$k=6$ (^1H)
λ_2	$\mathbf{S}^{(2)}\left(\begin{matrix} \lambda_{2,} \\ \sigma_{s,l=0,1}^{g' \rightarrow g} \end{matrix}\right)$ Max. value = 1.34×10^{-1} $g' = 12, g = 12$	$\mathbf{S}^{(2)}\left(\begin{matrix} \lambda_{2,} \\ \sigma_{s,l=0,2}^{g' \rightarrow g} \end{matrix}\right)$ Max. value = 8.89×10^{-3} $g' = 12, g = 12$	$\mathbf{S}^{(2)}\left(\begin{matrix} \lambda_{2,} \\ \sigma_{s,l=0,3}^{g' \rightarrow g} \end{matrix}\right)$ Max. value = 5.14×10^{-4} $g' = 12, g = 12$	$\mathbf{S}^{(2)}\left(\begin{matrix} \lambda_{2,} \\ \sigma_{s,l=0,4}^{g' \rightarrow g} \end{matrix}\right)$ Max. value = 3.30×10^{-4} $g' = 12, g = 12$	$\mathbf{S}^{(2)}\left(\begin{matrix} \lambda_{2,} \\ \sigma_{s,l=0,5}^{g' \rightarrow g} \end{matrix}\right)$ Max. value = 6.81×10^{-1} $g' = 12, g = 12$	$\mathbf{S}^{(2)}\left(\begin{matrix} \lambda_{2,} \\ \sigma_{s,l=0,6}^{g' \rightarrow g} \end{matrix}\right)$ Max. value = 1.26×10^{-1} $g' = 16, g = 17$
F_2^{SF}	$\mathbf{S}^{(2)}\left(\begin{matrix} F_2^{SF} \\ \sigma_{s,l=0,1}^{g' \rightarrow g} \end{matrix}\right)$ Max. value = 1.34×10^{-1} $g' = 12, g = 12$	$\mathbf{S}^{(2)}\left(\begin{matrix} F_2^{SF} \\ \sigma_{s,l=0,2}^{g' \rightarrow g} \end{matrix}\right)$ Max. value = 8.89×10^{-3} $g' = 12, g = 12$	$\mathbf{S}^{(2)}\left(\begin{matrix} F_2^{SF} \\ \sigma_{s,l=0,3}^{g' \rightarrow g} \end{matrix}\right)$ Max. value = 5.14×10^{-4} $g' = 12, g = 12$	$\mathbf{S}^{(2)}\left(\begin{matrix} F_2^{SF} \\ \sigma_{s,l=0,4}^{g' \rightarrow g} \end{matrix}\right)$ Max. value = 3.30×10^{-4} $g' = 12, g = 12$	$\mathbf{S}^{(2)}\left(\begin{matrix} F_2^{SF} \\ \sigma_{s,l=0,5}^{g' \rightarrow g} \end{matrix}\right)$ Max. value = 6.81×10^{-1} $g' = 12, g = 12$	$\mathbf{S}^{(2)}\left(\begin{matrix} F_2^{SF} \\ \sigma_{s,l=0,6}^{g' \rightarrow g} \end{matrix}\right)$ Max. value = 1.26×10^{-1} $g' = 16, g = 17$
a_2	$\mathbf{S}^{(2)}\left(\begin{matrix} a_{2,} \\ \sigma_{s,l=0,1}^{g' \rightarrow g} \end{matrix}\right)$ Max. value = 3.43×10^{-2} $g' = 7, g = 7$	$\mathbf{S}^{(2)}\left(\begin{matrix} a_{2,} \\ \sigma_{s,l=0,2}^{g' \rightarrow g} \end{matrix}\right)$ Max. value = 2.00×10^{-3} $g' = 7, g = 7$	$\mathbf{S}^{(2)}\left(\begin{matrix} a_{2,} \\ \sigma_{s,l=0,3}^{g' \rightarrow g} \end{matrix}\right)$ Max. value = 8.67×10^{-5} $g' = 7, g = 7$	$\mathbf{S}^{(2)}\left(\begin{matrix} a_{2,} \\ \sigma_{s,l=0,4}^{g' \rightarrow g} \end{matrix}\right)$ Max. value = 5.43×10^{-5} $g' = 7, g = 7$	$\mathbf{S}^{(2)}\left(\begin{matrix} a_{2,} \\ \sigma_{s,l=0,5}^{g' \rightarrow g} \end{matrix}\right)$ Max. value = 8.35×10^{-3} $g' = 7, g = 7$	$\mathbf{S}^{(2)}\left(\begin{matrix} a_{2,} \\ \sigma_{s,l=0,6}^{g' \rightarrow g} \end{matrix}\right)$ Min. value = -9.22×10^{-3} $g' = 16, g = 17$
b_2	$\mathbf{S}^{(2)}\left(\begin{matrix} b_{2,} \\ \sigma_{s,l=0,1}^{g' \rightarrow g} \end{matrix}\right)$ Max. value = 9.10×10^{-3} $g' = 7, g = 7$	$\mathbf{S}^{(2)}\left(\begin{matrix} b_{2,} \\ \sigma_{s,l=0,2}^{g' \rightarrow g} \end{matrix}\right)$ Max. value = 5.32×10^{-4} $g' = 7, g = 7$	$\mathbf{S}^{(2)}\left(\begin{matrix} b_{2,} \\ \sigma_{s,l=0,3}^{g' \rightarrow g} \end{matrix}\right)$ Max. value = 2.30×10^{-5} $g' = 7, g = 7$	$\mathbf{S}^{(2)}\left(\begin{matrix} b_{2,} \\ \sigma_{s,l=0,4}^{g' \rightarrow g} \end{matrix}\right)$ Max. value = 1.44×10^{-5} $g' = 7, g = 7$	$\mathbf{S}^{(2)}\left(\begin{matrix} b_{2,} \\ \sigma_{s,l=0,5}^{g' \rightarrow g} \end{matrix}\right)$ Max. value = 2.19×10^{-3} $g' = 7, g = 7$	$\mathbf{S}^{(2)}\left(\begin{matrix} b_{2,} \\ \sigma_{s,l=0,6}^{g' \rightarrow g} \end{matrix}\right)$ Min. value = -3.34×10^{-3} $g' = 16, g = 17$
ν_2^{SF}	$\mathbf{S}^{(2)}\left(\begin{matrix} \nu_2^{SF} \\ \sigma_{s,l=0,1}^{g' \rightarrow g} \end{matrix}\right)$ Max. value = 1.34×10^{-1} $g' = 12, g = 12$	$\mathbf{S}^{(2)}\left(\begin{matrix} \nu_2^{SF} \\ \sigma_{s,l=0,2}^{g' \rightarrow g} \end{matrix}\right)$ Max. value = 8.89×10^{-3} $g' = 12, g = 12$	$\mathbf{S}^{(2)}\left(\begin{matrix} \nu_2^{SF} \\ \sigma_{s,l=0,3}^{g' \rightarrow g} \end{matrix}\right)$ Max. value = 5.14×10^{-4} $g' = 12, g = 12$	$\mathbf{S}^{(2)}\left(\begin{matrix} \nu_2^{SF} \\ \sigma_{s,l=0,4}^{g' \rightarrow g} \end{matrix}\right)$ Max. value = 3.30×10^{-4} $g' = 12, g = 12$	$\mathbf{S}^{(2)}\left(\begin{matrix} \nu_2^{SF} \\ \sigma_{s,l=0,5}^{g' \rightarrow g} \end{matrix}\right)$ Max. value = 6.81×10^{-1} $g' = 12, g = 12$	$\mathbf{S}^{(2)}\left(\begin{matrix} \nu_2^{SF} \\ \sigma_{s,l=0,6}^{g' \rightarrow g} \end{matrix}\right)$ Max. value = 1.26×10^{-1} $g' = 16, g = 17$
$N_{2,1}$	$\mathbf{S}^{(2)}\left(\begin{matrix} N_{2,1,} \\ \sigma_{s,l=0,1}^{g' \rightarrow g} \end{matrix}\right)$ Max. value = 1.34×10^{-1} $g' = 12, g = 12$	$\mathbf{S}^{(2)}\left(\begin{matrix} N_{2,1,} \\ \sigma_{s,l=0,2}^{g' \rightarrow g} \end{matrix}\right)$ Max. value = 8.89×10^{-3} $g' = 12, g = 12$	$\mathbf{S}^{(2)}\left(\begin{matrix} N_{2,1,} \\ \sigma_{s,l=0,3}^{g' \rightarrow g} \end{matrix}\right)$ Max. value = 5.14×10^{-4} $g' = 12, g = 12$	$\mathbf{S}^{(2)}\left(\begin{matrix} N_{2,1,} \\ \sigma_{s,l=0,4}^{g' \rightarrow g} \end{matrix}\right)$ Max. value = 3.30×10^{-4} $g' = 12, g = 12$	$\mathbf{S}^{(2)}\left(\begin{matrix} N_{2,1,} \\ \sigma_{s,l=0,5}^{g' \rightarrow g} \end{matrix}\right)$ Max. value = 6.81×10^{-1} $g' = 12, g = 12$	$\mathbf{S}^{(2)}\left(\begin{matrix} N_{2,1,} \\ \sigma_{s,l=0,6}^{g' \rightarrow g} \end{matrix}\right)$ Max. value = 1.26×10^{-1} $g' = 16, g = 17$

The mixed 2nd-order relative sensitivities with respect to the source parameters a_2, b_2 of isotope ^{240}Pu and the 0th-order scattering cross sections for all isotopes, namely, $S^{(2)}(a_2, \sigma_{s,l=0,k}^{g' \rightarrow g}), S^{(2)}(b_2, \sigma_{s,l=0,k}^{g' \rightarrow g})$, for $k = 1, \dots, 6$, are small, having absolute values of the order of 10^{-2} or less. As shown in Table 10, the values of the largest elements of the respective sub-matrix are all positive, except for $S^{(2)}(a_2, \sigma_{s,l=0,k=6}^{16 \rightarrow 17})$ and $S^{(2)}(b_2, \sigma_{s,l=0,k=6}^{16 \rightarrow 17})$, which have small negative values; these elements involve (most of the time) either the 0th-order self-scattering cross sections for the 7th energy group of isotopes $^{239}\text{Pu}, ^{240}\text{Pu}, ^{69}\text{Ga}, ^{71}\text{Ga}$ and C, or (occasionally) the 0th-order out-scattering cross section $\sigma_{s,l=0,k=6}^{16 \rightarrow 17}$ for isotope ^1H .

4.3.2. Results for the Relative Sensitivities $\mathbf{S}^{(2)}(q_j, \sigma_{s,l=1,k}^{g' \rightarrow g})$

Table 11 presents the summary of the results for the mixed 2nd-order relative sensitivities of the leakage response with respect to the source parameters of isotope ^{240}Pu and the 1st-order scattering cross sections for all isotopes in the PERP benchmark; these 2nd-order sensitivities are elements of the matrix $\mathbf{S}^{(2)}(q_j, \sigma_{s,l=1,k}^{g' \rightarrow g}), j = 2, 4, 6, 8, 10, 12; k = 1, \dots, 6; g', g = 1, \dots, 30$. As shown in Table 11, the absolute values of all elements in the matrix $\mathbf{S}^{(2)}(q_j, \sigma_{s,l=1,k}^{g' \rightarrow g})$ are smaller than 1.0. The overall largest (absolute) value is $S^{(2)}(\lambda_2, \sigma_{s,l=1,k=6}^{12 \rightarrow 13}) = S^{(2)}(F_2^{SF}, \sigma_{s,l=1,k=6}^{12 \rightarrow 13}) = S^{(2)}(\nu_2^{SF}, \sigma_{s,l=1,k=6}^{12 \rightarrow 13}) = S^{(2)}(N_{2,1}, \sigma_{s,l=1,k=6}^{12 \rightarrow 13}) = -0.104$.

Table 11. Summary presentation of the matrix $\mathbf{S}^{(2)}(q_j, \sigma_{s,l=1,k}^{g' \rightarrow g})$, for 2nd-order relative sensitivities of the leakage response with respect to the source parameters of isotope ^{240}Pu and the 1st-order ($l = 1$) scattering cross sections for all isotopes in the PERP benchmark.

	$k=1$ (^{239}Pu)	$k=2$ (^{240}Pu)	$k=3$ (^{69}Ga)	$k=4$ (^{71}Ga)	$k=5$ (C)	$k=6$ (^1H)
λ_2	$\mathbf{S}^{(2)}\left(\begin{matrix} \lambda_{2,} \\ \sigma_{s,l=1,1}^{g' \rightarrow g} \end{matrix}\right)$ Min. value $= -8.72 \times 10^{-2}$ $g' = 7, g = 7$	$\mathbf{S}^{(2)}\left(\begin{matrix} \lambda_{2,} \\ \sigma_{s,l=1,2}^{g' \rightarrow g} \end{matrix}\right)$ Min. value $= -5.24 \times 10^{-3}$ $g' = 7, g = 7$	$\mathbf{S}^{(2)}\left(\begin{matrix} \lambda_{2,} \\ \sigma_{s,l=1,3}^{g' \rightarrow g} \end{matrix}\right)$ Min. value $= -1.76 \times 10^{-4}$ $g' = 7, g = 7$	$\mathbf{S}^{(2)}\left(\begin{matrix} \lambda_{2,} \\ \sigma_{s,l=1,4}^{g' \rightarrow g} \end{matrix}\right)$ Min. value $= -1.07 \times 10^{-4}$ $g' = 7, g = 7$	$\mathbf{S}^{(2)}\left(\begin{matrix} \lambda_{2,} \\ \sigma_{s,l=1,5}^{g' \rightarrow g} \end{matrix}\right)$ Min. value $= -2.74 \times 10^{-2}$ $g' = 12, g = 12$	$\mathbf{S}^{(2)}\left(\begin{matrix} \lambda_{2,} \\ \sigma_{s,l=1,6}^{g' \rightarrow g} \end{matrix}\right)$ Min. value $= -1.04 \times 10^{-1}$ $g' = 12, g = 13$
F_2^{SF}	$\mathbf{S}^{(2)}\left(\begin{matrix} F_2^{SF} \\ \sigma_{s,l=1,1}^{g' \rightarrow g} \end{matrix}\right)$ Min. value $= -8.72 \times 10^{-2}$ $g' = 7, g = 7$	$\mathbf{S}^{(2)}\left(\begin{matrix} F_2^{SF} \\ \sigma_{s,l=1,2}^{g' \rightarrow g} \end{matrix}\right)$ Min. value $= -5.24 \times 10^{-3}$ $g' = 7, g = 7$	$\mathbf{S}^{(2)}\left(\begin{matrix} F_2^{SF} \\ \sigma_{s,l=1,3}^{g' \rightarrow g} \end{matrix}\right)$ Min. value $= -1.76 \times 10^{-4}$ $g' = 7, g = 7$	$\mathbf{S}^{(2)}\left(\begin{matrix} F_2^{SF} \\ \sigma_{s,l=1,4}^{g' \rightarrow g} \end{matrix}\right)$ Min. value $= -1.07 \times 10^{-4}$ $g' = 7, g = 7$	$\mathbf{S}^{(2)}\left(\begin{matrix} F_2^{SF} \\ \sigma_{s,l=1,5}^{g' \rightarrow g} \end{matrix}\right)$ Min. value $= -2.74 \times 10^{-2}$ $g' = 12, g = 12$	$\mathbf{S}^{(2)}\left(\begin{matrix} F_2^{SF} \\ \sigma_{s,l=1,6}^{g' \rightarrow g} \end{matrix}\right)$ Min. value $= -1.04 \times 10^{-1}$ $g' = 12, g = 13$
a_2	$\mathbf{S}^{(2)}\left(\begin{matrix} a_{2,} \\ \sigma_{s,l=1,1}^{g' \rightarrow g} \end{matrix}\right)$ Min. value $= -2.91 \times 10^{-2}$ $g' = 7, g = 7$	$\mathbf{S}^{(2)}\left(\begin{matrix} a_{2,} \\ \sigma_{s,l=1,2}^{g' \rightarrow g} \end{matrix}\right)$ Min. value $= -1.75 \times 10^{-3}$ $g' = 7, g = 7$	$\mathbf{S}^{(2)}\left(\begin{matrix} a_{2,} \\ \sigma_{s,l=1,3}^{g' \rightarrow g} \end{matrix}\right)$ Min. value $= -5.88 \times 10^{-5}$ $g' = 7, g = 7$	$\mathbf{S}^{(2)}\left(\begin{matrix} a_{2,} \\ \sigma_{s,l=1,4}^{g' \rightarrow g} \end{matrix}\right)$ Min. value $= -3.57 \times 10^{-5}$ $g' = 7, g = 7$	$\mathbf{S}^{(2)}\left(\begin{matrix} a_{2,} \\ \sigma_{s,l=1,5}^{g' \rightarrow g} \end{matrix}\right)$ Min. value $= -7.36 \times 10^{-3}$ $g' = 7, g = 7$	$\mathbf{S}^{(2)}\left(\begin{matrix} a_{2,} \\ \sigma_{s,l=1,6}^{g' \rightarrow g} \end{matrix}\right)$ Max. value $= 7.46 \times 10^{-3}$ $g' = 16, g = 16$
b_2	$\mathbf{S}^{(2)}\left(\begin{matrix} b_{2,} \\ \sigma_{s,l=1,1}^{g' \rightarrow g} \end{matrix}\right)$ Min. value $= -7.73 \times 10^{-3}$ $g' = 7, g = 7$	$\mathbf{S}^{(2)}\left(\begin{matrix} b_{2,} \\ \sigma_{s,l=1,2}^{g' \rightarrow g} \end{matrix}\right)$ Min. value $= -4.65 \times 10^{-4}$ $g' = 7, g = 7$	$\mathbf{S}^{(2)}\left(\begin{matrix} b_{2,} \\ \sigma_{s,l=1,3}^{g' \rightarrow g} \end{matrix}\right)$ Min. value $= -1.56 \times 10^{-5}$ $g' = 7, g = 7$	$\mathbf{S}^{(2)}\left(\begin{matrix} b_{2,} \\ \sigma_{s,l=1,4}^{g' \rightarrow g} \end{matrix}\right)$ Min. value $= -9.48 \times 10^{-6}$ $g' = 7, g = 7$	$\mathbf{S}^{(2)}\left(\begin{matrix} b_{2,} \\ \sigma_{s,l=1,5}^{g' \rightarrow g} \end{matrix}\right)$ Min. value $= -1.93 \times 10^{-3}$ $g' = 7, g = 7$	$\mathbf{S}^{(2)}\left(\begin{matrix} b_{2,} \\ \sigma_{s,l=1,6}^{g' \rightarrow g} \end{matrix}\right)$ Max. value $= 2.71 \times 10^{-3}$ $g' = 16, g = 16$
ν_2^{SF}	$\mathbf{S}^{(2)}\left(\begin{matrix} \nu_2^{SF} \\ \sigma_{s,l=1,1}^{g' \rightarrow g} \end{matrix}\right)$ Min. value $= -8.72 \times 10^{-2}$ $g' = 7, g = 7$	$\mathbf{S}^{(2)}\left(\begin{matrix} \nu_2^{SF} \\ \sigma_{s,l=1,2}^{g' \rightarrow g} \end{matrix}\right)$ Min. value $= -5.24 \times 10^{-3}$ $g' = 7, g = 7$	$\mathbf{S}^{(2)}\left(\begin{matrix} \nu_2^{SF} \\ \sigma_{s,l=1,3}^{g' \rightarrow g} \end{matrix}\right)$ Min. value $= -1.76 \times 10^{-4}$ $g' = 7, g = 7$	$\mathbf{S}^{(2)}\left(\begin{matrix} \nu_2^{SF} \\ \sigma_{s,l=1,4}^{g' \rightarrow g} \end{matrix}\right)$ Min. value $= -1.07 \times 10^{-4}$ $g' = 7, g = 7$	$\mathbf{S}^{(2)}\left(\begin{matrix} \nu_2^{SF} \\ \sigma_{s,l=1,5}^{g' \rightarrow g} \end{matrix}\right)$ Min. value $= -2.74 \times 10^{-2}$ $g' = 12, g = 12$	$\mathbf{S}^{(2)}\left(\begin{matrix} \nu_2^{SF} \\ \sigma_{s,l=1,6}^{g' \rightarrow g} \end{matrix}\right)$ Min. value $= -1.04 \times 10^{-1}$ $g' = 12, g = 13$
$N_{2,1}$	$\mathbf{S}^{(2)}\left(\begin{matrix} N_{2,1,} \\ \sigma_{s,l=1,1}^{g' \rightarrow g} \end{matrix}\right)$ Min. value $= -8.72 \times 10^{-2}$ $g' = 7, g = 7$	$\mathbf{S}^{(2)}\left(\begin{matrix} N_{2,1,} \\ \sigma_{s,l=1,2}^{g' \rightarrow g} \end{matrix}\right)$ Min. value $= -5.24 \times 10^{-3}$ $g' = 7, g = 7$	$\mathbf{S}^{(2)}\left(\begin{matrix} N_{2,1,} \\ \sigma_{s,l=1,3}^{g' \rightarrow g} \end{matrix}\right)$ Min. value $= -1.76 \times 10^{-4}$ $g' = 7, g = 7$	$\mathbf{S}^{(2)}\left(\begin{matrix} N_{2,1,} \\ \sigma_{s,l=1,4}^{g' \rightarrow g} \end{matrix}\right)$ Min. value $= -1.07 \times 10^{-4}$ $g' = 7, g = 7$	$\mathbf{S}^{(2)}\left(\begin{matrix} N_{2,1,} \\ \sigma_{s,l=1,5}^{g' \rightarrow g} \end{matrix}\right)$ Min. value $= -2.74 \times 10^{-2}$ $g' = 12, g = 12$	$\mathbf{S}^{(2)}\left(\begin{matrix} N_{2,1,} \\ \sigma_{s,l=1,6}^{g' \rightarrow g} \end{matrix}\right)$ Min. value $= -1.04 \times 10^{-1}$ $g' = 12, g = 13$

The elements of $\mathbf{S}^{(2)}(\lambda_2, \sigma_{s,l=1,k}^{g' \rightarrow g})$, $\mathbf{S}^{(2)}(F_2^{SF}, \sigma_{s,l=1,k}^{g' \rightarrow g})$, $\mathbf{S}^{(2)}(\nu_2^{SF}, \sigma_{s,l=1,k}^{g' \rightarrow g})$, $\mathbf{S}^{(2)}(N_{2,1}, \sigma_{s,l=1,k}^{g' \rightarrow g})$ for $k = 1, \dots, 5$, namely the mixed 2nd-order relative sensitivities with respect to the source parameters $\lambda_2, F_2^{SF}, \nu_2^{SF}, N_{2,1}$ of isotope ^{240}Pu and the 1st-order scattering cross sections of isotopes ^{239}Pu , ^{240}Pu , ^{69}Ga and ^{71}Ga and C, can have either positive or negative values. For example, of the 900 elements of the submatrix $\mathbf{S}^{(2)}(\lambda_2, \sigma_{s,l=1,k=1}^{g' \rightarrow g})$, 263 elements have negative values, 75 elements have positive values, and the remaining elements are zero. Table 11 also indicates that all of the nonzero values of the elements of the matrices $\mathbf{S}^{(2)}(\lambda_2, \sigma_{s,l=1,k=6}^{g' \rightarrow g})$, $\mathbf{S}^{(2)}(F_2^{SF}, \sigma_{s,l=1,k=6}^{g' \rightarrow g})$, $\mathbf{S}^{(2)}(\nu_2^{SF}, \sigma_{s,l=1,k=6}^{g' \rightarrow g})$, $\mathbf{S}^{(2)}(N_{2,1}, \sigma_{s,l=1,k=6}^{g' \rightarrow g})$, which comprise the mixed 2nd-order relative sensitivities with respect to the source parameters $\lambda_2, F_2^{SF}, \nu_2^{SF}, N_{2,1}$ of isotope ^{240}Pu and the 1st-order scattering cross sections of isotope ^1H , are negative. The results presented in the Table 11 also reveal that the largest elements of the respective sub-matrix are all negative, involving either the 1st-order self-scattering cross sections for the 7th energy group of isotopes ^{239}Pu , ^{240}Pu , ^{69}Ga and ^{71}Ga (i.e., $\sigma_{s,l=1,k}^{7 \rightarrow 7}$, $k = 1, \dots, 4$) or the 12th energy group of isotope C (i.e., $\sigma_{s,l=0,k=5}^{12 \rightarrow 12}$), or the 1st-order out-scattering cross section $\sigma_{s,l=0,k=6}^{12 \rightarrow 13}$ of isotope ^1H .

As also shown in Table 11, the elements of $\mathbf{S}^{(2)}(a_2, \sigma_{s,l=1,k}^{g' \rightarrow g})$, $\mathbf{S}^{(2)}(b_2, \sigma_{s,l=1,k}^{g' \rightarrow g})$ for $k = 1, \dots, 6$ [i.e., the mixed 2nd-order relative sensitivities of the leakage response with respect to the source parameters a_2, b_2 of isotope ^{240}Pu and the 1st-order scattering cross sections for all isotopes] are all small and can have either positive or negative values. The value of the largest elements of these submatrices are generally negative, except for $\mathbf{S}^{(2)}(a_2, \sigma_{s,l=1,k=6}^{16 \rightarrow 16})$ and $\mathbf{S}^{(2)}(b_2, \sigma_{s,l=1,k=6}^{16 \rightarrow 16})$, which have positive values. The majority of these elements involve the 1st-order self-scattering cross sections for the 7th energy

group of isotopes ^{239}Pu , ^{240}Pu , ^{69}Ga , ^{71}Ga and C (namely, $\sigma_{s,l=0,k}^{7 \rightarrow 7}$, $k = 1, \dots, 5$) while a minority involve the 16th energy group of isotope ^1H (namely, $\sigma_{s,l=1,k=6}^{16 \rightarrow 16}$).

4.3.3. Results for the Relative Sensitivities $\mathbf{S}^{(2)}(q_j, \sigma_{s,l=2,k}^{g' \rightarrow g})$

The matrix $\mathbf{S}^{(2)}(q_j, \sigma_{s,l=2,k}^{g' \rightarrow g})$, $j = 2, 4, 6, 8, 10, 12$; $k = 1, \dots, 6$; $g', g = 1, \dots, 30$, comprises the 2nd-order mixed relative sensitivities of the leakage response with respect to the source parameters of isotope ^{240}Pu and the 2nd-order scattering cross sections for all isotopes in the PERP benchmark. As expected, based on the work previously performed in Part II [2], these 2nd-order mixed relative sensitivities with respect to the higher-order scattering cross sections are very small, of the order of 10^{-2} or less. The overall largest element in this matrix is $S^{(2)}(\lambda_2, \sigma_{s,l=2,k=6}^{12 \rightarrow 12}) = S^{(2)}(F_2^{SF}, \sigma_{s,l=2,k=6}^{12 \rightarrow 12}) = S^{(2)}(v_2^{SF}, \sigma_{s,l=2,k=6}^{12 \rightarrow 12}) = S^{(2)}(N_{2,1}, \sigma_{s,l=2,k=6}^{12 \rightarrow 12}) = 2.70 \times 10^{-2}$. Due to the small values of its elements, the detailed features of $\mathbf{S}^{(2)}(q_j, \sigma_{s,l=2,k}^{g' \rightarrow g})$ are not presented in work.

4.3.4. Results for the Relative Sensitivities $\mathbf{S}^{(2)}(q_j, \sigma_{s,l=3,k}^{g' \rightarrow g})$

The matrix $\mathbf{S}^{(2)}(q_j, \sigma_{s,l=3,k}^{g' \rightarrow g})$, $j = 2, 4, 6, 8, 10, 12$; $k = 1, \dots, 6$; $g', g = 1, \dots, 30$, comprises the 2nd-order mixed relative sensitivities of the leakage response with respect to the source parameters of isotope ^{240}Pu and the 3rd-order scattering cross sections for all isotopes in the PERP benchmark. The elements $S^{(2)}(\lambda_2, \sigma_{s,l=3,k=6}^{12 \rightarrow 12}) = S^{(2)}(F_2^{SF}, \sigma_{s,l=3,k=6}^{12 \rightarrow 12}) = S^{(2)}(v_2^{SF}, \sigma_{s,l=3,k=6}^{12 \rightarrow 12}) = S^{(2)}(N_{2,1}, \sigma_{s,l=3,k=6}^{12 \rightarrow 12}) = -5.35 \times 10^{-3}$ have the largest absolute values; the remaining elements are even smaller and will therefore not be discussed further.

5. Mixed Second-Order Sensitivities of the PERP Total Leakage Response with Respect to the Benchmark's Source Parameters and Fission Cross Sections

This Section presents the computation and analysis of the numerical results for the 2nd-order mixed sensitivities $\partial^2 L(\boldsymbol{\alpha}) / \partial \mathbf{q} \partial \sigma_f$, of the leakage response with respect to the source parameters and group-averaged fission microscopic cross sections of all isotopes of the PERP benchmark. These 2nd-order mixed sensitivities can also be obtained by alternatively computing the matrix $\partial^2 L(\boldsymbol{\alpha}) / \partial \sigma_f \partial \mathbf{q}$. As illustrated in Sections 5.1 and 5.2, respectively, these two distinct paths use distinct 2nd-level adjoint functions and therefore provide an intrinsic verification of the accuracy of the respective computations.

5.1. Computing the Second-Order Sensitivities $\partial^2 L(\boldsymbol{\alpha}) / \partial \mathbf{q} \partial \sigma_f$

The equations needed for deriving the expressions of the 2nd-order sensitivities $\partial^2 L(\boldsymbol{\alpha}) / \partial \mathbf{q} \partial \sigma_f$ are obtained by particularizing Equations (204) and (206) from Reference [6] to the PERP benchmark. Specifically, the expression obtained by particularizing Equation (204) from Reference [6], in conjunction with the relations $\frac{\partial^2 L}{\partial q_j \partial t_{m_2}} \frac{\partial t_{m_2}}{\partial f_{m_2}} = \frac{\partial^2 L}{\partial q_j \partial f_{m_2}}$ and $\frac{\partial \Sigma_t^g(t)}{\partial t_{m_2}} \frac{\partial t_{m_2}}{\partial f_{m_2}} = \frac{\partial \Sigma_t^g(t)}{\partial f_{m_2}}$, yields the following relation:

$$\left(\frac{\partial^2 L}{\partial q_j \partial f_{m_2}} \right)_{(f=\sigma_f)}^{(1)} = - \sum_{g=1}^G \int_V dV \int_{4\pi} d\boldsymbol{\Omega} h_{1,j}^{(2),g}(r, \boldsymbol{\Omega}) \psi^{(1),g}(r, \boldsymbol{\Omega}) \frac{\partial \Sigma_t^g(t)}{\partial f_{m_2}}, \quad (131)$$

for $j = 1, \dots, J_q$; $m_2 = 1, \dots, J_{\sigma_f}$,

where the 2nd-level adjoint functions $h_{1,j}^{(2),g}, j = 1, \dots, J_n; g = 1, \dots, G$, are the solutions of the 2nd-LASS presented previously in Equations (81) and (82). Noting that

$$\frac{\partial \Sigma_t^g}{\partial f_{m_2}} = \frac{\partial \left[\sum_{m=1}^M \sum_{i=1}^I N_{i,m} \sigma_{t,i}^g \right]}{\partial \sigma_{f,i_{m_2}}^{g_{m_2}}} = \frac{\partial \left[\sum_{m=1}^M \sum_{i=1}^I N_{i,m} \sigma_{f,i}^g \right]}{\partial \sigma_{f,i_{m_2}}^{g_{m_2}}} = \delta_{g_{m_2} g} N_{i_{m_2}, m_{m_2}}, \tag{132}$$

and inserting the result obtained in Equation (132) into Equation (131) yields the following expression:

$$\left(\frac{\partial^2 L}{\partial q_j \partial f_{m_2}} \right)_{(f=\sigma_f)}^{(1)} = -N_{i_{m_2}, m_{m_2}} \int_V dV \int_{4\pi} d\Omega h_{1,j}^{(2),g_{m_2}}(r, \Omega) \psi^{(1),g_{m_2}}(r, \Omega), \tag{133}$$

for $j = 1, \dots, J_q; m_2 = 1, \dots, J_{\sigma f}$.

Specializing Equation (206) from Reference [6] to the PERP benchmark yields the following expression:

$$\left(\frac{\partial^2 L}{\partial q_j \partial f_{m_2}} \right)_{(f=\sigma_f)}^{(2)} = \sum_{g=1}^G \int_V dV \int_{4\pi} d\Omega h_{1,j}^{(2),g}(r, \Omega) \frac{\partial [(v\Sigma_f)^g(f)]}{\partial f_{m_2}} \sum_{g'=1}^G \int_{4\pi} d\Omega' \chi^{g'} \psi^{(1),g'}(r, \Omega'), \tag{134}$$

for $j = 1, \dots, J_q; m_2 = 1, \dots, J_{\sigma f}$,

where:

$$\frac{\partial [(v\Sigma_f)^g]}{\partial f_{m_2}} = \frac{\partial \left[\sum_{m=1}^M \sum_{i=1}^I N_{i,m} (v\sigma_f)_i^g \right]}{\partial \sigma_{f,i_{m_2}}^{g_{m_2}}} = \frac{\partial \left[\sum_{m=1}^M \sum_{i=1}^I N_{i,m} v_i^g \sigma_{f,i}^g \right]}{\partial \sigma_{f,i_{m_2}}^{g_{m_2}}} = \delta_{g_{m_2} g} N_{i_{m_2}, m_{m_2}} v_{i_{m_2}}^g. \tag{135}$$

Inserting the result obtained in Equation (135) into Equation (134) yields the following expression:

$$\left(\frac{\partial^2 L}{\partial q_j \partial f_{m_2}} \right)_{(f=\sigma_f)}^{(2)} = N_{i_{m_2}, m_{m_2}} v_{i_{m_2}}^{g_{m_2}} \int_V dV H_{1,j;0}^{(2),g_{m_2}}(r) \sum_{g'=1}^G \chi^{g'} \xi_0^{(1),g'}(r), \tag{136}$$

for $j = 1, \dots, J_q; m_2 = 1, \dots, J_{\sigma f}$.

Collecting the partial contributions obtained in Equations (133) and (136) yields the following result:

$$\left(\frac{\partial^2 L}{\partial q_j \partial f_{m_2}} \right)_{(f=\sigma_f)} = \sum_i^2 \left(\frac{\partial^2 L}{\partial q_j \partial f_{m_2}} \right)_{(f=\sigma_f)}^{(i)} = -N_{i_{m_2}, m_{m_2}} \int_V dV \int_{4\pi} d\Omega h_{1,j}^{(2),g_{m_2}}(r, \Omega) \psi^{(1),g_{m_2}}(r, \Omega) \tag{137}$$

$$+ N_{i_{m_2}, m_{m_2}} v_{i_{m_2}}^{g_{m_2}} \int_V dV H_{1,j;0}^{(2),g_{m_2}}(r) \sum_{g'=1}^G \chi^{g'} \xi_0^{(1),g'}(r), \text{ for } j = 1, \dots, J_q; m_2 = 1, \dots, J_{\sigma f}.$$

5.2. Alternative Path: Computing the Second-Order Sensitivities $\partial^2 L(\alpha) / \partial \sigma_f \partial q$

The equations needed for deriving the alternative expression of the 2nd-order mixed sensitivities $\partial^2 L(\alpha) / \partial q \partial \sigma_f$ are obtained by particularizing Equations (162) and (181) from Reference [6] to the PERP benchmark, which yields:

$$\left(\frac{\partial^2 L}{\partial f_j \partial q_{m_2}} \right)_{(f=\sigma_f)} = \sum_{g=1}^G \int_V dV \int_{4\pi} d\Omega \psi_{2,j}^{(2),g}(r, \Omega) \frac{\partial Q^g(\mathbf{q}; r, \Omega)}{\partial q_{m_2}} \tag{138}$$

$$+ \sum_{g=1}^G \int_V dV \int_{4\pi} d\Omega u_{2,j}^{(2),g}(r, \Omega) \frac{\partial Q^g(\mathbf{q}; r, \Omega)}{\partial q_{m_2}}, \text{ for } j = 1, \dots, J_{\sigma f}; m_2 = 1, \dots, J_q.$$

In Equation (138), the adjoint functions $\psi_{2,j}^{(2),g}$, $j = 1, \dots, J_{\sigma f}$; $g = 1, \dots, G$ are the solutions of the 2nd-Level Adjoint Sensitivity System presented in Equations (35) and (40) of Part III [3], which are reproduced below for convenient reference:

$$A^{(1),g}(\alpha^0)\psi_{2,j}^{(2),g}(r, \Omega) = -\delta_{g,j} N_{i_j, m_j} \psi^{(1),g}(r, \Omega), \quad j = 1, \dots, J_{\sigma f}; \quad g = 1, \dots, G, \quad (139)$$

$$\psi_{2,j}^{(2),g}(r_d, \Omega) = 0, \quad \Omega \cdot \mathbf{n} > 0; \quad j = 1, \dots, J_{\sigma f}; \quad g = 1, \dots, G. \quad (140)$$

Furthermore, the 2nd-level adjoint functions $u_{2,j}^{(2),g}$, $j = 1, \dots, J_{\sigma f}$; $g = 1, \dots, G$ are the solutions of the 2nd-Level Adjoint Sensitivity System presented in Equations (21) and (30) of Part III [3], which are also reproduced below for convenient reference:

$$A^{(1),g}(\alpha^0)u_{2,j}^{(2),g}(r, \Omega) = \delta_{g,j} N_{i_j, m_j} v_{i_j}^g \sum_{g'=1}^G \chi^{g'} \xi_0^{(1),g'}(r), \quad j = 1, \dots, J_{\sigma f}; \quad g = 1, \dots, G, \quad (141)$$

$$u_{2,j}^{(2),g}(r_d, \Omega) = 0, \quad \Omega \cdot \mathbf{n} > 0; \quad j = 1, \dots, J_{\sigma f}; \quad g = 1, \dots, G. \quad (142)$$

Inserting the results obtained in Equations (18)–(25) into Equation (138) and performing the respective angular integrations yields the following simplified expression for Equation (138):

For $j = 1, \dots, J_{\sigma f}$; $m_2 = 1, 2$:

$$\left(\frac{\partial^2 L}{\partial f_j \partial q_{m_2}} \right)_{(f=\sigma_f)} = \frac{\partial^2 L}{\partial \sigma_{f,i_j}^{g_j} \partial \lambda_{i_{m_2}}} = \frac{1}{\lambda_{i_{m_2}}} \sum_{g=1}^G \int_V dV \left[\xi_{2,j;0}^{(2),g}(r) + U_{2,j;0}^{(2),g}(r) \right] Q_{SF,i_{m_2}}^g; \quad (143)$$

For $j = 1, \dots, J_{\sigma f}$; $m_2 = 3, 4$:

$$\left(\frac{\partial^2 L}{\partial f_j \partial q_{m_2}} \right)_{(f=\sigma_f)} = \frac{\partial^2 L}{\partial \sigma_{f,i_j}^{g_j} \partial F_{i_{m_2}}^{SF}} = \frac{1}{F_{i_{m_2}}^{SF}} \sum_{g=1}^G \int_V dV \left[\xi_{2,j;0}^{(2),g}(r) + U_{2,j;0}^{(2),g}(r) \right] Q_{SF,i_{m_2}}^g; \quad (144)$$

For $j = 1, \dots, J_{\sigma f}$; $m_2 = 5, 6$:

$$\left(\frac{\partial^2 L}{\partial f_j \partial q_{m_2}} \right)_{(f=\sigma_f)} = \frac{\partial^2 L}{\partial \sigma_{f,i_j}^{g_j} \partial a_{i_{m_2}}} = \lambda_{i_{m_2}} N_{i_{m_2},1} F_{i_{m_2}}^{SF} v_{i_{m_2}}^{SF} \sum_{g=1}^G \int_V dV \left[\xi_{2,j;0}^{(2),g}(r) + U_{2,j;0}^{(2),g}(r) \right] Da(g; a_{i_{m_2}}, b_{i_{m_2}}); \quad (145)$$

For $j = 1, \dots, J_{\sigma f}$; $m_2 = 7, 8$:

$$\left(\frac{\partial^2 L}{\partial f_j \partial q_{m_2}} \right)_{(f=\sigma_f)} = \frac{\partial^2 L}{\partial \sigma_{f,i_j}^{g_j} \partial b_{i_{m_2}}} = \lambda_{i_{m_2}} N_{i_{m_2},1} F_{i_{m_2}}^{SF} v_{i_{m_2}}^{SF} \sum_{g=1}^G \int_V dV \left[\xi_{2,j;0}^{(2),g}(r) + U_{2,j;0}^{(2),g}(r) \right] Db(g; a_{i_{m_2}}, b_{i_{m_2}}); \quad (146)$$

For $j = 1, \dots, J_{\sigma f}$; $m_2 = 9, 10$:

$$\left(\frac{\partial^2 L}{\partial f_j \partial q_{m_2}} \right)_{(f=\sigma_f)} = \frac{\partial^2 L}{\partial \sigma_{f,i_j}^{g_j} \partial v_{i_{m_2}}^{SF}} = \frac{1}{v_{i_{m_2}}^{SF}} \sum_{g=1}^G \int_V dV \left[\xi_{2,j;0}^{(2),g}(r) + U_{2,j;0}^{(2),g}(r) \right] Q_{SF,i_{m_2}}^g; \quad (147)$$

For $j = 1, \dots, J_{\sigma f}$; $m_2 = 11, 12$:

$$\left(\frac{\partial^2 L}{\partial f_j \partial q_{m_2}} \right)_{(f=\sigma_f)} = \frac{\partial^2 L(\alpha; Q_{SF}^g)}{\partial \sigma_{f,i_j}^{g_j} \partial N_{i_{m_2},1}} = \frac{1}{N_{i_{m_2},1}} \sum_{g=1}^G \int_V dV \left[\xi_{2,j;0}^{(2),g}(r) + U_{2,j;0}^{(2),g}(r) \right] Q_{SF,i_{m_2}}^g, \quad (148)$$

where:

$$U_{2,j;0}^{(2),g}(r) \triangleq \int_{4\pi} d\Omega u_{2,j}^{(2),g}(r,\Omega). \quad (149)$$

5.3. Numerical Results for $\partial^2 L(\alpha) / \partial \mathbf{q} \partial \sigma_f$

The second-order absolute sensitivities, $\partial^2 L(\alpha) / \partial \mathbf{q} \partial \sigma_f$, of the leakage response with respect to the source parameters and the fission cross sections for all isotopes of the PERP benchmark have been computed using Equation (137), and have been independently verified by computing $\partial^2 L(\alpha) / \partial \sigma_f \partial \mathbf{q}$ using Equations (143)–(148). For the PERP benchmark, computing the second-order absolute sensitivities, $\partial^2 L(\alpha) / \partial \mathbf{q} \partial \sigma_f$, using Equation (137) requires 12 PARTISN computations (using the forward transport equation with a modified source) to obtain all the adjoint functions needed in Equation (137). On the other hand, computing the alternative expression $\partial^2 L(\alpha) / \partial \sigma_f \partial \mathbf{q}$ by using Equations (143)–(148) requires 120 adjoint PARTISN computations to obtain the second level adjoint functions needed in Equations (143)–(148). Thus, computing $\partial^2 L(\alpha) / \partial \mathbf{q} \partial \sigma_f$ using Equation (137) is 10 (=120/12) times more efficient than computing $\partial^2 L(\alpha) / \partial \sigma_f \partial \mathbf{q}$ by using Equations (143)–(148).

The matrix $\partial^2 L / \partial q_j \partial f_{m_2}$, $j = 1, \dots, J_q$; $m_2 = 1, \dots, J_{\sigma_f}$ has dimensions $J_q \times J_{\sigma_f}$ ($= 12 \times 60$), where $J_{\sigma_f} = G \times N_f = 30 \times 2$ and where $N_f = 2$ denotes the total number of fissionable isotopes in the PERP benchmark. The matrix of 2nd-order relative sensitivities corresponding to $\partial^2 L / \partial q_j \partial f_{m_2}$, $j = 1, \dots, J_q$; $m_2 = 1, \dots, J_{\sigma_f}$, will be denoted as $\mathbf{S}^{(2)}(q_j, \sigma_{f,k}^g)$ and is defined as follows:

$$\mathbf{S}^{(2)}(q_j, \sigma_{f,k}^g) \triangleq \frac{\partial^2 L}{\partial q_j \partial \sigma_{f,k}^g} \left(\frac{q_j \sigma_{f,k}^g}{L} \right), \quad j = 1, \dots, 12; \quad k = 1, 2; \quad g = 1, \dots, 30. \quad (150)$$

Applying Equation (150) to Equations (143), (144), (147) and (148) yields the following result:

$$\begin{aligned} S^{(2)}(\sigma_{f,k}^g, \lambda_i) &= S^{(2)}(\sigma_{f,k}^g, F_i^{SF}) = S^{(2)}(\sigma_{f,k}^g, \nu_i^{SF}) = S^{(2)}(\sigma_{f,k}^g, N_{i,1}) \\ &= \frac{1}{L} \sum_{g=1}^G \sigma_{f,k}^g \int_V dV \left[\xi_{2,j;0}^{(2),g}(r) + U_{2,j;0}^{(2),g}(r) \right] Q_{SF,i}^g, \text{ for } i = 1, 2; \quad k = 1, 2; \quad g = 1, \dots, 30. \end{aligned} \quad (151)$$

As indicated by Equation (151), the mixed 2nd-order relative sensitivities with respect to the microscopic fission cross section $\sigma_{f,k}^g$ and the source parameters $\lambda_i, F_i^{SF}, \nu_i^{SF}, N_{i,1}$, namely, $S^{(2)}(\lambda_i, \sigma_{f,k}^g)$, $S^{(2)}(F_i^{SF}, \sigma_{f,k}^g)$, $S^{(2)}(\nu_i^{SF}, \sigma_{f,k}^g)$ and $S^{(2)}(N_{i,1}, \sigma_{f,k}^g)$, have the same value. This result has also been confirmed by using Equation (137) together with Equation (150).

Table 12 summarizes the results for the $J_q \times J_{\sigma_f}$ ($= 6 \times 60$) matrix $\mathbf{S}^{(2)}(q_j, \sigma_{f,k}^g)$, $j = 2, 4, 6, 8, 10, 12$; $k = 1, 2$; $g = 1, \dots, 30$, which comprises the 2nd-order relative sensitivities of the leakage response with respect to the source parameters of isotope ^{240}Pu and the fission cross sections for all isotopes in the PERP benchmark. To facilitate the presentation of the numerical results, the matrix $\mathbf{S}^{(2)}(q_j, \sigma_{f,k}^g)$ has been partitioned into $J_q \times N_f$ ($= 6 \times 2$) submatrices, each of dimensions $1 \times G = 1 \times 30$. It has been found that the absolute values of all elements of $\mathbf{S}^{(2)}(q_j, \sigma_{f,k}^g)$ are all smaller than 1.0. Of the sensitivities summarized in Table 12, the single largest relative value is $S^{(2)}(\lambda_2, \sigma_{f,1}^{g=12}) = S^{(2)}(F_2^{SF}, \sigma_{f,1}^{g=12}) = S^{(2)}(\nu_2^{SF}, \sigma_{f,1}^{g=12}) = S^{(2)}(N_{2,1}, \sigma_{f,1}^{g=12}) = 0.882$. All elements of the submatrices $\mathbf{S}^{(2)}(\lambda_2, \sigma_{f,k}^g)$, $\mathbf{S}^{(2)}(F_2^{SF}, \sigma_{f,k}^g)$, $\mathbf{S}^{(2)}(\nu_2^{SF}, \sigma_{f,k}^g)$ and $\mathbf{S}^{(2)}(N_{2,1}, \sigma_{f,k}^g)$ have positive values, and the element with the largest value in each of these submatrices involves the microscopic fission cross sections for the 12th energy group of isotopes ^{239}Pu and ^{240}Pu (namely, $\sigma_{f,k}^{g=12}$, $k = 1, 2$). On the other hand, the elements of the submatrices $\mathbf{S}^{(2)}(a_2, \sigma_{f,k}^g)$ and $\mathbf{S}^{(2)}(b_2, \sigma_{f,k}^g)$, have positive values for

$g = 1, \dots, 10$, and negative values for $g = 11, \dots, 30$. Furthermore, the element having the largest absolute value in each of the submatrices $\mathbf{S}^{(2)}(a_2, \sigma_{f,k}^g)$ and $\mathbf{S}^{(2)}(b_2, \sigma_{f,k}^g)$ involves the microscopic fission cross sections for the 7th energy group of isotopes ^{239}Pu and ^{240}Pu , respectively.

Table 12. Summary of the matrix $\mathbf{S}^{(2)}(q_j, \sigma_{f,k}^g)$, $j = 2, 4, 6, 8, 10, 12$; $k = 1, 2$; $g = 1, \dots, 30$, for 2nd-order relative sensitivities of the leakage response with respect to the source parameters of isotope ^{240}Pu and fission cross sections for all fissionable isotopes.

	$k=1$ (^{239}Pu)	$k=2$ (^{240}Pu)
λ_2	$\mathbf{S}^{(2)}(\lambda_2, \sigma_{f,1}^g)$ Max. value = 8.82×10^{-1} , at $g = 12$	$\mathbf{S}^{(2)}(\lambda_2, \sigma_{f,2}^g)$ Max. value = 4.57×10^{-2} , at $g = 12$
F_2^{SF}	$\mathbf{S}^{(2)}(F_2^{SF}, \sigma_{f,1}^g)$ Max. value = 8.82×10^{-1} , at $g = 12$	$\mathbf{S}^{(2)}(F_2^{SF}, \sigma_{f,2}^g)$ Max. value = 4.57×10^{-2} , at $g = 12$
a_2	$\mathbf{S}^{(2)}(a_2, \sigma_{f,1}^g)$ Max. value = 1.90×10^{-1} , at $g = 7$	$\mathbf{S}^{(2)}(a_2, \sigma_{f,2}^g)$ Max. value = 1.07×10^{-2} , at $g = 7$
b_2	$\mathbf{S}^{(2)}(b_2, \sigma_{f,1}^g)$ Max. value = 5.02×10^{-1} , at $g = 7$	$\mathbf{S}^{(2)}(b_2, \sigma_{f,2}^g)$ Max. value = 2.84×10^{-3} , at $g = 7$
v_2^{SF}	$\mathbf{S}^{(2)}(v_2^{SF}, \sigma_{f,1}^g)$ Max. value = 8.82×10^{-1} , at $g = 12$	$\mathbf{S}^{(2)}(v_2^{SF}, \sigma_{f,2}^g)$ Max. value = 4.57×10^{-2} , at $g = 12$
$N_{2,1}$	$\mathbf{S}^{(2)}(N_{2,1}, \sigma_{f,1}^g)$ Max. value = 8.82×10^{-1} , at $g = 12$	$\mathbf{S}^{(2)}(N_{2,1}, \sigma_{f,2}^g)$ Max. value = 4.57×10^{-2} , at $g = 12$

6. Mixed Second-Order Sensitivities of the PERP Total Leakage Response with Respect to the Benchmark’s Source Parameters and the Average Number of Neutrons per Fission

This Section presents the computation and analysis of the numerical results for the 2nd-order mixed sensitivities $\partial^2 L(\boldsymbol{\alpha}) / \partial \mathbf{q} \partial \mathbf{v}$ of the leakage response with respect to the source parameters and the average number of neutrons per fission of all isotopes in the PERP benchmark. These 2nd-order mixed sensitivities can also be computed by using the alternative expression $\partial^2 L(\boldsymbol{\alpha}) / \partial \mathbf{v} \partial \mathbf{q}$, which requires adjoint functions that are distinct from those required for computing $\partial^2 L(\boldsymbol{\alpha}) / \partial \mathbf{q} \partial \mathbf{v}$. These two distinct paths are illustrated in Sections 6.1 and 6.2, respectively, as follows.

6.1. Computing the Second-Order Sensitivities $\partial^2 L(\boldsymbol{\alpha}) / \partial \mathbf{q} \partial \mathbf{v}$

The equations needed for deriving the expressions of the 2nd-order sensitivities $\partial^2 L(\boldsymbol{\alpha}) / \partial \mathbf{q} \partial \mathbf{v}$ are obtained by particularizing Equation (206) from Reference [6] to the PERP benchmark, which yields the following expression:

$$\left(\frac{\partial^2 L}{\partial q_j \partial f_{m_2}} \right)_{(f=\nu)} = \sum_{g=1}^G \int_V dV \int_{4\pi} d\boldsymbol{\Omega} h_{1,j}^{(2),g}(r, \boldsymbol{\Omega}) \frac{\partial[(v\Sigma_f)^g(\mathbf{f})]}{\partial f_{m_2}} \sum_{g'=1}^G \int_{4\pi} d\boldsymbol{\Omega}' \chi^{g'} \psi^{(1),g'}(r, \boldsymbol{\Omega}'), \tag{152}$$

for $j = 1, \dots, J_q$; $m_2 = J_{\sigma f} + 1, \dots, J_{\sigma f} + J_v$,

where the 2nd-level adjoint functions $h_{1,j}^{(2),g}, j = 1, \dots, J_n; g = 1, \dots, G$, are the solutions of the 2nd-LASS presented previously in Equations (81) and (82). Noting that

$$\frac{\partial[(v\Sigma_f)^g]}{\partial f_{m_2}} = \frac{\partial\left[\sum_{m=1}^M \sum_{i=1}^I N_{i,m}(v\sigma_f)_i^g\right]}{\partial v_{i_{m_2}}^{g_{m_2}}} = \frac{\partial\left[\sum_{m=1}^M \sum_{i=1}^I N_{i,m} v_i^g \sigma_{f,i}^g\right]}{\partial v_{i_{m_2}}^{g_{m_2}}} = \delta_{g_{m_2} g} N_{i_{m_2}, m_{m_2}} \sigma_{f, i_{m_2}}^g, \quad (153)$$

and inserting the result obtained in Equation (153) into Equation (152) yields the following simplified expression for Equation (152):

$$\left(\frac{\partial^2 L}{\partial q_j \partial f_{m_2}}\right)_{(f=v)} = N_{i_{m_2}, m_{m_2}} \sigma_{f, i_{m_2}}^{g_{m_2}} \int_V dV H_{1,j,0}^{(2),g_{m_2}}(r) \sum_{g'=1}^G \chi^{g'} \xi_0^{(1),g'}(r), \quad j = 1, \dots, J_q; \quad m_2 = J_{\sigma f} + 1, \dots, J_{\sigma f} + J_v. \quad (154)$$

6.2. Alternative Path: Computing the Second-Order Sensitivities $\partial^2 L(\alpha) / \partial v \partial q$

The equations needed for deriving the alternative expression of the 2nd-order mixed sensitivities $\partial^2 L(\alpha) / \partial v \partial q$ are obtained by particularizing Equation (181) from Reference [6] to the PERP benchmark. This procedure yields:

$$\left(\frac{\partial^2 L}{\partial f_j \partial q_{m_2}}\right)_{(f=v)} = \sum_{g=1}^G \int_V dV \int_{4\pi} d\Omega u_{2,j}^{(2),g}(r, \Omega) \frac{\partial Q^g(q; r, \Omega)}{\partial q_{m_2}}, \quad j = J_{\sigma f} + 1, \dots, J_{\sigma f} + J_v; \quad m_2 = 1, \dots, J_q, \quad (155)$$

where the 2nd-level adjoint functions, $u_{2,j}^{(2),g}, j = 1, \dots, J_{\sigma f}; g = 1, \dots, G$, are the solutions of the 2nd-Level Adjoint Sensitivity System presented in Equations (118) and (125) of Part III [3], which is reproduced below for convenient reference:

$$A^{(1),g}(\alpha^0) u_{2,j}^{(2),g}(r, \Omega) = \delta_{g,j} N_{i_j, m_j} \sigma_{f, i_j}^{g_j} \sum_{g'=1}^G \chi^{g'} \xi_0^{(1),g'}(r), \quad j = J_{\sigma f} + 1, \dots, J_{\sigma f} + J_v; \quad g = 1, \dots, G, \quad (156)$$

$$u_{2,j}^{(2),g}(r_d, \Omega) = 0, \quad \Omega \cdot \mathbf{n} > 0; \quad j = J_{\sigma f} + 1, \dots, J_{\sigma f} + J_v; \quad g = 1, \dots, G. \quad (157)$$

Inserting the results obtained in Equations (18)–(25) into Equation (155) and performing the respective angular integrations yields the following particular expressions for Equation (155):

For $j = J_{\sigma f} + 1, \dots, J_{\sigma f} + J_v; m_2 = 1, 2$:

$$\left(\frac{\partial^2 L}{\partial f_j \partial q_{m_2}}\right)_{(f=v)} = \frac{\partial^2 L}{\partial v_{i_j}^{g_j} \partial \lambda_{i_{m_2}}} = \frac{1}{\lambda_{i_{m_2}}} \sum_{g=1}^G \int_V dV U_{2,j,0}^{(2),g}(r) Q_{SF, i_{m_2}}^g; \quad (158)$$

For $j = J_{\sigma f} + 1, \dots, J_{\sigma f} + J_v; m_2 = 3, 4$:

$$\left(\frac{\partial^2 L}{\partial f_j \partial q_{m_2}}\right)_{(f=v)} = \frac{\partial^2 L}{\partial v_{i_j}^{g_j} \partial F_{i_{m_2}}^{SF}} = \frac{1}{F_{i_{m_2}}^{SF}} \sum_{g=1}^G \int_V dV U_{2,j,0}^{(2),g}(r) Q_{SF, i_{m_2}}^g; \quad (159)$$

For $j = J_{\sigma f} + 1, \dots, J_{\sigma f} + J_v; m_2 = 5, 6$:

$$\left(\frac{\partial^2 L}{\partial f_j \partial q_{m_2}}\right)_{(f=v)} = \frac{\partial^2 L}{\partial v_{i_j}^{g_j} \partial a_{i_{m_2}}} = \lambda_{i_{m_2}} N_{i_{m_2}, 1} F_{i_{m_2}}^{SF} v_{i_{m_2}}^{SF} \sum_{g=1}^G \int_V dV U_{2,j,0}^{(2),g}(r) Da(g; a_{i_{m_2}}, b_{i_{m_2}}); \quad (160)$$

For $j = J_{\sigma f} + 1, \dots, J_{\sigma f} + J_v; m_2 = 7, 8$:

$$\left(\frac{\partial^2 L}{\partial f_j \partial q_{m_2}} \right)_{(f=v)} = \frac{\partial^2 L}{\partial v_{i_j}^{s_j} \partial b_{i_{m_2}}} = \lambda_{i_{m_2}} N_{i_{m_2},1} F_{i_{m_2}}^{SF} v_{i_{m_2}}^{SF} \sum_{g=1}^G \int_V dV U_{2,j;0}^{(2),g}(r) Db(g; a_{i_{m_2}}, b_{i_{m_2}}); \quad (161)$$

For $j = J_{\sigma f} + 1, \dots, J_{\sigma f} + J_v; m_2 = 9, 10$:

$$\left(\frac{\partial^2 L}{\partial f_j \partial q_{m_2}} \right)_{(f=v)} = \frac{\partial^2 L}{\partial v_{i_j}^{s_j} \partial v_{i_{m_2}}^{SF}} = \frac{1}{v_{i_{m_2}}^{SF}} \sum_{g=1}^G \int_V dV U_{2,j;0}^{(2),g}(r) Q_{SF,i_{m_2}}^g; \quad (162)$$

For $j = J_{\sigma f} + 1, \dots, J_{\sigma f} + J_v; m_2 = 11, 12$:

$$\left(\frac{\partial^2 L}{\partial f_j \partial q_{m_2}} \right)_{(f=v)} = \frac{\partial^2 L(\alpha; Q_{SF}^g)}{\partial v_{i_j}^{s_j} \partial N_{i_{m_2},1}} = \frac{1}{N_{i_{m_2},1}} \sum_{g=1}^G \int_V dV U_{2,j;0}^{(2),g}(r) Q_{SF,i_{m_2}}^g. \quad (163)$$

6.3. Numerical Results for $\partial^2 L(\alpha) / \partial q \partial v$

The second-order absolute sensitivities, $\partial^2 L(\alpha) / \partial q \partial v$, of the leakage response with respect to the source parameters and the average number of neutrons per fission for all isotopes of the PERP benchmark have been computed using Equation (154) and have been independently verified by computing $\partial^2 L(\alpha) / \partial v \partial q$ using Equations (158)–(163). Computing the second-order absolute sensitivities $\partial^2 L(\alpha) / \partial q \partial v$ using Equation (154) requires 12 forward PARTISN computations to obtain all the required 2nd-level adjoint functions. On the other hand, computing the alternative expression $\partial^2 L(\alpha) / \partial v \partial q$ using Equations (158)–(163), requires 60 adjoint PARTISN computations to obtain the required second-level adjoint functions. Thus, computing $\partial^2 L(\alpha) / \partial q \partial v$ using Equation (154) is 5 times more efficient than computing $\partial^2 L(\alpha) / \partial v \partial q$ by using Equations (158)–(163).

The matrix $\partial^2 L / \partial q_j \partial f_{m_2}$, $j = 1, \dots, J_q$; $m_2 = J_{\sigma f} + 1, \dots, J_{\sigma f} + J_v$ has dimensions $J_q \times J_v$ ($= 12 \times 60$), where $J_v = G \times N_f = 30 \times 2$. The matrix of 2nd-order relative sensitivities corresponding to $\partial^2 L / \partial q_j \partial f_{m_2}$, $j = 1, \dots, J_q$; $m_2 = J_{\sigma f} + 1, \dots, J_{\sigma f} + J_v$, will be denoted as $\mathbf{S}^{(2)}(q_j, v_k^g)$ and is defined as follows:

$$\mathbf{S}^{(2)}(q_j, v_k^g) \triangleq \frac{\partial^2 L}{\partial q_j \partial v_k^g} \left(\frac{q_j v_k^g}{L} \right), \quad j = 1, \dots, 12; k = 1, 2; g = 1, \dots, 30. \quad (164)$$

Applying Equation (164) to Equations (158), (159), (162) and (163) yields the following relation:

$$S^{(2)}(v_k^g, \lambda_i) = S^{(2)}(v_k^g, F_i^{SF}) = S^{(2)}(v_k^g, v_i^{SF}) = S^{(2)}(v_k^g, N_{i,1}) = \frac{1}{L} \sum_{g=1}^G v_k^g \int_V dV U_{2,j;0}^{(2),g}(r) Q_{SF,i}^g, \quad (165)$$

for $i = 1, 2; k = 1, 2; g = 1, \dots, 30$.

As indicated in Equation (165), the mixed 2nd-order relative sensitivities $S^{(2)}(\lambda_i, v_k^g)$, $S^{(2)}(F_i^{SF}, v_k^g)$, $S^{(2)}(v_i^{SF}, v_k^g)$ and $S^{(2)}(N_{i,1}, v_k^g)$ of the leakage response with respect to the average number of neutrons per fission v_k^g and the source parameters $\lambda_i, F_i^{SF}, v_i^{SF}, N_{i,1}$, respectively, are all equal to each other. The relation expressed by Equation (165) has also been confirmed independently by using Equation (154) together with Equation (164).

Table 13 summarizes the results for the 12 submatrices, each of dimensions $1 \times G = 1 \times 30$, of the matrix $\mathbf{S}^{(2)}(q_j, v_k^g)$, $j = 2, 4, 6, 8, 10, 12; k = 1, 2; g = 1, \dots, 30$, comprising the 2nd-order relative sensitivities of the leakage response with respect to the source parameters of isotope ^{240}Pu and the average number of neutrons per fission of all fissionable isotopes of the PERP benchmark.

Table 13. Summary results for $\mathbf{S}^{(2)}(q_j, v_k^g)$, $j = 2, 4, 6, 8, 10, 12$; $k = 1, 2$; $g = 1, \dots, 30$, for 2nd-order relative sensitivities of the leakage response with respect to the source parameters of isotope ^{240}Pu and the average number of neutrons per fission for all fissionable isotopes.

	$k=1$ (^{239}Pu)	$k=2$ (^{240}Pu)
λ_2	$\mathbf{S}^{(2)}(\lambda_2, v_{k=1}^g)$ 1 element with absolute value >1.0	$\mathbf{S}^{(2)}(\lambda_2, v_{k=2}^g)$ Max. value = 6.31×10^{-2} , at $g = 12$
F_2^{SF}	$\mathbf{S}^{(2)}(F_2^{SF}, v_{k=1}^g)$ 1 element with absolute value >1.0	$\mathbf{S}^{(2)}(F_2^{SF}, v_{k=2}^g)$ Max. value = 6.31×10^{-2} , at $g = 12$
a_2	$\mathbf{S}^{(2)}(a_2, v_{k=1}^g)$ Max. value = 2.47×10^{-1} , at $g = 7$	$\mathbf{S}^{(2)}(a_2, v_{k=2}^g)$ Max. value = 1.40×10^{-2} , at $g = 7$
b_2	$\mathbf{S}^{(2)}(b_2, v_{k=1}^g)$ Max. value = 6.53×10^{-2} , at $g = 7$	$\mathbf{S}^{(2)}(b_2, v_{k=2}^g)$ Max. value = 3.70×10^{-3} , at $g = 7$
v_2^{SF}	$\mathbf{S}^{(2)}(v_2^{SF}, v_{k=1}^g)$ 1 element with absolute value >1.0	$\mathbf{S}^{(2)}(v_2^{SF}, v_{k=2}^g)$ Max. value = 6.31×10^{-2} , at $g = 12$
$N_{2,1}$	$\mathbf{S}^{(2)}(N_{2,1}, v_{k=1}^g)$ 1 element with absolute value >1.0	$\mathbf{S}^{(2)}(N_{2,1}, v_{k=2}^g)$ Max. value = 6.31×10^{-2} , at $g = 12$

As shown in Table 13, most of the elements of $\mathbf{S}^{(2)}(q_j, v_k^g)$ have absolute values smaller than 1.0. Only 4 elements in the shaded submatrices have absolute values greater than 1.0. All elements of the submatrices $\mathbf{S}^{(2)}(\lambda_2, v_k^g)$, $\mathbf{S}^{(2)}(F_2^{SF}, v_k^g)$, $\mathbf{S}^{(2)}(v_2^{SF}, v_k^g)$ and $\mathbf{S}^{(2)}(N_{2,1}, v_k^g)$, $k = 1, 2$, have positive values. In each of these submatrices, the element having the largest absolute value involves the average number of neutrons per fission for the 12th energy group of the isotopes (i.e., $v_k^{g=12}$, $k = 1, 2$). For the submatrices $\mathbf{S}^{(2)}(a_2, v_k^g)$ and $\mathbf{S}^{(2)}(b_2, v_k^g)$, the values of the mixed 2nd-order relative sensitivities are positive for $g = 1, \dots, 10$, and negative for $g = 11, \dots, 30$; the largest elements in these submatrices involve the average number of neutrons per fission for the 7th energy group of the two fissionable isotopes ^{239}Pu and ^{240}Pu , respectively. Table 14 presents the values of the components of submatrices $\mathbf{S}^{(2)}(\lambda_2, v_{k=1}^g)$, $\mathbf{S}^{(2)}(F_2^{SF}, v_{k=1}^g)$, $\mathbf{S}^{(2)}(v_2^{SF}, v_{k=1}^g)$ and $\mathbf{S}^{(2)}(N_{2,1}, v_{k=1}^g)$, which are shaded in Table 13. As shown (in bold) in Table 14, the only elements that have absolute values greater than 1.0 are $S^{(2)}(\lambda_2, v_{k=1}^{g=12}) = S^{(2)}(F_2^{SF}, v_{k=1}^{g=12}) = S^{(2)}(v_2^{SF}, v_{k=1}^{g=12}) = S^{(2)}(N_{2,1}, v_{k=1}^{g=12}) = 1.214$, i.e., the 2nd-order relative sensitivities of the leakage response with respect to the source parameters λ_2 , F_2^{SF} , v_2^{SF} , $N_{2,1}$, respectively, for isotope ^{240}Pu and the average number of neutrons per fission for isotope ^{239}Pu in the 12th energy group.

Table 14. Second-Order Relative Sensitivities $\mathbf{S}^{(2)}(\lambda_2, v_{k=1}^g)$, $\mathbf{S}^{(2)}(F_2^{SF}, v_{k=1}^g)$, $\mathbf{S}^{(2)}(v_2^{SF}, v_{k=1}^g)$ and $\mathbf{S}^{(2)}(N_{2,1}, v_{k=1}^g)$, $g = 1, \dots, 30$.

g	Relative Sensitivities	g	Relative Sensitivities
1	5.265×10^{-4}	16	0.297
2	1.069×10^{-3}	17	0.117
3	3.064×10^{-3}	18	0.068
4	0.014	19	0.060
5	0.067	20	0.065
6	0.169	21	0.071
7	0.762	22	0.063
8	0.658	23	0.064
9	0.802	24	0.042
10	0.842	25	0.055
11	0.786	26	0.051
12	1.214	27	0.026
13	0.847	28	0.012
14	0.555	29	0.034
15	0.321	30	0.461

7. Mixed Second-Order Sensitivities of the PERP Total Leakage Response with Respect to the Benchmark’s Source Parameters and Isotopic Number Densities

The 2nd-order sensitivities of the leakage response with respect to the source parameters $\lambda_i, F_i^{SF}, a_i, b_i, v_i^{SF}$ and the fissionable isotope number densities $N_{i,1}, i = 1, 2$, namely $\frac{\partial^2 L(\alpha; Q_{SF}^g)}{\partial \lambda_i \partial N_{i,1}}$, $\frac{\partial^2 L(\alpha; Q_{SF}^g)}{\partial F_i^{SF} \partial N_{i,1}}$, $\frac{\partial^2 L(\alpha; Q_{SF}^g)}{\partial a_i \partial N_{i,1}}$, $\frac{\partial^2 L(\alpha; Q_{SF}^g)}{\partial b_i \partial N_{i,1}}$, and $\frac{\partial^2 L(\alpha; Q_{SF}^g)}{\partial v_i^{SF} \partial N_{i,1}}$, have been computed using Equations (62), (66), (70), (73) and (74), respectively, and the respective numerical results have been presented in Table 6. As denoted by the presence of Q_{SF}^g in the argument of the leakage response $L(\alpha; Q_{SF}^g)$, only the contributions stemming from the spontaneous fission source were considered in the computation of these mixed 2nd-order sensitivities.

In order to account for the partial contributions stemming from the macroscopic total, scattering and fission cross sections, as well as the source, this Section presents the computation and analysis of the numerical results for the 2nd-order mixed sensitivities $\partial^2 L(\alpha) / \partial \mathbf{q} \partial \mathbf{N}$ of the leakage response with respect to the source parameters and isotopic number densities of all (including the non-fissionable) isotopes of the PERP benchmark. Note that the 2nd-order mixed sensitivities $\partial^2 L(\alpha) / \partial \mathbf{q} \partial \mathbf{N}$ can also be computed using the alternative expressions for $\partial^2 L(\alpha) / \partial \mathbf{N} \partial \mathbf{q}$. These two distinct paths are illustrated in Sections 7.1 and 7.2, respectively.

7.1. Computing the Second-Order Sensitivities $\partial^2 L(\alpha) / \partial \mathbf{q} \partial \mathbf{N}$

The equations needed for deriving the expressions of the 2nd-order sensitivities $\partial^2 L(\alpha) / \partial \mathbf{q} \partial \mathbf{N}$ are obtained by particularizing Equations (204), (205), (206) and (208) from Reference [6] to the PERP benchmark. Specifically, the contribution stemming from the macroscopic total cross sections is obtained by particularizing Equation (204) from Reference [6], which yields:

$$\left(\frac{\partial^2 L}{\partial q_j \partial n_{m_2}} \right)^{(1)} = \left[\frac{\partial^2 L}{\partial q_j \partial t_{j_{ot}+m_2}} \right]_{t=N} = - \sum_{g=1}^G \int_V dV \int_{4\pi} d\Omega h_{1,j}^{(2),g}(r, \Omega) \psi^{(1),g}(r, \Omega) \frac{\partial \Sigma_t^g(t)}{\partial n_{m_2}}, \tag{166}$$

for $j = 1, \dots, 10; m_2 = 1, \dots, J_n$,

where the 2nd-level adjoint functions $h_{1,j}^{(2),g}$, $j = 1, \dots, J_n$; $g = 1, \dots, G$, are the solutions of the 2nd-LASS presented previously in Equations (81) and (82), and where the parameters n_{m_2} , $m_2 = 1, \dots, J_n$ are the components of the vector \mathbf{N} as defined in [1] and reproduced in Appendix A, namely:

$$\mathbf{N} \triangleq [n_1, \dots, n_{J_n}]^\dagger \triangleq [N_{1,1}, N_{2,1}, N_{3,1}, N_{4,1}, N_{5,2}, N_{6,2}]^\dagger, \quad J_n = 6. \tag{167}$$

Noting that:

$$\frac{\partial \Sigma_t^g(\mathbf{t})}{\partial n_{m_2}} = \frac{\partial \Sigma_t^g(\mathbf{t})}{\partial N_{i_{m_2}, m_{m_2}}} = \frac{\partial \left(\sum_{m=1}^M \sum_{i=1}^I N_{i,m} \sigma_{t,i}^g \right)}{\partial N_{i_{m_2}, m_{m_2}}} = \sigma_{t,i_{m_2}}^g, \tag{168}$$

and inserting the result obtained in Equation (168) into Equation (166) yields the following simplified expression for Equation (166):

$$\left(\frac{\partial^2 L}{\partial q_j \partial n_{m_2}} \right)^{(1)} = \left[\frac{\partial^2 L}{\partial q_j \partial t_{j,ot+m_2}} \right]_{t=N} = - \sum_{g=1}^G \int_V dV \sigma_{t,i_{m_2}}^g \int_{4\pi} d\Omega h_{1,j}^{(2),g}(r, \Omega) \psi^{(1),g}(r, \Omega), \tag{169}$$

for $j = 1, \dots, 10$; $m_2 = 1, \dots, J_n$.

The contribution stemming from the macroscopic scattering cross sections is obtained by particularizing Equation (205) from Reference [6] to the PERP benchmark, which yields:

$$\left(\frac{\partial^2 L}{\partial q_j \partial n_{m_2}} \right)^{(2)} = \left[\frac{\partial^2 L}{\partial q_j \partial s_{j,os+m_2}} \right]_{s=N} = \sum_{g=1}^G \int_V dV \int_{4\pi} d\Omega h_{1,j}^{(2),g}(r, \Omega) \sum_{g'=1}^G \int_{4\pi} d\Omega' \psi^{(1),g'}(r, \Omega') \frac{\partial \Sigma_s^{g \rightarrow g'}(s; \Omega \rightarrow \Omega')}{\partial n_{m_2}}, \quad j = 1, \dots, 10; m_2 = 1, \dots, J_n. \tag{170}$$

Noting that:

$$\frac{\partial \Sigma_s^{g \rightarrow g'}(s; \Omega \rightarrow \Omega')}{\partial n_{m_2}} = \frac{\partial \Sigma_s^{g \rightarrow g'}(s; \Omega \rightarrow \Omega')}{\partial N_{i_{m_2}, m_{m_2}}} = \sum_{l=0}^{ISCT} (2l+1) \sigma_{s,l,i_{m_2}}^{g \rightarrow g'} P_l(\Omega' \cdot \Omega), \tag{171}$$

inserting Equation (171) into Equation (170) and performing the respective angular integrations yields the following simplified expression for Equation (170):

$$\left(\frac{\partial^2 L}{\partial q_j \partial n_{m_2}} \right)^{(2)} = \sum_{g=1}^G \sum_{l=0}^{ISCT} (2l+1) \int_V dV H_{1,j;l}^{(2),g}(r) \sum_{g'=1}^G \sigma_{s,l,i_{m_2}}^{g \rightarrow g'} \xi_l^{(1),g'}(r), \quad j = 1, \dots, 10; m_2 = 1, \dots, J_n. \tag{172}$$

The contribution stemming from the macroscopic fission cross sections is obtained by particularizing Equation (206) from Reference [6] to the PERP benchmark, which yields:

$$\left(\frac{\partial^2 L}{\partial q_j \partial n_{m_2}} \right)^{(3)} = \left[\frac{\partial^2 L}{\partial q_j \partial f_{j,of+J_v+m_2}} \right]_{f=N} = \sum_{g=1}^G \int_V dV \int_{4\pi} d\Omega h_{1,j}^{(2),g}(r, \Omega) \frac{\partial [(\nu \Sigma_f)^g(\mathbf{t})]}{\partial n_{m_2}} \sum_{g'=1}^G \int_{4\pi} d\Omega' \chi^{g'} \psi^{(1),g'}(r, \Omega'), \quad j = 1, \dots, 10; m_2 = 1, \dots, J_n. \tag{173}$$

Noting that:

$$\frac{\partial (\nu \Sigma_f)^g(\mathbf{t})}{\partial n_{m_2}} = \frac{\partial \sum_{m=1}^M \sum_{i=1}^I N_{i,m} (\nu \sigma_f)_i^g}{\partial N_{i_{m_2}, m_{m_2}}} = \frac{\partial \sum_{m=1}^M \sum_{i=1}^I N_{i,m} \nu_i^g \sigma_{f,i}^g}{\partial N_{i_{m_2}, m_{m_2}}} = \nu_{i_{m_2}}^g \sigma_{f,i_{m_2}}^g, \tag{174}$$

inserting Equation (174) into Equation (173) and performing the respective angular integrations, yields the following simplified expression for Equation (173):

$$\left(\frac{\partial^2 L}{\partial q_j \partial n_{m_2}}\right)^{(3)} = \sum_{g=1}^G \int_V dV V_{i_{m_2}}^g \sigma_{f,i_{m_2}}^g H_{1,j;0}^{(2),g}(r) \sum_{g'=1}^G \chi^{g'} \xi_0^{(1),g'}(r), \quad j = 1, \dots, 10; m_2 = 1, \dots, J_n. \quad (175)$$

Finally, the contribution stemming from the source term is obtained by particularizing Equation (208) from Reference [6] to the PERP benchmark, which yields:

$$\left(\frac{\partial^2 L}{\partial q_j \partial n_{m_2}}\right)^{(4)} = \left[\frac{\partial^2 L}{\partial q_j \partial q_{lq+m_2}} \right]_{q=N} = \sum_{g=1}^G \int_V dV \int_{4\pi} d\Omega \psi^{(1),g}(r, \Omega) \frac{\partial Q^g(\mathbf{q}; r, \Omega)}{\partial q_j \partial n_{m_2}}, \quad (176)$$

for $j = 1, \dots, 10; m_2 = 1, \dots, J_n,$

where the derivatives $\frac{\partial Q^g(\mathbf{q}; r, \Omega)}{\partial q_j \partial n_{m_2}}$ have been derived previously in Equations (42), (46), (52), (56) and (57), respectively. The simplified expression in Equation (176) has been obtained and solved previously in Equations (62), (66), (70), (73) and (74), respectively.

Collecting the partial contributions obtained in Equations (169), (172), (175) and (176) yields the following expression:

$$\begin{aligned} \frac{\partial^2 L}{\partial q_j \partial n_{m_2}} &= \sum_i^4 \left(\frac{\partial^2 L}{\partial q_j \partial n_{m_2}}\right)^{(i)} = - \sum_{g=1}^G \int_V dV \int_{4\pi} d\Omega \sigma_{t,i_{m_2}}^g h_{1,j}^{(2),g}(r, \Omega) \psi^{(1),g}(r, \Omega) \\ &+ \sum_{g=1}^G \sum_{l=0}^{ISCT} (2l+1) \int_V dV H_{1,j;l}^{(2),g}(r) \sum_{g'=1}^G \sigma_{s,l,i_{m_2}}^{g \rightarrow g'} \xi_l^{(1),g'}(r) + \sum_{g=1}^G \int_V dV V_{i_{m_2}}^g \sigma_{f,i_{m_2}}^g H_{1,j;0}^{(2),g}(r) \sum_{g'=1}^G \chi^{g'} \xi_0^{(1),g'}(r) \\ &+ \sum_{g=1}^G \int_V dV \xi_0^{(1),g}(r) \frac{\partial Q^g(\mathbf{q}; r, \Omega)}{\partial q_j \partial n_{m_2}}, \end{aligned} \quad (177)$$

for $j = 1, \dots, 10; m_2 = 1, \dots, J_n.$

7.2. Alternative Path: Computing the Second-Order Sensitivities $\partial^2 L(\boldsymbol{\alpha}) / \partial \mathbf{N} \partial \mathbf{q}$

The equations needed for deriving the alternative expression of the 2nd-order mixed sensitivities $\partial^2 L(\boldsymbol{\alpha}) / \partial \mathbf{N} \partial \mathbf{q}$ are obtained by particularizing Equations (162), (171), (181) and (208) from Reference [6] to the PERP benchmark. The combined expression obtained by particularizing these equations takes on the following form:

$$\begin{aligned} \frac{\partial^2 L}{\partial n_j \partial q_{m_2}} &= \sum_{g=1}^G \int_V dV \int_{4\pi} d\Omega \psi_{2,j}^{(2),g}(r, \Omega) \frac{\partial Q^g(\mathbf{q}; r, \Omega)}{\partial q_{m_2}} + \sum_{g=1}^G \int_V dV \int_{4\pi} d\Omega \theta_{2,j}^{(2),g}(r, \Omega) \frac{\partial Q^g(\mathbf{q}; r, \Omega)}{\partial q_{m_2}} \\ &+ \sum_{g=1}^G \int_V dV \int_{4\pi} d\Omega u_{2,j}^{(2),g}(r, \Omega) \frac{\partial Q^g(\mathbf{q}; r, \Omega)}{\partial q_{m_2}} + \sum_{g=1}^G \int_V dV \int_{4\pi} d\Omega \psi^{(1),g}(r, \Omega) \frac{\partial Q^g(\mathbf{q}; r, \Omega)}{\partial n_j \partial q_{m_2}}, \end{aligned} \quad (178)$$

for $j = 1, \dots, J_n; m_2 = 1, \dots, 10.$

The adjoint functions $\psi_{2,j}^{(2),g}, j = 1, \dots, J_n; g = 1, \dots, G,$ which appear in Equation (178), are the solutions of the 2nd-Level Adjoint Sensitivity System presented in Equations (165)–(166) of [6] and reproduced below, for easy reference:

$$A^{(1),g}(\boldsymbol{\alpha}^0) \psi_{2,i}^{(2),g}(r, \Omega) = -\psi^{(1),g}(r, \Omega) \frac{\partial \Sigma_t^g(\mathbf{t})}{\partial n_j}, \quad i = 1, \dots, J_n; g = 1, \dots, G, \quad (179)$$

$$\psi_{2,i}^{(2),g}(r_d, \Omega) = 0, \quad \Omega \cdot \mathbf{n} > 0; \quad i = 1, \dots, J_n; g = 1, \dots, G. \quad (180)$$

The 2nd-level adjoint functions $\theta_{2,j}^{(2),g}, j = 1, \dots, J_n; g = 1, \dots, G$, are the solutions of the following 2nd-Level Adjoint Sensitivity System presented in Equations (174)–(175) of [6] and reproduced below, for easy reference:

$$A^{(1),g}(\alpha^0)\theta_{2,j}^{(2),g}(r, \Omega) = \sum_{g'=1}^G \int_{4\pi} d\Omega' \psi^{(1),g'}(r, \Omega') \frac{\partial \Sigma_s^{g \rightarrow g'}(s; \Omega \rightarrow \Omega')}{\partial n_j}, j = 1, \dots, J_n; g = 1, \dots, G, \tag{181}$$

$$\theta_{2,j}^{(2),g}(r_d, \Omega) = 0, \Omega \cdot \mathbf{n} > 0; j = 1, \dots, J_n; g = 1, \dots, G. \tag{182}$$

The 2nd-level adjoint functions $u_{2,j}^{(2),g}, j = 1, \dots, J_{\sigma f}; g = 1, \dots, G$ are the solutions of the 2nd-Level Adjoint Sensitivity System presented in Equations (184)–(185) of [6], and reproduced below for convenient reference:

$$A^{(1),g}(\alpha^0)u_{2,j}^{(2),g}(r, \Omega) = \frac{\partial [(v\Sigma_f)^g(\mathbf{f})]}{\partial n_j} \sum_{g'=1}^G \int_{4\pi} d\Omega' \psi^{(1),g'}(r, \Omega') \chi^{g'}, j = 1, \dots, J_n; g = 1, \dots, G, \tag{183}$$

$$u_{2,j}^{(2),g}(r_d, \Omega) = 0, \Omega \cdot \mathbf{n} > 0; j = 1, \dots, J_n; g = 1, \dots, G. \tag{184}$$

Noting that:

$$\frac{\partial Q^g(\mathbf{q}; r, \Omega)}{\partial n_j \partial q_{m_2}} = 0 \quad j \neq m_2 \text{ and } j \neq 1, 2, \tag{185}$$

inserting the results obtained in Equations (18)–(24), (42), (46), (52), (56) and (57) into Equation (178), and performing the respective angular integrations yields the following expression for Equation (178):

For $j = 1, \dots, J_n; m_2 = 1, 2$:

$$\begin{aligned} \frac{\partial^2 L}{\partial n_j \partial q_{m_2}} &= \frac{\partial^2 L}{\partial n_j \partial \lambda_k} = \frac{1}{\lambda_k} \sum_{g=1}^G \int_V dV \left[\xi_{2,j;0}^{(2),g}(r) + \Theta_{2,j;0}^{(2),g}(r) + U_{2,j;0}^{(2),g}(r) \right] Q_{SF,k}^g \\ &+ \delta_{jk} \frac{1}{n_j \lambda_k} \sum_{g=1}^G \int_V dV \xi_0^{(1),g}(r) Q_{SF,k'}^g \quad k = 1, 2; \end{aligned} \tag{186}$$

For $j = 1, \dots, J_n; m_2 = 3, 4$:

$$\begin{aligned} \frac{\partial^2 L}{\partial n_j \partial q_{m_2}} &= \frac{\partial^2 L}{\partial n_j \partial F_k^{SF}} = \frac{1}{F_k^{SF}} \sum_{g=1}^G \int_V dV \left[\xi_{2,j;0}^{(2),g}(r) + \Theta_{2,j;0}^{(2),g}(r) + U_{2,j;0}^{(2),g}(r) \right] Q_{SF,k}^g \\ &+ \delta_{jk} \frac{1}{n_j F_k^{SF}} \sum_{g=1}^G \int_V dV \xi_0^{(1),g}(r) Q_{SF,k'}^g \quad k = 1, 2; \end{aligned} \tag{187}$$

For $j = 1, \dots, J_n; m_2 = 5, 6$:

$$\begin{aligned} \frac{\partial^2 L}{\partial n_j \partial q_{m_2}} &= \frac{\partial^2 L}{\partial n_j \partial a_k} = \lambda_k N_{k,1} F_k^{SF} v_k^{SF} \sum_{g=1}^G \int_V dV \left[\xi_{2,j;0}^{(2),g}(r) + \Theta_{2,j;0}^{(2),g}(r) + U_{2,j;0}^{(2),g}(r) \right] Da(g; a_k, b_k) \\ &+ \delta_{jk} \lambda_k F_k^{SF} v_k^{SF} \sum_{g=1}^G \int_V dV \xi_0^{(1),g}(r) Da(g; a_k, b_k), \quad k = 1, 2; \end{aligned} \tag{188}$$

For $j = 1, \dots, J_n; m_2 = 7, 8$:

$$\begin{aligned} \frac{\partial^2 L}{\partial n_j \partial q_{m_2}} &= \frac{\partial^2 L}{\partial n_j \partial b_k} = \lambda_k N_{k,1} F_k^{SF} v_k^{SF} \sum_{g=1}^G \int_V dV \left[\xi_{2,j;0}^{(2),g}(r) + \Theta_{2,j;0}^{(2),g}(r) + U_{2,j;0}^{(2),g}(r) \right] Db(g; a_k, b_k) \\ &+ \delta_{jk} \lambda_k F_k^{SF} v_k^{SF} \sum_{g=1}^G \int_V dV \xi_0^{(1),g}(r) Db(g; a_k, b_k), \quad k = 1, 2; \end{aligned} \tag{189}$$

For $j = 1, \dots, J_n; m_2 = 9, 10$:

$$\begin{aligned} \frac{\partial^2 L}{\partial n_j \partial q_{m_2}} &= \frac{\partial^2 L}{\partial n_j \partial v_k^{SF}} = \frac{1}{v_k^{SF}} \sum_{g=1}^G \int_V dV \left[\xi_{2,j;0}^{(2),g}(r) + \Theta_{2,j;0}^{(2),g}(r) + U_{2,j;0}^{(2),g}(r) \right] Q_{SF,k}^g \\ &+ \delta_{jk} \frac{1}{n_j v_k^{SF}} \sum_{g=1}^G \int_V dV \xi_0^{(1),g}(r) Q_{SF,k}^g \quad k = 1, 2. \end{aligned} \tag{190}$$

7.3. Numerical Results for $\partial^2 L(\alpha) / \partial q \partial N$

The second-order absolute sensitivities, $\partial^2 L(\alpha) / \partial q \partial N$, of the leakage response with respect to the source parameters and the isotopic number densities for all isotopes of the PERP benchmark have been computed using Equation (177), and have been independently verified by computing $\partial^2 L(\alpha) / \partial N \partial q$ using Equations (186)–(190). The matrix $\partial^2 L / \partial q_j \partial n_{m_2}$, $j = 1, \dots, 10; m_2 = 1, \dots, J_n$ has dimensions 10×6 . The matrix of 2nd-order relative sensitivities corresponding to $\partial^2 L / \partial q_j \partial n_{m_2}$, $j = 1, \dots, 10; m_2 = 1, \dots, J_n$, will be denoted as $S^{(2)}(q_j, N_{i,m})$ and is defined as follows:

$$S^{(2)}(q_j, N_{k,m}) \triangleq \frac{\partial^2 L}{\partial q_j \partial N_{k,m}} \left(\frac{q_j N_{k,m}}{L} \right), \quad j = 1, \dots, 10; k = 1, \dots, 6; m = 1, 2. \tag{191}$$

Table 15 summarizes the results for the elements of the matrix $S^{(2)}(q_j, N_{k,m})$, $j = 2, 4, 6, 8, 10; k = 1, \dots, 6; m = 1, 2$ of 2nd-order relative sensitivities of the leakage response with respect to the source parameters of isotope ^{240}Pu and the isotopic number densities for all isotopes in the PERP benchmark.

Table 15. Results for the elements of $S^{(2)}(q_j, N_{k,m})$, $j = 2, 4, 6, 8, 10; k = 1, \dots, 6; m = 1, 2$.

	$k=1$ (^{239}Pu)	$k=2$ (^{240}Pu)	$k=3$ (^{69}Ga)	$k=4$ (^{71}Ga)	$k=5$ (C)	$k=6$ (^1H)
λ_2	$S^{(2)}(\lambda_2, N_{1,1})$ = 5.967	$S^{(2)}(\lambda_2, N_{2,1})$ = 1.219	$S^{(2)}(\lambda_2, N_{3,1})$ $= 2.228 \times 10^{-3}$	$S^{(2)}(\lambda_2, N_{4,1})$ $= 1.364 \times 10^{-3}$	$S^{(2)}(\lambda_2, N_{5,2})$ $= 6.310 \times 10^{-1}$	$S^{(2)}(\lambda_2, N_{6,2})$ = 1.001
F_2^{SF}	$S^{(2)}(F_2^{SF}, N_{1,1})$ = 5.967	$S^{(2)}(F_2^{SF}, N_{2,1})$ = 1.219	$S^{(2)}(F_2^{SF}, N_{3,1})$ $= 2.228 \times 10^{-3}$	$S^{(2)}(F_2^{SF}, N_{4,1})$ $= 1.364 \times 10^{-3}$	$S^{(2)}(F_2^{SF}, N_{5,2})$ $= 6.310 \times 10^{-1}$	$S^{(2)}(F_2^{SF}, N_{6,2})$ = 1.001
a_2	$S^{(2)}(a_2, N_{1,1})$ $= 3.065 \times 10^{-1}$	$S^{(2)}(a_2, N_{2,1})$ $= 2.592 \times 10^{-2}$	$S^{(2)}(a_2, N_{3,1})$ $= 7.758 \times 10^{-5}$	$S^{(2)}(a_2, N_{4,1})$ $= 7.537 \times 10^{-5}$	$S^{(2)}(a_2, N_{5,2})$ $= 1.078 \times 10^{-2}$	$S^{(2)}(a_2, N_{6,2})$ $= -1.709 \times 10^{-2}$
b_2	$S^{(2)}(b_2, N_{1,1})$ $= 8.202 \times 10^{-2}$	$S^{(2)}(b_2, N_{2,1})$ $= 7.648 \times 10^{-3}$	$S^{(2)}(b_2, N_{3,1})$ $= 1.934 \times 10^{-5}$	$S^{(2)}(b_2, N_{4,1})$ $= 2.083 \times 10^{-5}$	$S^{(2)}(b_2, N_{5,2})$ $= 2.386 \times 10^{-3}$	$S^{(2)}(b_2, N_{6,2})$ $= -6.788 \times 10^{-3}$
v_2^{SF}	$S^{(2)}(v_2^{SF}, N_{1,1})$ = 5.967	$S^{(2)}(v_2^{SF}, N_{2,1})$ = 1.219	$S^{(2)}(v_2^{SF}, N_{3,1})$ $= 2.228 \times 10^{-3}$	$S^{(2)}(v_2^{SF}, N_{4,1})$ $= 1.364 \times 10^{-3}$	$S^{(2)}(v_2^{SF}, N_{5,2})$ $= 6.310 \times 10^{-1}$	$S^{(2)}(v_2^{SF}, N_{6,2})$ = 1.001

As shown (in bold) in Table 15, the values of 9 elements in the matrix $S^{(2)}(q_j, N_{k,m})$ are greater than 1.0. The elements $S^{(2)}(\lambda_2, N_{k,m})$, $S^{(2)}(F_2^{SF}, N_{k,m})$ and $S^{(2)}(v_2^{SF}, N_{k,m})$, $k = 1, \dots, 6; m = 1, 2$, have identical values. Of the sensitivities presented in Table 15, the largest relative sensitivities are $S^{(2)}(\lambda_2, N_{1,1}) = S^{(2)}(F_2^{SF}, N_{1,1}) = S^{(2)}(v_2^{SF}, N_{1,1}) = 5.967$. Adding ^{239}Pu will considerably affect the sensitivity of other parameters. Also, all the mixed 2nd-order sensitivities of the leakage response with respect to the source parameters and the isotopic number densities are positive, except for $S^{(2)}(a_2, N_{6,2})$ and $S^{(2)}(b_2, N_{6,2})$, which have negative values.

8. Quantification of Uncertainties in the PERP Leakage Response due to Uncertainties in Source Parameters

Correlations between the source parameters or correlations between these source parameters and other cross section parameters are not available for the PERP benchmark. As discussed in [1–3], when such correlations are unavailable, the maximum entropy principle (see, e.g., Ref. [14]) indicates that neglecting them minimizes the inadvertent introduction of spurious information into the computations

of the various moments of the response's distribution in parameter space. Considering the PERP leakage response 1st- and 2nd-order sensitivities with respect to the PERP benchmark's source parameters, the formulas for computing the expected value, variance and skewness of the leakage response distribution are as follows:

1) The expected value, $[E(L)]_q$, of the leakage response $L(\alpha)$ has the following expression:

$$[E(L)]_q = L(\alpha^0) + [E(L)]_q^{(2,U)}, \quad (192)$$

where the superscript "U" indicates contributions solely from the *uncorrelated* source parameters, and where the term $[E(L)]_q^{(2,U)}$, which provides the 2nd-order contributions, is given by the following expression:

$$[E(L)]_q^{(2,U)} = \frac{1}{2} \sum_{i=1}^{J_q} \frac{\partial^2 L(\alpha)}{\partial q_i \partial q_i} (s_{q_i})^2, \quad J_q = 12. \quad (193)$$

In Equation (193), the quantity s_{q_i} denotes the standard deviation associated with the imprecisely known model parameter q_i , $i = 1, \dots, J_q$.

2) Taking into account contributions solely from the uncorrelated and normally-distributed source parameters (which will be indicated by using the superscript "(U,N)" in the following equations), the expression for computing the variance, denoted as $[\text{var}(L)]_q^{(U,N)}$, of the PERP leakage response has the following form:

$$[\text{var}(L)]_q^{(U,N)} = [\text{var}(L)]_q^{(1,U,N)} + [\text{var}(L)]_q^{(2,U,N)}, \quad (194)$$

where the first-order contribution term, $[\text{var}(L)]_q^{(1,U,N)}$, to the variance $[\text{var}(L)]_q^{(U,N)}$ is defined as follows:

$$[\text{var}(L)]_q^{(1,U,N)} \triangleq \sum_{i=1}^{J_q} \left[\frac{\partial L(\alpha)}{\partial q_i} \right]^2 (s_{q_i})^2, \quad J_q = 12, \quad (195)$$

while the second-order contribution term, $[\text{var}(L)]_q^{(2,U,N)}$, to the variance $[\text{var}(L)]_q^{(U,N)}$ is defined as follows:

$$[\text{var}(L)]_q^{(2,U,N)} \triangleq \frac{1}{2} \sum_{i=1}^{J_q} \left[\frac{\partial^2 L(\alpha)}{\partial q_i \partial q_i} (s_{q_i})^2 \right]^2, \quad J_q = 12. \quad (196)$$

3) Considering contributions solely from the uncorrelated normally-distributed source parameters, the third-order moment, $[\mu_3(L)]_q^{(U,N)}$, of the leakage response for the PERP benchmark takes on the following form:

$$[\mu_3(L)]_q^{(U,N)} = 3 \sum_{i=1}^{J_q} \left[\frac{\partial L(\alpha)}{\partial q_i} \right]^2 \frac{\partial^2 L(\alpha)}{\partial q_i \partial q_i} (s_{q_i})^4, \quad J_q = 12. \quad (197)$$

As Equation (197) indicates, if the 2nd-order sensitivities were unavailable, the third moment $[\mu_3(L)]_q^{(U,N)}$ would vanish and the response distribution would by default be assumed to be Gaussian.

4) The skewness, $[\gamma_1(L)]_q^{(U,N)}$, due to the variances of source parameters in the leakage response, L , is defined as follows:

$$[\gamma_1(L)]_q^{(U,N)} = [\mu_3(L)]_q^{(U,N)} / \left\{ [\text{var}(L)]_q^{(U,N)} \right\}^{3/2}. \quad (198)$$

The effects of the first- and second-order sensitivities on the response's expected value, variance and skewness are quantified by considering typical values for the standard deviations for the uncorrelated source parameters, using these values together with the respective sensitivities computed in Section 2 in Equations (192) through (198). The results thus obtained are presented in Table 16, considering uniform parameter standard deviations of 1%, 5%, and 10%, respectively. These results indicate that

the effects of both the first- and second-order sensitivities on the expected response value, its standard deviation and skewness are negligible, which is expected in view of the small values for the first- and second-order sensitivities presented in Tables 4 and 5.

Table 16. Comparison of Response Moments Induced by Various Relative Standard Deviations Assumed for the Source Parameters q_i .

Relative Standard Deviation	10%	5%	1%
$L(\alpha^0)$	1.7648×10^6	1.7648×10^6	1.7648×10^6
$[E(L)]_q^{(2,U)}$	5.9586×10^2	1.4897×10^2	5.9586×10^0
$[E(L)]_q = L(\alpha^0) + [E(L)]_q^{(2,U)}$	1.7654×10^6	1.7649×10^6	1.7648×10^6
$[\text{var}(L)]_q^{(1,U,N)}$	1.2459×10^{11}	3.1147×10^{10}	1.2459×10^9
$[\text{var}(L)]_q^{(2,U,N)}$	6.7741×10^5	4.2338×10^4	6.7741×10^1
$[\text{var}(L)]_q^{(U,N)} =$ $[\text{var}(L)]_q^{(1,U,N)} +$ $[\text{var}(L)]_q^{(2,U,N)}$	1.2459×10^{11}	3.1147×10^{10}	1.2459×10^9
$[\mu_3(L)]_q^{(U,N)}$	2.0825×10^{11}	1.3016×10^{10}	2.0825×10^7
$[\gamma_1(L)]_q^{(U,N)} =$ $[\mu_3(L)]_q^{(U,N)} / \{[\text{var}(L)]_q^{(U,N)}\}^{3/2}$	4.7356×10^{-6}	2.3678×10^{-6}	4.7356×10^{-7}

The relative effects of uncertainties in the source parameters can be compared to the corresponding effects stemming from the total and scattering cross sections, respectively, by considering standard deviations of 10% for all of these parameters and by comparing the corresponding results shown in Table 16 with the corresponding results presented in Table 25 from Part I [1] and Table 19 from Part II [2]. This comparison reveals that the following relations hold:

$$\begin{aligned}
 [E(L)]_q^{(2,U)} &= 5.9586 \times 10^2 \ll |[E(L)]_s^{(2,U)}| = 1.3473 \times 10^4 \ll [E(L)]_f^{(2,U)} = 4.5980 \times 10^6, \\
 [\text{var}(L)]_s^{(1,U,N)} &= 1.2379 \times 10^{10} < [\text{var}(L)]_q^{(1,U,N)} = 1.2459 \times 10^{11} \ll [\text{var}(L)]_f^{(1,U,N)} = 3.4196 \times 10^{12}, \\
 [\text{var}(L)]_q^{(2)} &= 6.7741 \times 10^5 \ll [\text{var}(L)]_s^{(2)} = 4.3207 \times 10^7 \ll [\text{var}(L)]_f^{(2)} = 2.8789 \times 10^{13}, \\
 [\gamma_1(L)]_q^{(U,N)} &= 4.7356 \times 10^{-4} < |[\gamma_1(L)]_s^{(U,N)}| = 3.5595 \times 10^{-3} \ll [\gamma_1(L)]_f^{(U,N)} = 0.3407.
 \end{aligned}$$

The above relations indicate that the contributions to the expected value, second-order variance and skewness stemming from the uncorrelated source parameters are much smaller than the corresponding contributions stemming from the group-averaged uncorrelated microscopic scattering and total cross sections. However, the contributions to the first-order variance stemming from uncorrelated source parameters are larger than those stemming from the uncorrelated microscopic scattering cross sections but are much smaller than those stemming from the uncorrelated microscopic total cross sections.

Correlations between the source parameters are not available in the literature. Hence, the results presented in Table 16 consider only illustrative values for the standard deviations of the source parameters and unmixed 2nd-order sensitivities, in addition to the 1st-order sensitivities. On the other hand, the results presented in Sections 3–7 indicated that several mixed 2nd-order sensitivities in matrices $\partial^2 L(\alpha) / \partial \mathbf{q} \partial \sigma_t$, $\partial^2 L(\alpha) / \partial \mathbf{q} \partial \nu$ and $\partial^2 L(\alpha) / \partial \mathbf{q} \partial \mathbf{N}$, have large values, as follows:

(a) 32 elements of the matrix $\mathbf{S}^{(2)}(q_j, \sigma_{t,k}^g)$, $j = 2, 4, 6, 8, 10, 12$; $k = 1, \dots, 6$; $g = 1, \dots, 30$, presented in Table 7;

(b) four elements of the matrix $\mathbf{S}^{(2)}(q_j, v_k^g)$, $j = 2, 4, 6, 8, 10, 12$; $k = 1, 2$; $g = 1, \dots, 30$, presented in Table 13.

(c) nine elements of the matrix $\mathbf{S}^{(2)}(q_j, N_{k,m})$, $j = 2, 4, 6, 8, 10$; $k = 1, \dots, 6$; $m = 1, 2$, presented in Table 15.

It would be very important to establish if correlations among the model parameters mentioned in items (a)–(c), above, since such correlations could contribute, in conjunction with the respective mixed second-order sensitivities, to the values of the response moments. Since the mixed second-order sensitivities of the leakage response to the source parameters and group-averaged total microscopic cross sections are significantly larger than the unmixed second-order sensitivities of the leakage response to the source parameters, it is likely that the correlations among the respective source parameters and the total cross sections could provide significantly larger contributions to the response moments than just the standard deviations of the source parameters.

9. Discussions and Conclusions Related to the Sensitivities and Uncertainties to the Source Parameters

This work has presented results for the first-order sensitivities, $\partial L(\alpha)/\partial \mathbf{q}$, and the second-order sensitivities $\partial^2 L(\alpha)/\partial \mathbf{q} \partial \mathbf{q}$ of the PERP total leakage response with respect to the source parameters. In addition, this work has also presented the results for the mixed second-order sensitivities $\partial^2 L(\alpha)/\partial \mathbf{q} \partial \sigma_t$, $\partial^2 L(\alpha)/\partial \mathbf{q} \partial \sigma_s$, $\partial^2 L(\alpha)/\partial \mathbf{q} \partial \sigma_f$, $\partial^2 L(\alpha)/\partial \mathbf{q} \partial \mathbf{v}$ and $\partial^2 L(\alpha)/\partial \mathbf{q} \partial \mathbf{N}$. The following conclusions can be drawn from the results reported in this work:

- (1) The 1st-order relative sensitivities of the PERP leakage response with respect to the source parameters for the fissionable isotopes are all positive, signifying that an increase in the source parameters will cause an increase in the total neutron leakage from the PERP sphere.
- (2) The 1st-order relative sensitivities for $S^{(1)}(\lambda_i)$, $S^{(1)}(F_i^{SF})$, $S^{(1)}(v_i^{SF})$ and $S^{(1)}(N_{i,1})$ for $i = 1, 2$ have the same value, although their absolute sensitivities differ from each other. The 1st-order relative sensitivities with respect to the source parameters of isotope ^{239}Pu are very small, of the order of 10^{-4} or less. However, the 1st-order relative sensitivities with respect to the source parameters λ_2 , F_2^{SF} , v_2^{SF} , and $N_{2,1}$ of isotope ^{240}Pu are quite large, with values close to 1.0.
- (3) The following relations hold for the 1st- and 2nd-order sensitivities to the source parameters: $S^{(1)}(\lambda_i) = S^{(1)}(F_i^{SF}) = S^{(1)}(v_i^{SF}) = S^{(1)}(N_{i,1}) = S^{(2)}(\lambda_i, F_i^{SF}) = S^{(2)}(\lambda_i, v_i^{SF}) = S^{(2)}(\lambda_i, N_{i,1}) = S^{(2)}(F_i^{SF}, v_i^{SF}) = S^{(2)}(F_i^{SF}, N_{i,1}) = S^{(2)}(v_i^{SF}, N_{i,1})$; $S^{(1)}(a_i) = S^{(2)}(\lambda_i, a_i) = S^{(2)}(F_i^{SF}, a_i) = S^{(2)}(a_i, v_i^{SF}) = S^{(2)}(a_i, N_{i,1})$; and $S^{(1)}(b_i) = S^{(2)}(\lambda_i, b_i) = S^{(2)}(F_i^{SF}, b_i) = S^{(2)}(b_i, v_i^{SF}) = S^{(2)}(b_i, N_{i,1})$ for $i = 1, 2$.
- (4) The 2nd-order sensitivities $\partial^2 L(\alpha)/\partial \mathbf{q} \partial \mathbf{q}$ are all positive. The 2nd-order relative sensitivities of the leakage response with respect to the source parameters of isotope ^{239}Pu are very small, of the order of 10^{-4} or less. However, several mixed 2nd-order relative sensitivities of the leakage response with respect to the source parameters of isotope ^{240}Pu are quite large, having values close to 1.0. The unmixed 2nd-order sensitivities in the matrix $\mathbf{S}^{(2)}(q_j, q_{m_2})$, $j, m_2 = 1, \dots, J_q$ are mostly zero, except for $S^{(2)}(a_i, a_i)$ and $S^{(2)}(b_i, b_i)$, $i = 1, 2$. Moreover, the unmixed 2nd-order relative sensitivity with respect to the Watt's coefficient a_2 , namely, $S^{(2)}(a_2, a_2)$, is about 50% larger than the corresponding 1st-order one; whereas the value of the 2nd-order relative sensitivity with respect to the Watt's coefficient b_2 , namely, $S^{(2)}(b_2, b_2)$, is about 1/7 of the value of the corresponding 1st-order sensitivity $S^{(1)}(b_2)$.
- (5) For the 2nd-order mixed sensitivities $\partial^2 L(\alpha)/\partial \mathbf{q} \partial \sigma_t$, among the $J_q \times J_{\sigma_t}$ ($= 2160$) elements of the matrix $\mathbf{S}^{(2)}(q_j, \sigma_{t,k}^g)$, $j = q_j$; $k = 1, \dots, 6$; $g = 1, \dots, 30$, 32 elements have relative sensitivities greater than 1.0. These large sensitivities involve the total cross sections of isotopes ^{239}Pu or ^1H . However, when the source parameters a_i or b_i , or the total cross sections of isotopes ^{240}Pu , ^{69}Ga , ^{71}Ga and C are involved, the absolute values of the mixed 2nd-order relative

sensitivities are all smaller than 1.0. The largest absolute values in the matrix $\mathbf{S}^{(2)}(q_j, \sigma_{t,k}^g)$ are $\mathbf{S}^{(2)}(\lambda_2, \sigma_{t,6}^{g=30}) = \mathbf{S}^{(2)}(F_2^{SF}, \sigma_{t,6}^{g=30}) = \mathbf{S}^{(2)}(v_2^{SF}, \sigma_{t,6}^{g=30}) = \mathbf{S}^{(2)}(N_{2,1}, \sigma_{t,6}^{g=30}) = -9.364$. Also, all the elements in the submatrices $\mathbf{S}^{(2)}(\lambda_2, \sigma_{t,k}^g)$, $\mathbf{S}^{(2)}(F_2^{SF}, \sigma_{t,k}^g)$, $\mathbf{S}^{(2)}(v_2^{SF}, \sigma_{t,k}^g)$ and $\mathbf{S}^{(2)}(N_{2,1}, \sigma_{t,k}^g)$ have negative values; whereas the elements in submatrices $\mathbf{S}^{(2)}(a_2, \sigma_{t,k}^g)$ and $\mathbf{S}^{(2)}(b_2, \sigma_{t,k}^g)$ can have positive or negative values, depending on the energy group as well as the isotope of the microscopic total cross sections.

- (6) For the 2nd-order mixed sensitivities $\partial^2 L(\alpha) / \partial \mathbf{q} \partial \sigma_s$, the corresponding relative sensitivities are all smaller than 1.0. The overall largest value in the matrix $\mathbf{S}^{(2)}(q_j, \sigma_{s,l=0,k}^{g' \rightarrow g})$ is $S^{(2)}(\lambda_2, \sigma_{s,l=0,5}^{12 \rightarrow 12}) = S^{(2)}(F_2^{SF}, \sigma_{s,l=0,5}^{12 \rightarrow 12}) = S^{(2)}(v_2^{SF}, \sigma_{s,l=0,5}^{12 \rightarrow 12}) = S^{(2)}(N_{2,1}, \sigma_{s,l=0,5}^{12 \rightarrow 12}) = 0.681$. All of these (largest) sensitivities are related to the 0th-order self-scattering cross section for the 12th energy group of isotope 5 (C). For the 2nd-order mixed relative sensitivities with respect to the source parameters and the 0th-order (i.e., $l = 0$) scattering microscopic cross sections, the values of the relative sensitivities can be positive or negative, but there are more positive values than negative ones. For the 2nd-order mixed relative sensitivities with respect to the source parameters and the 1st-order (i.e., $l = 1$) scattering microscopic cross sections, the overall largest (absolute) value is $S^{(2)}(\lambda_2, \sigma_{s,l=1,k=6}^{12 \rightarrow 13}) = S^{(2)}(F_2^{SF}, \sigma_{s,l=1,k=6}^{12 \rightarrow 13}) = S^{(2)}(v_2^{SF}, \sigma_{s,l=1,k=6}^{12 \rightarrow 13}) = S^{(2)}(N_{2,1}, \sigma_{s,l=1,k=6}^{12 \rightarrow 13}) = -0.104$; these sensitivities involve the 1st-order out-scattering cross section $\sigma_{s,l=0,k=6}^{12 \rightarrow 13}$ of isotope ^1H . In addition, for the scattering order $l = 1$, the values of the relative sensitivities can also be positive or negative, but there are more negative values than positive ones. The values for the 2nd-order mixed relative sensitivities of the leakage response with respect to the source parameters of isotope ^{240}Pu and the higher-order (i.e., $l = 2, 3$) scattering cross sections for all isotopes in the PERP benchmark are all very small, in the order of 10^{-2} or less.
- (7) For the 2nd-order mixed sensitivities $\partial^2 L(\alpha) / \partial \mathbf{q} \partial \sigma_f$, it has been found that the values of the corresponding relative sensitivities are all smaller than 1.0. The single largest relative value is $S^{(2)}(\lambda_2, \sigma_{f,1}^{g=12}) = S^{(2)}(F_2^{SF}, \sigma_{f,1}^{g=12}) = S^{(2)}(v_2^{SF}, \sigma_{f,1}^{g=12}) = S^{(2)}(N_{2,1}, \sigma_{f,1}^{g=12}) = 0.882$. All elements in the submatrices $\mathbf{S}^{(2)}(\lambda_2, \sigma_{f,k}^g)$, $\mathbf{S}^{(2)}(F_2^{SF}, \sigma_{f,k}^g)$, $\mathbf{S}^{(2)}(v_2^{SF}, \sigma_{f,k}^g)$ and $\mathbf{S}^{(2)}(N_{2,1}, \sigma_{f,k}^g)$ have positive values, and the element with the maximum absolute value in each of these submatrices relates to the microscopic fission cross sections for the 12th energy group of isotopes ^{239}Pu and ^{240}Pu (namely, $\sigma_{f,k}^{g=12}$, $k = 1, 2$). For the submatrices $\mathbf{S}^{(2)}(a_2, \sigma_{f,k}^g)$ and $\mathbf{S}^{(2)}(b_2, \sigma_{f,k}^g)$, the values of the elements can be positive or negative, and the element with the maximum absolute value in each of the submatrices $\mathbf{S}^{(2)}(a_2, \sigma_{f,k}^g)$ and $\mathbf{S}^{(2)}(b_2, \sigma_{f,k}^g)$ relates to the microscopic fission cross sections for the 7th energy group of isotopes ^{239}Pu and ^{240}Pu (i.e., $\sigma_{f,k}^{g=7}$, $k = 1, 2$).
- (8) For the 2nd-order mixed sensitivities $\partial^2 L(\alpha) / \partial \mathbf{q} \partial \nu$, the corresponding relative sensitivities are mostly smaller than 1.0; only 4 elements with absolute values greater than 1.0, which are $S^{(2)}(\lambda_2, \nu_{k=1}^{g=12}) = S^{(2)}(F_2^{SF}, \nu_{k=1}^{g=12}) = S^{(2)}(v_2^{SF}, \nu_{k=1}^{g=12}) = S^{(2)}(N_{2,1}, \nu_{k=1}^{g=12}) = 1.214$. Similarly, all elements in the submatrices $\mathbf{S}^{(2)}(\lambda_2, \nu_k^g)$, $\mathbf{S}^{(2)}(F_2^{SF}, \nu_k^g)$, $\mathbf{S}^{(2)}(v_2^{SF}, \nu_k^g)$ and $\mathbf{S}^{(2)}(N_{2,1}, \nu_k^g)$ for $k = 1, 2$ have positive values, and the element with the maximum absolute value in each of these submatrices relates to the average number of neutrons per fission for the 12th energy group of the isotopes (namely, $\nu_k^{g=12}$, $k = 1, 2$). The elements in submatrices $\mathbf{S}^{(2)}(a_2, \nu_k^g)$ and $\mathbf{S}^{(2)}(b_2, \nu_k^g)$ have positive values for $g = 1, \dots, 10$, and have negative values for $g = 11, \dots, 30$. The elements having the maximum absolute value in each of the submatrices $\mathbf{S}^{(2)}(a_2, \nu_k^g)$ and $\mathbf{S}^{(2)}(b_2, \nu_k^g)$ pertain to the average number of neutrons per fission for the 7th energy group of the isotopes ^{239}Pu and ^{240}Pu (namely, $\nu_k^{g=7}$, $k = 1, 2$). The reason that the maximum absolute value in each of submatrices mostly relates to energy groups 7 and 12 is because those groups have high leakage, as shown in Figure 1. The high leakage in those groups is due to the fission spectrum of the isotopes ^{239}Pu and ^{240}Pu , as illustrated in Figure 4 from Part III [3], where most of the spectrum is concentrated

in the energy region $g = 7, \dots, 14$, with the largest portion contained in group 12, and the next largest contained in group 7.

- (9) For the 2nd-order mixed sensitivities $\partial^2 L(\boldsymbol{\alpha}) / \partial \mathbf{q} \partial \mathbf{N}$, it has been found that among the 60 elements in the relative sensitivity matrix $\mathbf{S}^{(2)}(q_j, N_{k,m})$, there are 9 elements having values greater than 1.0; these are: $S^{(2)}(\lambda_2, N_{1,1}) = S^{(2)}(F_2^{SF}, N_{1,1}) = S^{(2)}(v_2^{SF}, N_{1,1}) = 5.967$; $S^{(2)}(\lambda_2, N_{2,1}) = S^{(2)}(F_2^{SF}, N_{2,1}) = S^{(2)}(\lambda_2, N_{2,1}) = 1.219$; and $S^{(2)}(\lambda_2, N_{6,2}) = S^{(2)}(F_2^{SF}, N_{6,2}) = S^{(2)}(v_2^{SF}, N_{6,2}) = 1.001$. The elements $S^{(2)}(\lambda_2, N_{k,m})$, $S^{(2)}(F_2^{SF}, N_{k,m})$, and $S^{(2)}(v_2^{SF}, N_{k,m})$, $k = 1, \dots, 6$; $m = 1, 2$, have identical values. Also, all of the mixed 2nd-order sensitivities of the leakage response with respect to the source parameters and the isotopic number densities are positive, except for $S^{(2)}(a_2, N_{6,2})$ and $S^{(2)}(b_2, N_{6,2})$, which have negative values.
- (9) By considering typical values for the standard deviations for the uncorrelated source parameters, it has been found that the effects of both the first- and second-order sensitivities on the expected response value, its standard deviation and skewness are negligible. However, many mixed 2nd-order sensitivities in matrices $\partial^2 L(\boldsymbol{\alpha}) / \partial \mathbf{q} \partial \sigma_t$, $\partial^2 L(\boldsymbol{\alpha}) / \partial \mathbf{q} \partial \mathbf{v}$ and $\partial^2 L(\boldsymbol{\alpha}) / \partial \mathbf{q} \partial \mathbf{N}$ are significantly larger than the unmixed 2nd-order sensitivities of the leakage response with respect to the source parameters. Therefore, it would be very important to obtain correlations among the various model parameters, since the correlations among the source parameters and other model parameters (e.g., total cross sections, average number of neutrons per fission, and isotopic number densities) could provide significantly larger contributions to the response moments than the standard deviations of the source parameters.

Author Contributions: D.G.C. conceived and directed the research reported herein, developed the general theory of the second-order comprehensive adjoint sensitivity analysis methodology to compute 1st- and 2nd-order sensitivities of flux functionals in a multiplying system with source, and the uncertainty equations for response moments. R.F. derived the expressions of the various derivatives with respect to the model parameters to the PERP benchmark and performed all the numerical calculations. All authors have read and agreed to the published version of the manuscript.

Acknowledgments: This work was partially funded by the United States National Nuclear Security Administration's Office of Defense Nuclear Nonproliferation Research & Development, grand number 155040-FD50.

Conflicts of Interest: The authors declare no conflict of interest. The founding sponsors had no role in the design of the study; in the collection, analyses, or interpretation of data; in the writing of the manuscript, and in the decision to publish the results.

Appendix A Definitions of PERP Model Parameters

As presented in Part I [1], the components of the vector of 1st-order sensitivities of the leakage response with respect to the model parameters, denoted as $\mathbf{S}^{(1)}(\boldsymbol{\alpha})$, is defined as follows:

$$\mathbf{S}^{(1)}(\boldsymbol{\alpha}) \triangleq \left[\frac{\partial L(\boldsymbol{\alpha})}{\partial \sigma_t}; \frac{\partial L(\boldsymbol{\alpha})}{\partial \sigma_s}; \frac{\partial L(\boldsymbol{\alpha})}{\partial \sigma_f}; \frac{\partial L(\boldsymbol{\alpha})}{\partial \mathbf{v}}; \frac{\partial L(\boldsymbol{\alpha})}{\partial \mathbf{p}}; \frac{\partial L(\boldsymbol{\alpha})}{\partial \mathbf{q}}; \frac{\partial L(\boldsymbol{\alpha})}{\partial \mathbf{N}} \right]^{\dagger}. \quad (\text{A1})$$

The symmetric matrix of 2nd-order sensitivities of the leakage response with respect to the model parameters, denoted as $\mathbf{S}^{(2)}(\boldsymbol{\alpha})$, is defined as follows:

$$\mathbf{S}^{(2)}(\boldsymbol{\alpha}) \triangleq \begin{bmatrix} \frac{\partial^2 L(\boldsymbol{\alpha})}{\partial \sigma_t \partial \sigma_t} & * & * & * & * & * & * \\ \frac{\partial^2 L(\boldsymbol{\alpha})}{\partial \sigma_s \partial \sigma_t} & \frac{\partial^2 L(\boldsymbol{\alpha})}{\partial \sigma_s \partial \sigma_s} & * & * & * & * & * \\ \frac{\partial^2 L(\boldsymbol{\alpha})}{\partial \sigma_f \partial \sigma_t} & \frac{\partial^2 L(\boldsymbol{\alpha})}{\partial \sigma_f \partial \sigma_s} & \frac{\partial^2 L(\boldsymbol{\alpha})}{\partial \sigma_f \partial \sigma_f} & * & * & * & * \\ \frac{\partial^2 L(\boldsymbol{\alpha})}{\partial \mathbf{v} \partial \sigma_t} & \frac{\partial^2 L(\boldsymbol{\alpha})}{\partial \mathbf{v} \partial \sigma_s} & \frac{\partial^2 L(\boldsymbol{\alpha})}{\partial \mathbf{v} \partial \sigma_f} & \frac{\partial^2 L(\boldsymbol{\alpha})}{\partial \mathbf{v} \partial \mathbf{v}} & * & * & * \\ \frac{\partial^2 L(\boldsymbol{\alpha})}{\partial \mathbf{p} \partial \sigma_t} & \frac{\partial^2 L(\boldsymbol{\alpha})}{\partial \mathbf{p} \partial \sigma_s} & \frac{\partial^2 L(\boldsymbol{\alpha})}{\partial \mathbf{p} \partial \sigma_f} & \frac{\partial^2 L(\boldsymbol{\alpha})}{\partial \mathbf{p} \partial \mathbf{v}} & \frac{\partial^2 L(\boldsymbol{\alpha})}{\partial \mathbf{p} \partial \mathbf{p}} & * & * \\ \frac{\partial^2 L(\boldsymbol{\alpha})}{\partial \mathbf{q} \partial \sigma_t} & \frac{\partial^2 L(\boldsymbol{\alpha})}{\partial \mathbf{q} \partial \sigma_s} & \frac{\partial^2 L(\boldsymbol{\alpha})}{\partial \mathbf{q} \partial \sigma_f} & \frac{\partial^2 L(\boldsymbol{\alpha})}{\partial \mathbf{q} \partial \mathbf{v}} & \frac{\partial^2 L(\boldsymbol{\alpha})}{\partial \mathbf{q} \partial \mathbf{p}} & \frac{\partial^2 L(\boldsymbol{\alpha})}{\partial \mathbf{q} \partial \mathbf{q}} & * \\ \frac{\partial^2 L(\boldsymbol{\alpha})}{\partial \mathbf{N} \partial \sigma_t} & \frac{\partial^2 L(\boldsymbol{\alpha})}{\partial \mathbf{N} \partial \sigma_s} & \frac{\partial^2 L(\boldsymbol{\alpha})}{\partial \mathbf{N} \partial \sigma_f} & \frac{\partial^2 L(\boldsymbol{\alpha})}{\partial \mathbf{N} \partial \mathbf{v}} & \frac{\partial^2 L(\boldsymbol{\alpha})}{\partial \mathbf{N} \partial \mathbf{p}} & \frac{\partial^2 L(\boldsymbol{\alpha})}{\partial \mathbf{N} \partial \mathbf{q}} & \frac{\partial^2 L(\boldsymbol{\alpha})}{\partial \mathbf{N} \partial \mathbf{N}} \end{bmatrix}. \quad (\text{A2})$$

As defined in Equation (1), the vector $\boldsymbol{\alpha} \triangleq [\sigma_t; \sigma_s; \sigma_f; \mathbf{v}; \mathbf{p}; \mathbf{q}; \mathbf{N}]^\dagger$ denotes the “vector of imprecisely known model parameters”, with vector-components $\sigma_t, \sigma_s, \sigma_f, \mathbf{v}, \mathbf{p}, \mathbf{q}$ and \mathbf{N} , comprising the various model parameters for the microscopic total cross sections, scattering cross sections, fission cross sections, average number of neutrons per fission, fission spectra, sources, and isotopic number densities, which have been described in Part I [1]. For easy referencing, however, the definitions of these model parameters will be provided in the remainder of this Appendix.

The total cross section Σ_t^g for energy group $g, g = 1, \dots, G$, is computed for the PERP benchmark using the following expression:

$$\Sigma_t^g = \sum_{m=1}^{M=2} \Sigma_{t,m}^g; \quad \Sigma_{t,m}^g = \sum_i^I N_{i,m} \sigma_{t,i}^g = \sum_i^I N_{i,m} \left[\sigma_{f,i}^g + \sigma_{c,i}^g + \sum_{g'=1}^G \sigma_{s,l=0,i}^{g \rightarrow g'} \right], \quad m = 1, 2, \quad (\text{A3})$$

where m denotes the materials in the PERP benchmark; $\sigma_{f,i}^g$ and $\sigma_{c,i}^g$ denote, respectively, the tabulated group microscopic fission and neutron capture cross sections for group $g, g = 1, \dots, G$. Other nuclear reactions are negligible in the PERP benchmark. As discussed in Part I [1], the total cross section $\Sigma_t^g \rightarrow \Sigma_t^g(\mathbf{t})$ will depend on the vector of parameters \mathbf{t} , which is defined as follows:

$$\mathbf{f} \triangleq [f_1, \dots, f_{J_{\sigma_f}}; f_{J_{\sigma_f}+1}, \dots, f_{J_{\sigma_f}+J_v}; f_{J_{\sigma_f}+J_v+1}, \dots, f_{J_f}]^\dagger \triangleq [\sigma_f; \mathbf{v}; \mathbf{N}]^\dagger, \quad J_f = J_{\sigma_f} + J_v + J_n, \quad (\text{A4})$$

where:

$$\mathbf{N} \triangleq [n_1, \dots, n_{J_n}]^\dagger \triangleq [N_{1,1}, N_{2,1}, N_{3,1}, N_{4,1}, N_{5,2}, N_{6,2}]^\dagger, \quad J_n = 6, \quad (\text{A5})$$

$$\sigma_t \triangleq [t_1, \dots, t_{J_{\sigma_t}}]^\dagger \triangleq [\sigma_{t,i=1}^1, \sigma_{t,i=1}^2, \dots, \sigma_{t,i=1}^G, \dots, \sigma_{t,i=I'}^g, \dots, \sigma_{t,i=I'}^1, \dots, \sigma_{t,i=I}^G]^\dagger, \quad (\text{A6})$$

$i = 1, \dots, I = 6; \quad g = 1, \dots, G = 30; \quad J_{\sigma_t} = I \times G.$

In Equations (A4) through (A6), the dagger denotes “transposition,” $\sigma_{t,i}^g$ denotes the microscopic total cross section for isotope i and energy group $g, N_{i,m}$ denotes the respective isotopic number density, and J_n denotes the total number of isotopic number densities in the model. Thus, the vector \mathbf{t} comprises a total of $J_t = J_{\sigma_t} + J_n = 30 \times 6 + 6 = 186$ imprecisely known “model parameters” as its components.

The scattering transfer cross section $\Sigma_s^{g' \rightarrow g}(\boldsymbol{\Omega}' \rightarrow \boldsymbol{\Omega})$ from energy group $g', g' = 1, \dots, G$ into energy group $g, g = 1, \dots, G$, is computed using the finite Legendre polynomial expansion of order $ISCT = 3$:

$$\begin{aligned} \Sigma_s^{g' \rightarrow g}(\boldsymbol{\Omega}' \rightarrow \boldsymbol{\Omega}) &= \sum_{m=1}^{M=2} \Sigma_{s,m}^{g' \rightarrow g}(\boldsymbol{\Omega}' \rightarrow \boldsymbol{\Omega}), \\ \Sigma_{s,m}^{g' \rightarrow g}(\boldsymbol{\Omega}' \rightarrow \boldsymbol{\Omega}) &\cong \sum_{i=1}^{I=6} N_{i,m} \sum_{l=0}^{ISCT=3} (2l+1) \sigma_{s,l,i}^{g' \rightarrow g} P_l(\boldsymbol{\Omega}' \cdot \boldsymbol{\Omega}), \quad m = 1, 2, \end{aligned} \quad (\text{A7})$$

where $\sigma_{s,l,i}^{g' \rightarrow g}$ denotes the l -th order Legendre-expanded microscopic scattering cross section from energy group g' into energy group g for isotope i . In view of Equation (A7), the scattering cross section $\Sigma_s^{g' \rightarrow g}(\Omega' \rightarrow \Omega) \rightarrow \Sigma_s^{g' \rightarrow g}(\mathbf{s}; \Omega' \rightarrow \Omega)$ depends on the vector of parameters \mathbf{s} , which is defined as follows:

$$\mathbf{s} \triangleq [s_1, \dots, s_{J_s}]^\dagger \triangleq [s_1, \dots, s_{J_{os}}; n_1, \dots, n_{J_n}]^\dagger \triangleq [\sigma_s; \mathbf{N}]^\dagger, \quad J_s = J_{os} + J_n, \quad (\text{A8})$$

$$\sigma_s \triangleq [s_1, \dots, s_{J_{os}}]^\dagger \triangleq [\sigma_{s,l=0,i=1}^{g'=1 \rightarrow g=1}, \sigma_{s,l=0,i=1}^{g'=2 \rightarrow g=1}, \dots, \sigma_{s,l=0,i=1}^{g'=G \rightarrow g=1}, \sigma_{s,l=0,i=1}^{g'=1 \rightarrow g=2}, \sigma_{s,l=0,i=1}^{g'=2 \rightarrow g=2}, \dots, \sigma_{s,l,i}^{g' \rightarrow g}, \dots, \sigma_{s,ISCT,i=1}^{G \rightarrow G}]^\dagger, \quad (\text{A9})$$

$l = 0, \dots, ISCT; \quad i = 1, \dots, I; \quad g, g' = 1, \dots, G; \quad J_{os} = (G \times G) \times I \times (ISCT + 1).$

The expressions in Equations (A7) and (A3) indicate that the zeroth order (i.e., $l = 0$) scattering cross sections must be considered separately from the higher order (i.e., $l \geq 1$) scattering cross sections, since the former contribute to the total cross sections, while the latter do not. Therefore, the total number of zeroth-order scattering cross section comprise in σ_s is denoted as $J_{os,l=0}$, where $J_{os,l=0} = G \times G \times I$; and the total number of higher order (i.e., $l \geq 1$) scattering cross sections comprised in σ_s is denoted as $J_{os,l \geq 1}$, where $J_{os,l \geq 1} = G \times G \times I \times ISCT$, with $J_{os,l=0} + J_{os,l \geq 1} = J_{os}$. Thus, the vector \mathbf{s} comprises a total of $J_{os} + J_n = 30 \times 30 \times 6 \times (3 + 1) + 6 = 21,606$ imprecisely known components (“model parameters”).

The transport code PARTISN [10] computes the quantity $(\nu \Sigma_f)^g$ using directly the quantities $(\nu \sigma)_{f,i}^g$, which are provided in data files for each isotope i , and energy group g , as follows

$$(\nu \Sigma_f)^g = \sum_{m=1}^{M=2} (\nu \Sigma_f)_m^g; \quad (\nu \Sigma_f)_m^g = \sum_{i=1}^{I=6} N_{i,m} (\nu \sigma_f)_i^g, \quad m = 1, 2. \quad (\text{A10})$$

In view of Equation (A10), the quantity $(\nu \Sigma_f)^g \rightarrow (\nu \Sigma_f)^g(\mathbf{f}; r)$ depends on the vector of parameters \mathbf{f} , which is defined as follows:

$$\mathbf{f} \triangleq [f_1, \dots, f_{J_{\sigma_f}}; f_{J_{\sigma_f}+1}, \dots, f_{J_{\sigma_f}+J_v}; f_{J_{\sigma_f}+J_v+1}, \dots, f_{J_f}]^\dagger \triangleq [\sigma_f; \mathbf{v}; \mathbf{N}]^\dagger, \quad J_f = J_{\sigma_f} + J_v + J_n, \quad (\text{A11})$$

where:

$$\sigma_f \triangleq [\sigma_{f,i=1}^1, \sigma_{f,i=1}^2, \dots, \sigma_{f,i=1}^G, \sigma_{f,i'}^g, \dots, \sigma_{f,i=N_f}^1, \dots, \sigma_{f,i=N_f}^G]^\dagger \triangleq [f_1, \dots, f_{J_{\sigma_f}}]^\dagger, \quad (\text{A12})$$

$i = 1, \dots, N_f; \quad g = 1, \dots, G; \quad J_{\sigma_f} = G \times N_f,$

$$\mathbf{v} \triangleq [v_{i=1}^1, v_{i=1}^2, \dots, v_{i=1}^G, v_i^g, \dots, v_{i=N_f}^1, \dots, v_{i=N_f}^G]^\dagger \triangleq [f_{J_{\sigma_f}+1}, \dots, f_{J_{\sigma_f}+J_v}]^\dagger, \quad (\text{A13})$$

$i = 1, \dots, N_f; \quad g = 1, \dots, G; \quad J_v = G \times N_f,$

and where $\sigma_{f,i}^g$ denotes the microscopic fission cross section for isotope i and energy group g , v_i^g denotes the average number of neutrons per fission for isotope i and energy group g , and N_f denotes the total number of fissionable isotopes. For the purposes of sensitivity analysis, the quantity v_i^g can be obtained by using the relation $v_{f,i}^g = (\nu \sigma)_{f,i}^g / \sigma_{f,i}^g$, where the isotopic fission cross sections $\sigma_{f,i}^g$ are available in data files for computing reaction rates.

The quantity χ^g in Equation (3) quantifies the material fission spectrum in energy group g , and is defined in PARTISN [10] as follows:

$$\chi^g \triangleq \frac{\sum_{i=1}^{N_f} \chi_i^g N_{i,m} \sum_{g'=1}^G (\nu \sigma_f)_i^{g'} f_i^{g'}}{\sum_{i=1}^{N_f} N_{i,m} \sum_{g'=1}^G (\nu \sigma_f)_i^{g'} f_i^{g'}}, \quad \text{with} \quad \sum_{g=1}^G \chi_i^g = 1, \quad (\text{A14})$$

where the quantity χ_i^g denotes the isotopic fission spectrum in energy group g , while the quantity f_i^g denotes the corresponding spectrum weighting function.

The fission spectrum is considered to depend on the vector of parameters \mathbf{p} , defined as follows:

$$\mathbf{p} \triangleq [p_1, \dots, p_{J_p}]^\dagger \triangleq [\chi_{i=1}^{g=1}, \chi_{i=1}^{g=2}, \dots, \chi_{i=1}^G, \dots, \chi_i^g, \dots, \chi_{N_f}^G]^\dagger, \quad i = 1, \dots, N_f; \quad g = 1, \dots, G; \quad J_p = G \times N_f. \quad (\text{A15})$$

The source $Q^g(r) \rightarrow Q^g(\mathbf{q}; \mathbf{N})$ depends on the vector of model parameters \mathbf{q} , which is defined as follows:

$$\mathbf{q} \triangleq [q_1, \dots, q_{J_q}]^\dagger \triangleq [\lambda_1, \lambda_2; F_1^{SF}, F_2^{SF}; a_1, a_2; b_1, b_2; v_1^{SF}, v_2^{SF}]^\dagger, \quad J_q = 10. \quad (\text{A16})$$

In view of Equations (A4)–(A16), the model parameters characterizing the PERP benchmark can all be considered to be the components of the following “vector of model parameters:”

$$\boldsymbol{\alpha} \triangleq [\alpha_1, \dots, \alpha_{J_\alpha}]^\dagger \triangleq [\boldsymbol{\sigma}_t; \boldsymbol{\sigma}_s; \boldsymbol{\sigma}_f; \mathbf{v}; \mathbf{p}; \mathbf{q}; \mathbf{N}]^\dagger, \quad J_\alpha = J_{\sigma t} + J_{\sigma s} + J_{\sigma f} + J_v + J_p + J_q + J_n. \quad (\text{A17})$$

References

1. Cacuci, D.G.; Fang, R.; Favorite, J.A. Comprehensive Second-Order Adjoint Sensitivity Analysis Methodology (2nd-ASAM) Applied to a Subcritical Experimental Reactor Physics Benchmark: I. Effects of Imprecisely Known Microscopic Total and Capture Cross Sections. *Energies* **2019**, *12*, 4219. [\[CrossRef\]](#)
2. Fang, R.; Cacuci, D.G. Comprehensive second-order adjoint sensitivity analysis methodology (2nd-ASAM) applied to a subcritical experimental reactor physics benchmark: II. Effects of imprecisely known microscopic scattering cross sections. *Energies* **2019**, *12*, 4114. [\[CrossRef\]](#)
3. Cacuci, D.G.; Fang, R.; Favorite, J.A.; Badea, M.C.; di Rocco, F. Comprehensive second-order adjoint sensitivity analysis methodology (2nd-ASAM) applied to a subcritical experimental reactor physics benchmark: III. Effects of imprecisely known microscopic fission cross sections and average number of neutrons per fission. *Energies* **2019**, *12*, 4100. [\[CrossRef\]](#)
4. Cacuci, D.G. Second-Order Adjoint Sensitivity Analysis Methodology (2nd-ASAM) for Computing Exactly and Efficiently First- and Second-Order Sensitivities in Large-Scale Linear Systems: I. Computational Methodology. *J. Comput. Phys.* **2015**, *284*, 687–699. [\[CrossRef\]](#)
5. Cacuci, D.G. *The Second-Order Adjoint Sensitivity Analysis Methodology*; CRC Press, Taylor & Francis Group: Boca Raton, FL, USA, 2018.
6. Cacuci, D.G. Application of the Second-Order Comprehensive Adjoint Sensitivity Analysis Methodology to Compute 1st- and 2nd-Order Sensitivities of Flux Functionals in a Multiplying System with Source. *Nucl. Sci. Eng.* **2019**, *193*, 555–600. [\[CrossRef\]](#)
7. Valentine, T.E. Polyethylene-Reflected Plutonium Metal Sphere Subcritical Noise Measurements, SUB-PU-METMIXED-001. In *International Handbook of Evaluated Criticality Safety Benchmark Experiments, NEA/NSC/DOC(95)03/I-IX*; Report NEA/NSC/DOC(95)03/I, OECD-NEA (2008); Organization for Economic Co-operation and Development, Nuclear Energy Agency: Paris, France, 2008.
8. Fang, R.; Cacuci, D.G. Comprehensive second-order adjoint sensitivity analysis methodology (2nd-ASAM) applied to a subcritical experimental reactor physics benchmark: V. Computation of mixed 2nd-order sensitivities involving isotopic number densities. *Energies*. submitted.
9. Cacuci, D.G.; Fang, R.; Favorite, J.A. Comprehensive second-order adjoint sensitivity analysis methodology (2nd-ASAM) applied to a subcritical experimental reactor physics benchmark: VI. Overall impact of 1st- and 2nd-order sensitivities on response uncertainties. *Energies*. submitted.
10. Wilson, W.B.; Perry, R.T.; Shores, E.F.; Charlton, W.S.; Parish, T.A.; Estes, G.P.; Brown, T.H.; Arthur, E.D.; Bozoian, M.; England, T.R.; et al. SOURCES4C: A Code for Calculating (α, n), Spontaneous Fission, and Delayed Neutron Sources and Spectra. In Proceedings of the 12th Biennial Topical Meeting of the Radiation Protection and Shielding Division of the American Nuclear Society, Santa Fe, NM, USA, 14–18 April 2002. LA-UR-02-1839.

11. Alcouffe, R.E.; Baker, R.S.; Dahl, J.A.; Turner, S.A.; Ward, R. *PARTISN: A Time-Dependent, Parallel Neutral Particle Transport Code System*; LA-UR-08-07258; Los Alamos National Laboratory: Los Alamos, NM, USA, 2008.
12. Conlin, J.L.; Parsons, D.K.; Gardiner, S.J.; Gray, M.; Lee, M.B.; White, M.C. *MENDF71X: Multigroup Neutron Cross-Section Data Tables Based upon ENDF/B-VII.1X*; Los Alamos National Laboratory Report LA-UR-15-29571 (October 7, 2013); Los Alamos National Lab. (LANL): Los Alamos, NM, USA, 2013.
13. Chadwick, M.B.; Herman, M.; Obložinský, P.; Dunn, M.E.; Danon, Y.; Kahler, A.C.; Smith, D.L.; Pritychenko, B.; Arbanas, G.; Arcilla, R.; et al. ENDF/B-VII.1: Nuclear Data for Science and Technology: Cross Sections, Covariances, Fission Product Yields and Decay Data. *Nuclear Data Sheets* **2011**, *112*, 2887–2996. [[CrossRef](#)]
14. Cacuci, D.G. *BERRU Predictive Modeling: Best Estimate Results with Reduced Uncertainties*; Springer: Berlin/Heidelberg, Germany, 2018.



© 2020 by the authors. Licensee MDPI, Basel, Switzerland. This article is an open access article distributed under the terms and conditions of the Creative Commons Attribution (CC BY) license (<http://creativecommons.org/licenses/by/4.0/>).